6th International Conference
on Stability and Handling of Liquid Fuels
Vancouver, B. C., Canada
October 13-17, 1997

EXPERIMENTAL EVALUATION OF THE TWO-TIERED JFTOT TEMPERATURE PROVISION FOR JET A FUEL

Cliff Moses*[1], Stan Seto[2], and Steve Anderson[3]

[1]Southwest Research Institute, P.O. Drawer 28510, San Antonio, TX 78228-05210. [2]General Electric Aircraft Engines, 1 Neumann Way, Cincinnati, OH 45215-6301. [3]WL/POSF, Wright-Patterson AFB, OH 45433-7521.

ABSTRACT

An experimental program is being conducted to assess the potential impact to fuel-nozzle fouling life of using Jet A fuels which pass the JFTOT at 245°C but not at 260°C. Since the JP-8 fuel specification allows only the 260°C minimum temperature, this is an important consideration for military aircraft which upon occasion refuel with Jet A at commercial airports. The methodology of accelerated fuel-nozzle fouling tests and subsequent analysis follows previous projects for the US Navy to answer similar questions on the effect of reductions in thermal stability. Although the project is underway, unforseen delays precluded the presentation of actual results at this meeting. Anticipated results are presented and discussed.

INTRODUCTION

Aircraft of the US Air Force on occasion are refueled at commercial airports with fuel meeting the ASTM D 1655 fuel specification for Jet A, but not necessarily meeting the MIL-T-83133D fuel specification for JP-8. Specifically, there is a two-tiered temperature provision for thermal stability in ASTM D 1655 that allows for a fuel that does not pass the JFTOT test at 260°C to be retested at 245°C and approved for use if the fuel passes the test at the lower temperature, providing both results are reported. MIL-T-83133D requires that all fuels pass the JFTOT at 260°C. Many military aircraft engines have less margin available for thermal stability than do commercial engines, and there is concern that operating on fuels with a 245°C pass on the JFTOT may compromise reliability and mission readiness.

It is generally not possible to predict the effect of using a fuel with a JFTOT breakpoint temperature between 245 and 260°C since, with some exceptions as discussed below, there are no correlations

between JFTOT results and fouling rates in real engine hardware. It is therefore important to develop data on the fouling tendency of an atomizer from an Air Force engine when operated on fuels of marginal or "off-spec" thermal stability. It is also desirable to determine the effect of the "+100" additive package on atomizer fouling with such fuels to determine if that is a viable means of "upgrading" the fuel.

PREVIOUS RELATED STUDIES

During the late 1970's and early 1980's, some atomizer fouling tests were conducted for the US Air Force and US Navy as part of their alternative fuel programs. Some of these fouling tests were conducted by the engine manufacturers[1-6] while others were conducted at Southwest Research Institute (SwRI)[7-9].

The purpose of the fouling tests sponsored by the US Navy [7-9] was to determine the impact of using JP-5 that had been contaminated either by diesel fuel, i.e. DFM/NATO F-76, or by copper so as to cause the jet fuel to fail the JFTOT test for thermal stability, a problem very similar to the Air Force concern described earlier.

The nozzle fouling tests in the Navy program were conducted at SwRI. Test nozzles were immersed in an air flow which simulated the thermal environment of the engine installation. The surface temperature of the nozzle and the fuel flow rate were that of the beginning of idle-descent, which is considered to be the worst-case flight condition for deposition since the fuel and engine parts are still hot, but the fuel flow rate has been greatly reduced. The fuel inlet temperature was a variable among tests and was higher than normal engine experience to accelerate the tests. Fuels of different thermal stability, as determined by JFTOT breakpoint temperature, T_{BP}, were tested at three fuel inlet temperatures each. The test nozzle was instrumented for surface temperatures, inlet fuel temperature, flow rate, and pressure drop. A new nozzle was used for each test. The fuel was discarded after passing through the nozzle, and was not recirculated or reused.

Figure 1 illustrates typical fouling histories for five fuels of varying T_{BP}; these data came from the Navy program to determine the effect of contamination of JP-5 by diesel fuel and by copper on nozzle

fouling[8]. In this comparison, the inlet fuel temperature was constant. It is evident from these results that fouling takes place rather linearly with time and that fuels of lower thermal stability, i.e., lower T_{BP}, cause fouling at a higher rate.

From test results such as these, it is possible to compare the fouling rates caused by the fuels and develop expressions of equivalent fouling life, i.e., number of hours on a good fuel that it would take to produce the same amount of flow degradation in the nozzle. Figure 2 illustrates such results by comparing the equivalent fouling life for several different fuel nozzles as the breakpoint of the fuel is reduced beyond the minimum of 500°F (260°C)[7]. Considering one extreme, nozzle "a", the results indicate that a decrease in T_{BP} of 75°F(42°C) would cause about a 10-fold increase in fouling rate, i.e., one flight would produce the same deposit as 10 flights on a fuel of minimum acceptable thermal stability of 500°F (260°C). For the other extreme, nozzle "b", the effect of a 75°F (42°C) decrease in T_{BP} would be negligible.

The methodology used in the tests just described has been incorporated into a project for the US Air Force to determine the following while avoiding the expense of multiple engine endurance tests:

- the effect of the two-tiered JFTOT on military aircraft
- the effect of the "+100" additive package on fuels of marginal or sub-standard thermal stability

The test schedule has been delayed, so only the project description and anticipated results will be discussed.

OBJECTIVE

The objectives of this project are to experimentally determine the effect of using fuels with JFTOT breakpoint temperatures less that 260C on the fouling rate of a relevant fuel atomizer and subsequently determine the effect of the JP-8+100 additive on fuels of marginal or sub-standard thermal stability.

APPROACH AND SCOPE

Accelerated fuel-nozzle fouling tests are being conducted on a candidate nozzle using three fuels of different JFTOT breakpoint temperature to quantify the effect of breakpoint temperature on fouling rate. These results will then be used to evaluate the effect of using a fuel with a 245°C breakpoint. The tests will then be rerun with the "+100" additive added to the test fuels.

The three test fuels were supplied by the Fuels Branch at Wright-Patterson AFB following an initial screening of five fuels to select three JP-8 type fuels with the following thermal stability characteristics as determined by JFTOT breakpoint (T_{BP}):

- $T_{BP} \approx 245°C$
- $T_{BP} \approx 260°C$
- $T_{BP} >> 260°C$

The fouling rates are accelerated by raising the fuel inlet temperature. Test times of 25 to 75 hours are desirable, representing a compromise between excessively high temperatures and long test times. Nozzle tests are being conducted at three inlet temperatures.

The nozzle being tested is a dual-orifice pressure atomizer of the type used in the General Electric F108 and F110 engines. Figure 3 shows an outline schematic of the nozzle along with the locations of the thermocouples used to monitor test conditions.

EXPERIMENTAL CONDITIONS

The nozzle fouling tests are conducted by suspending the test nozzle in a heated air flow so as to reproduce surface temperatures on the nozzle that are typical of engine-installed conditions. The fuel flow rate is that of the beginning of idle-descent, which is considered to be the worst-case flight condition for deposition since the fuel and engine parts are still hot, but the fuel flow rate has been greatly reduced. The test nozzle is instrumented for surface temperatures, flow rate, and pressure drop.

Figure 4 presents a flow schematic of the experiments. The test nozzle is submerged in a heated fluidized bed of sand which serves to increase the heat transfer between the heated air and the nozzle body. The temperature of the air flowing through the bed is adjusted to maintain a constant temperature at the tip of the test nozzle for all the tests. Since the fuel flow rate and pressure drop across the nozzle are constantly monitored, it is possible to see the results of the fouling occur in real time.

The fuel inlet temperatures are being chosen to achieve test times on the order of 25 to 75 hours. The test time is the time required to develop a 10 percent increase in pressure drop across the nozzle. This is a value that is large enough to be significant and easily measured without extending test times unnecessarily.

ANTICIPATED RESULTS

Figure 5 illustrates the type of data results that are anticipated to determine the effect of fuel thermal stability on fouling rate for the three test fuels. Each of the lines will be a least-squares fit to data at three temperatures. Figure 6 illustrates the possible analyses of the data of Figure 5 in a manner similar to the results presented in Figure 2; a large increase represents a significant reduction in fouling life. If the three lines of Figure 5 are very close together, there will be little effect of a decrease in breakpoint temperature. The larger the separation of the three lines, the greater the effect will be on the equivalent-life analysis of Figure 6.

If the "+100 additive package" performs as expected, the lines of Figure 5 should be shifted to the right to higher fuel temperatures. The degree of the shift and whether or not the effect will be the same on all three fuels can not be predicted.

REFERENCES

1. Gleason, C.C., et al., "Evaluation of Fuel Character Effects on J79 Engine Combustion System," US Air Force AFAPL-TR-79-2015, June 1977.

2. Gleason, C.C., et al., "Evaluation of Fuel Character Effects on F101 Engine Combustion System," US Air Force AFAPL-TR-79-2018, June 1979.

3. Vogel, R.E. et al., "Fuel Character Effects on Current High Pressure Ratio, Can-Type Turbine Combustion Systems," US Air Force AFAPL-TR-79-2072, April 1980.

4. Gleason, C.C., et al., "Evaluation of Fuel Character Effects on J79 Smokeless Combustor," US Air Force AFAPL-TR-80-2092, November 1980.

5. Oller, T.L., et al., "Fuel Mainburner/Turbine Effects," US Air Force AFAPL-TR-81-2100, May 1982.

6. Russell, P.L., "Fuel Mainburner/Turbine Effects," US Air Force AFAPL-TR-81-2081, September 1982.

7. Moses, C.A., et al., "An Alternate Test Procedure to Qualify Fuels for Navy Aircraft: Phase II," US Navy NAPC-PE-145C, August 1984.

8. Tyler, J.C. et al., "An Alternate Test Procedure to Qualify Fuels for Navy Aircraft: Phase II Continuation," US Navy NAPC-PE-176C, August 1987.

9. Moses, C.A., "Effect of a Metal Deactivator Fuel Additive on Fuel Deposition in Fuel Atomizers at High Temperature," US Army BFLRF Report No. 281, AD A260915, August 1992.

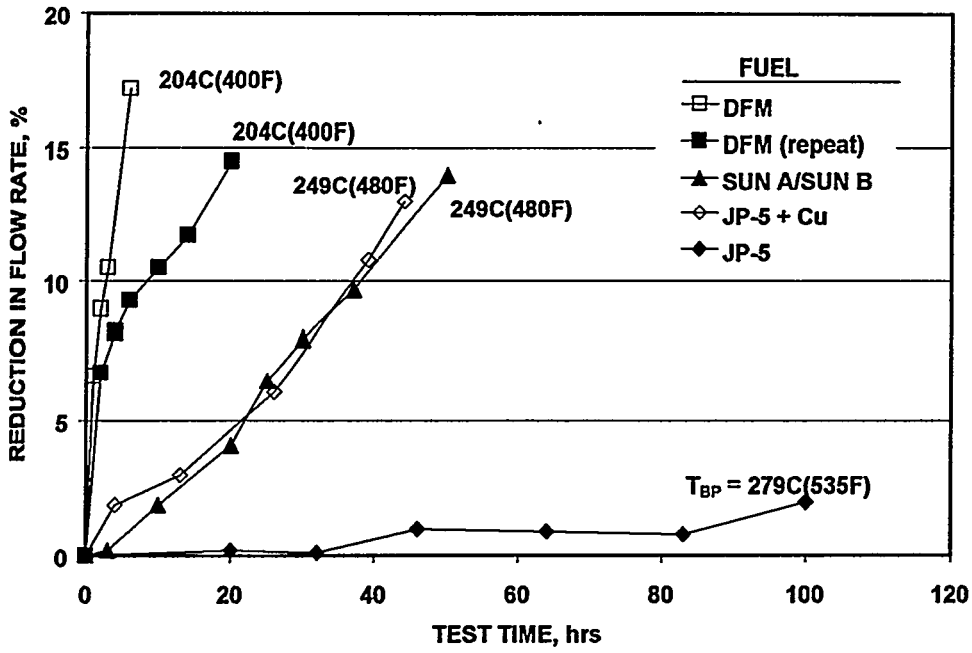

FIGURE 1. EFFECT OF JFTOT BREAKPOINT TEMPERATURE ON NOZZLE FOULING (from Ref. 8)

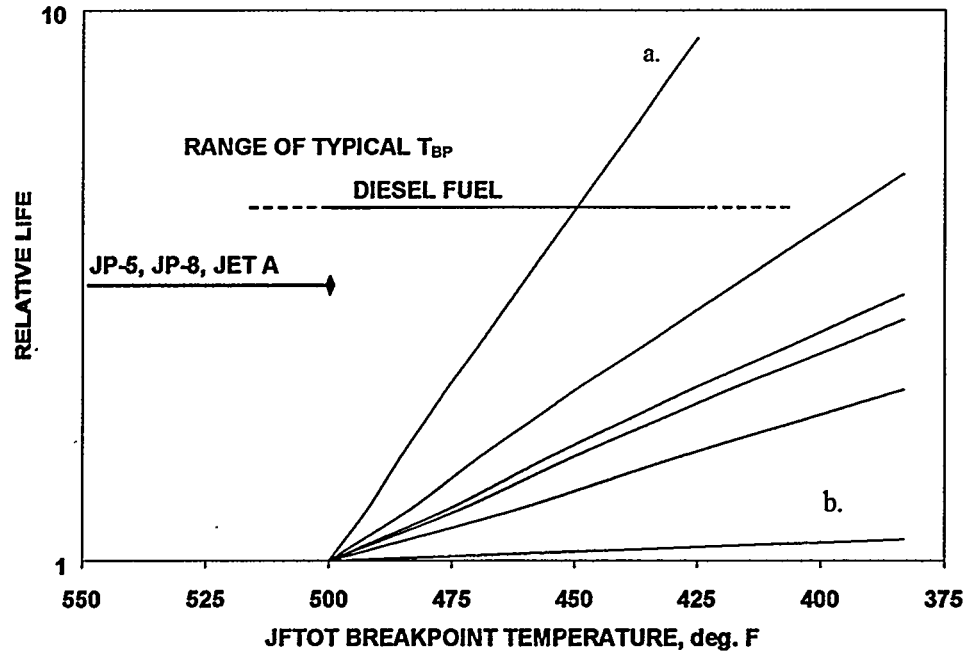

FIGURE 2. EFFECT OF BREAKPOINT TEMPERATURE ON RELATIVE FOULING LIFE (from Ref. 7)

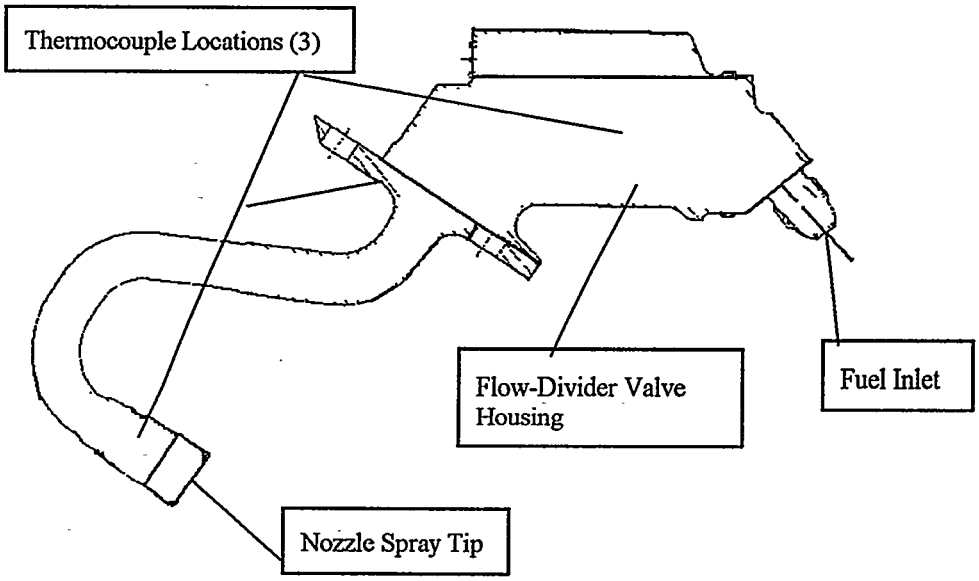

FIGURE 3. TEST ATOMIZER SHOWING THERMOCOUPLE LOCATIONS

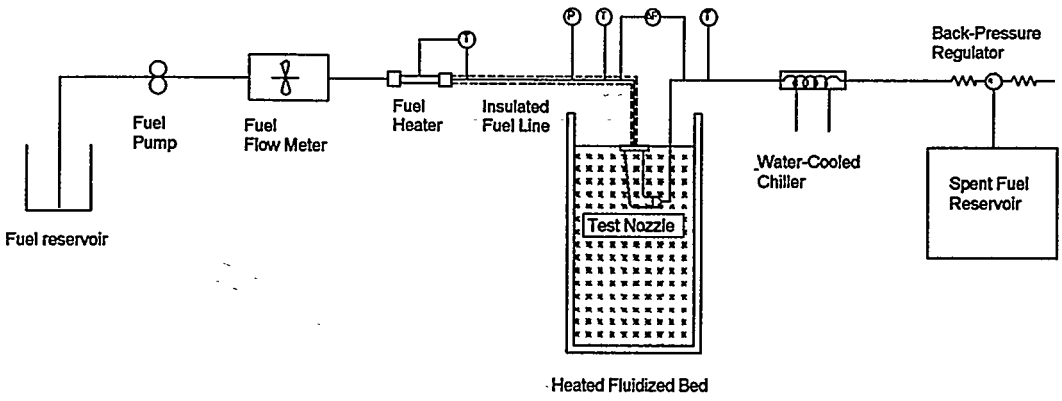

FIGURE 4. FLOW SCHEMATIC OF NOZZLE FOULING TESTS

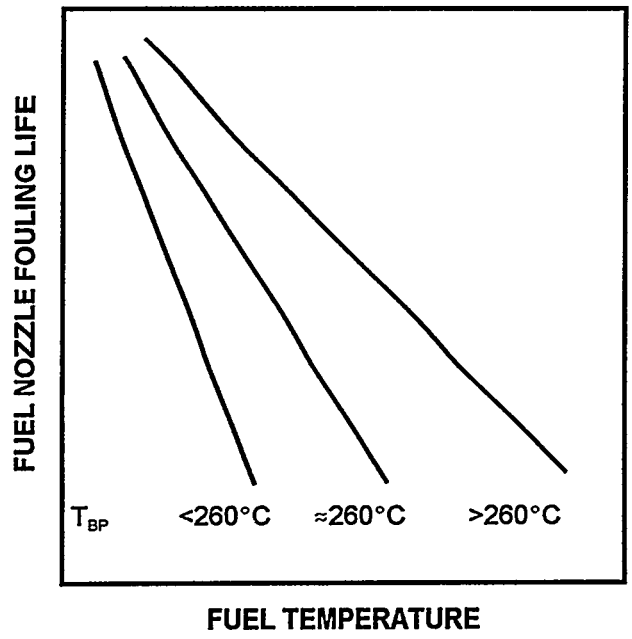

FIGURE 5. ANTICIPATED RESULTS FROM FUEL-NOZZLE FOULING EXPERIMENTS

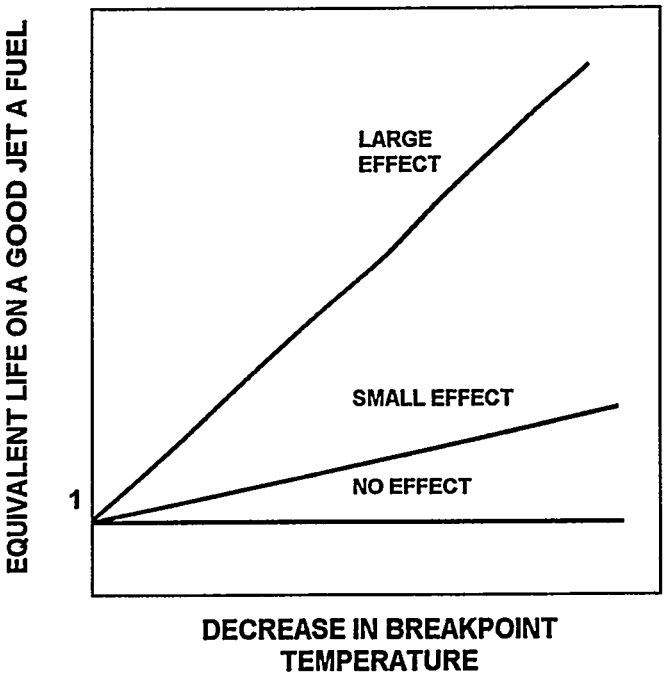

FIGURE 6. POSSIBLE RESULTS FROM THE ANALYSIS OF NOZZLE FOULING DATA TO QUANTIFY THE EFFECT OF BREAKPOINT TEMPERATURE ON FOULING LIFE

6th International Conference
on Stability and Handling of Liquid Fuels
Vancouver, B. C., Canada
October 13-17, 1997

STUDIES OF JET FUEL OXIDATION USING OXYGEN MONITORING AND CHEMICAL KINETIC MODELING

Steven Zabarnick*, Shawn D. Whitacre, Mark S. Mick, and Jamie S. Ervin

University of Dayton Research Institute, Aerospace Mechanics Division, 300 College Park, KL-463, Dayton, OH 45469-0140, USA.

A quartz crystal microbalance (QCM)/Parr bomb system with a headspace oxygen sensor is used to measure oxidation and deposition during thermal oxidative stressing of jet fuel. In studies of jet fuel antioxidants, we find that rapid increases in oxidation rate occur upon consumption of the antioxidant. The antioxidant appears to be consumed by reaction with alkylperoxy radicals. In studies of metal deactivator (MDA) additives, we find that MDA is consumed during thermal stressing, and this consumption results in large increases in the oxidation rate of metal containing fuels. Mechanisms of MDA consumption are hypothesized. Chemical kinetic modeling was used to simulate the autoxidation of jet fuel including the chemistry of peroxy radical inhibiting antioxidants and hydroperoxide decomposing species. Recent experimental measurements of oxygen concentration during autoxidation of jet fuel were used to "calibrate" the rate parameters of the mechanism. The model showed excellent agreement with oxygen profiles of static measurements at 140°C. At 185°C, the model predicts that peroxy radical inhibiting antioxidants and hydroperoxide decomposers both slow and/or delay oxidation, but the resulting oxygen profiles display different characteristics. We have shown that comparison of these profiles with fuel blending and fuel dilution measurements have the potential to differentiate between the two types of oxidation slowing species. The modeling predicts that the presence of both types of species in a fuel results in a synergistic slowing of the oxidation rate.

Introduction

Jet fuel undergoes oxidative chemistry upon being heated in the fuel systems of advanced military aircraft. Besides being heated by heat transfer from the hot turbine compressor air (or in the afterburner by combustor exhaust), the fuel is also heated while being used as a coolant for various engine and airframe components.[1] It has been predicted that this coolant usage will become even more important in future advanced aircraft.[2] Air saturated fuel typically contains

≈60 ppm (w/w) or 1.8×10^{-3} M of oxygen. This very small amount of oxygen can result in the formation of gums and deposits which are capable of impairing proper performance of the fuel system and grounding of the aircraft. In a flowing fuel system, the mass of deposits formed per volume of fuel is small, on the order of 1 μg/mL (≈1.2 ppm w/w) for complete oxygen consumption;[3] but, the volumes of fuel used in military aircraft are extremely large over the lifetime of an aircraft. Thus the small amounts of deposits which form can build up over time, ultimately resulting in filter plugging, fouling of close tolerance valves, valve hysteresis, and other problems.

Antioxidants have been used for many decades to slow and/or delay autoxidation. Indeed, the development of antioxidants has been so successful that they are used routinely in many industrial and consumer products, including foods and gasoline. There are many types of antioxidants that have been used in hydrocarbon liquids: hindered phenols, phenylenediamines, peroxide decomposers, and metal deactivators. It is believed that hindered phenols and phenylenediamines slow oxidation by intercepting the alkylperoxy free radicals that carry the autoxidation chain. Peroxide decomposers react with hydroperoxides and prevent their decomposition into free radicals. Metal deactivators complex with metal ions and prevent their catalysis of processes which form free radicals. Thus each of these antioxidant types is thought to lower the concentration of free radicals either by preventing their formation or rapidly removing them after they are formed.

Although antioxidants are widely used and have proven very successful in preventing the formation of detrimental products, chemical kinetic modeling of the chemical mechanism of antioxidant action has received little attention. Fortunately, the primary reactions by which hindered phenol antioxidants intercept alkylperoxy radicals have been studied extensively. Previously, we have performed chemical kinetic modeling of antioxidant action for jet fuel applications.[4] This study was limited to relatively short reaction times before significant consumption of the antioxidant species occurred. Also, because of the lack of suitable experimental data, no comparison with laboratory measurements was included. Recent measurements of oxygen concentration during the autoxidation of jet fuel, jet fuel mixtures, and

model jet fuel species have provided reasonable data for comparison with modeling.[5-8] In the present study we utilize these experimental data for "calibration" of the kinetic parameters of the model. Also, we compare the predicted and measured oxygen profiles to provide insight into the antioxidant mechanism. In addition, we explore the type of behavior expected by the presence of peroxide decomposing species. This study will also address relatively long reaction times, where the antioxidant species may become completely consumed. In experimental studies, we also explore the mechanisms by which metal deactivators and hindered phenols slow and/or delay the autoxidation process.

Experimental

The QCM/Parr bomb system has been described in detail previously and will only be outlined briefly here.[9,10] The Parr bomb is a 100 mL stainless steel reactor. It is heated with a clamp-on band heater and its temperature is controlled by a PID controller through a thermocouple immersed in the fuel. The reactor contains an rf feedthrough, through which the connection for the quartz crystal resonator is attached. The crystals are 2.54 cm in diameter, 0.33 mm thick and have a nominal resonant frequency of 5 MHz. The crystals were acquired from Maxtek Inc. and are available in crystal electrode surfaces of gold, silver, platinum, and aluminum. For the studies reported here gold crystal electrodes were used. The QCM measures deposition (i.e., an increase in mass) which occurs on overlapping sections of the two sided electrodes. Thus, the device responds to deposition which occurs on the metal surface and does not respond to deposition on the exposed quartz.

The device is also equipped with a pressure transducer (Sensotec) to measure the absolute headspace pressure and a polarographic oxygen sensor (Ingold) to measure the headspace oxygen concentration. Previous studies have demonstrated the value of determining the oxidation characteristics of fuels and fuels with additives. A personal computer is used to acquire data at one minute intervals during the experimental run. The following data are recorded during a run:

temperature, crystal frequency, headspace pressure, headspace oxygen concentration, and crystal damping voltage.

BHT (2,6 di-*tert*-butyl-4-methylphenol) was quantified by gas chromatography-mass spectrometry (GC-MS). 500 μL fuel samples were withdrawn from the reactor through a GC septum and extracted with 500 μL of methanol. 2 μL samples of the methanol solution were injected into a Hewlett-Packard GC-MS operating in single-ion monitoring (SIM) mode. The mass spectrometer was set to follow the intensity of the 205 amu fragment ion and the 220 amu parent ion of BHT. Calibration curves were obtained by injecting standard solutions of BHT in methanol.

MDA was quantified by a procedure developed by Striebich.[11] 10 mL of fuel is passed through a silica gel solid phase extraction cartridge. The polar components, including MDA, are retained on the cartridge and subsequently eluted with methanol. The methanol is evaporated and the remaining condensate is dissolved in 200 μL of toluene. This toluene solution is injected into a GC/MS operated with base deactivated injector liner and column. Single ion monitoring of the 161 amu fragment ion and the 282 amu parent ion were used for quantitation.

Chemical Kinetic Modeling Methodology

The methodology used in the chemical kinetic modeling reported here has been reported previously,[4] and therefore will only be described briefly. The chemical kinetic modeling was performed using the modeling package REACT.[12] This is a relatively simple package that integrates the multiple differential equations that result from a detailed chemical kinetic mechanism and yields species concentrations as a function of time. The following is input to the code: reaction mechanism with rate constants, initial concentrations for each species present in the mechanism, reaction time and time intervals for output, and various tolerances for the precision of the computation. The code outputs the individual species concentrations at each time interval.

As jet fuels are mixtures of hundreds of chemical species, it is impractical to model the chemical changes of all components of the mixture. Instead we have chosen to model the bulk fuel as a single compound, RH. RH has the chemical properties of a straight-chain alkane, such as n-dodecane; this is a reasonable simplification as alkanes comprise a large proportion of a jet fuel mixture. This single compound "fuel" can also contain dissolved oxygen (O_2), an antioxidant species (AH), and a peroxide decomposer (SH). The reaction mechanism used in the present study is shown in Table 1. The mechanism is a modification of that used previously.[4] Modifications involve adjustment of rate parameters to better match experimental measurements and the inclusion of a "peroxide decomposer" species.

Results and Discussion

Studies of peroxy radical intercepting antioxidants

Peroxy radical intercepting antioxidants are widely used in the petroleum industry to slow the oxidation of petroleum distillates. Military jet fuels which are hydrotreated require the addition of antioxidants to prevent the formation of gums and peroxides during storage and handling. In addition the US Air Force is considering the use of an antioxidant additive in the JP-8+100 thermal stability additive package. We have noted, in rapidly oxidizing fuels stressed at 140°C in the QCM system,[10] that the addition of an antioxidant additive can significantly delay oxidation and deposition. But, in such fast oxidizing fuels, after some time the oxygen removal process will begin.

This behavior is illustrated in Fig. 1 for a hydrocarbon solvent, Exxsol D-110. Exxsol D-110 is a dearomatized, narrow-cut aliphatic solvent with <1% aromatics and 3 ppm sulfur. As it is highly refined, it contains few naturally occurring antioxidants and therefore oxidizes quite rapidly. The figure shows that complete oxygen consumption occurs in two hours at 140°C. As it contains few naturally occurring antioxidants, Exxsol D-110 is an ideal model fuel in which to study antioxidants. We have added the antioxidant BHT over the concentration range 4.2 to 50

mg/L and measured the headspace oxygen concentration. Deposition is not reported as it is quite low for this solvent. The figure shows that as the concentration of added BHT is increased the oxidation process is delayed. But, after the delay period, oxidation occurs at a very similar rate to the neat fuel. Chemical kinetic schemes can reproduce this delay in oxidation;[4] but, it is not clear why the oxidation rate increases at longer times. One possible explanation is that the antioxidant molecule is consumed during the slow oxidation time until it is reduced below some critical level, then the oxidation process can proceed. This explanation is supported by the concentration dependence of the oxygen curves of Fig. 1. The more antioxidant that is present the longer is the delay before rapid oxidation occurs. A second explanation is that oxidation products build up slowly during the slow oxidation, and reach a critical level at which point they can help initiate faster oxidation.

To test the first theory, we have measured the concentration of BHT during a run by withdrawing 500 μL samples and performing the GC-MS analysis for BHT described in the experimental section. These experiments were performed in fuel F-3139, a fast oxidizing Jet A fuel. The results are shown in Fig. 2. The neat fuel consumes all of the headspace oxygen in three hours, and the addition of 25 mg/L of BHT delays the time of complete oxygen consumption out to seven hours. The figure shows that the BHT concentration decreases to near zero over the first 5 hours of the run. The oxidation rate increases when the BHT concentration begins to get quite low (<5 mg/L). Unfortunately, not enough data were taken during the 3 to 6 hour range to better determine the critical BHT concentration below which the oxidation rate increases. We believe that these BHT concentration measurements support the first explanation hypothesized above. Recently performed chemical kinetic modeling also supports the supposition that the consumption of the antioxidant will precipitate rapid oxidation.[13] Presumably the antioxidant is being consumed by reaction with peroxy radicals in its role as a peroxy radical inhibitor.

Studies of metal deactivator additives

Metal deactivator species have been used for many years in the petroleum industry to inhibit the catalytic effect of metals in petroleum distillates.[14] These metals, and copper in

particular, act to catalyze the autoxidation chemistry thereby greatly increasing oxidation and deposition rates. This catalytic effect occurs at the part per billion level of dissolved metal. It was realized early on that the presence of these metals in petroleum distillates had the effect of greatly reducing the antioxidant capabilities of peroxy radical inhibiting antioxidant species. Thus, metal deactivator additives were developed as an inexpensive solution to suppressing the catalytic activity of the metals without removing them from the system. The metal deactivators, N,N'-disalicylidene-1,2-propanediamine and N,N'-disalicylidene-1,2-cyclohexanediamine, are optional additives in the JP-8 military specification (MIL-T-83133D). In the jet fuel community the use of metal deactivators is controversial due to their possible over response in the JFTOT thermal stability fuel specification test.[15]

Although originally designed to chelate metal ions in solution, it has been proposed that these metal deactivators may also act by surface passivation of exposed metal surfaces and as antioxidants by radical inhibition.[16] To further explore the nature of metal deactivators as thermal stability additives we have performed a series of experiments in the QCM system. In these studies we use fuel F-3145, which has been doped with 285 ppb copper, and the metal deactivator, N,N'-disalicylidene-1,2-propanediamine, hereafter referred to simply as MDA. In Figs. 3a and 3b are shown plots of deposition and headspace oxygen at 140°C for fuel F-3145 neat and with 3.0, 5.8, and 12.0 mg/L added MDA. The neat fuel produces deposition during the first four hours, after which the deposition levels. The oxygen sensor data show that oxidation occurs during this initial four hour period, and oxygen is completely consumed at five hours. The addition of MDA delays both the oxidation and deposition processes. Increasing amounts of MDA allow longer delays in oxidation and deposition. With 3 mg/L added MDA, these processes are delayed for one hour, with 5.8 mg/L the delay is five hours, and with 12 mg/L the delay is 10 hours. The final deposit amounts for all of the MDA concentrations are near 4 $\mu g/cm^2$, reduced from the 7 $\mu g/cm^2$ produced by the neat fuel.

As fuel F-3145 contains 285 ppb copper, a delay in the oxidation and deposition process is fully expected. Clark[15] reported a chelation ratio for MDA:Cu of 1.1:1 mol/mol or 5:1 w/w.

Thus all of the copper can be complexed by the addition of approximately 1.1 mg/L MDA. Therefore even the smallest amount of added MDA shown in Fig. 3, 3 mg/L, is enough to completely complex all of the copper in the fuel. If MDA acted only as a simple complexing agent of copper and was not depleted during the test, we would expect the oxidation and deposition results to be identical for these three concentrations of MDA, because addition of excess MDA (>1.1 mg/L) should have no effect on oxidation or deposition. But instead we see that the oxidation delay is a function of the concentration of MDA.

The two previously reported secondary behaviors of MDA, surface passivation and free radical inhibition, may be able to yield the observed behavior. In addition, if MDA is consumed by chemical reaction, the observed behavior would be expected. To date, we are not aware of any previous reports of MDA consumption during thermal stressing of a fuel. To test this third mechanism we have measured the concentration of MDA present during an experimental run and the results are shown in Fig. 4. A separate experimental run was used for each MDA concentration point shown in the figure, as the analysis required 10 mL of fuel. The figure shows that the MDA concentration drops during the entire run, resulting in an MDA concentration below the detection limit at 15 hours. The figure also shows that oxygen consumption is moderately slow until seven hours, after which the oxidation rate increases substantially. The time of rapid increase in the oxidation rate occurs when the MDA concentration drops below approximately 1 mg/L. This is close to the predicted concentration requirement (1.1 mg/L) for chelation of all of the copper as determined by the binding ratio. It would appear that when the MDA concentration falls below this level, unchelated copper becomes available to catalyze the initiation reactions and thereby accelerates the oxidation process. These results clearly show that the consumption of MDA controls the time delays observed from MDA addition to fuel.

However, the mechanism by which MDA is depleted is uncertain. We are not aware of any MDA consumption reactions reported in the literature. Presumably MDA could be removed by chemical reaction, complexation with reaction products, or adsorption to the reactor walls. MDA contains phenolic hydrogen atoms which may be amenable to attack by peroxy radicals. Complexation of acidic reaction products is also a possible pathway for MDA consumption.

Chemical kinetic modeling

Modeling of BHT addition at 140°C

Recent measurements of the antioxidant behavior of jet fuel, jet fuel mixtures, and model jet fuel species have shown a distinctive behavior of the oxidation profiles as the antioxidant concentration is varied.[6-8] An example of this behavior is shown in Figure 1 for the autoxidation of Exxsol D-110 with various levels of added BHT at 140°C in a Parr bomb reactor.[6] It is apparent from the figure that increasing levels of added BHT result in increasing delays in the oxidation process. The oxidation behavior with added antioxidant is characterized by a slow initial oxidation followed by a sudden rapid increase in the oxidation rate.

Previous chemical kinetic modeling of antioxidants in jet fuel concentrated on relatively short reaction times, where significant consumption of the antioxidant species had not occurred.[4] In the present work, we extend the modeling to longer times to determine if the model can predict and corroborate the sudden increase in oxidation rate upon antioxidant consumption. The results at various levels of added BHT antioxidant are shown in Fig. 5. The figure shows plots of oxygen concentration versus time for modeling performed at 140°C. The rate parameters of Table 1 were used and the concentration of the peroxide decomposing species, SH, was held at zero to "turn off" reaction 17. The plot shows that without added antioxidant the "fuel" oxidizes rapidly, completely consuming the available oxygen in less than one hour. In the presence of added antioxidant there is an initial slow oxidation followed by a change to a more rapid loss of oxygen. As the antioxidant concentration is increased, the delay until the onset of rapid oxidation increases. This qualitative behavior is remarkably similar to the experimental measurements of Figure 1. As the antioxidant concentration is varied over the range 0 to 50 mg/L the time at which the oxidation rate rapidly increases, matches the measurements quite well. Note that a direct quantitative comparison between Figs. 1 and 5 cannot be performed as the Parr bomb technique is complicated by the presence of headspace oxygen and diffusional effects.[9] Also the first 45 minutes to one hour of the measurements in Figure 1 corresponds to the heat-up period of the reactor, and thus significant reaction does not occur during this time.

Modeling of autoxidation at 185°C

Figure 6 shows results for the modeling at a temperature of 185°C. Without antioxidant the "fuel" oxidizes rapidly, completely consuming the oxygen in 60 seconds. As at 140°C, at relatively low concentrations of added antioxidant (0.5 to 8 x 10^{-4} M) there is an initial slow oxidation followed by a change to a more rapid oxygen loss. The figure also shows predicted oxygen profiles at relatively high concentrations of added antioxidant, up to 3.2 x 10^{-3} M (704 mg/L based on the molecular weight of BHT). As the antioxidant concentration is increased above 8 x 10^{-4} M, the rate of the initial oxidation increases significantly, eroding the gains in slowing the oxidation at lower concentrations of antioxidant. This increase in oxidation rate with added antioxidant is similar to that observed in the blending of slow and fast oxidizing fuels.[8] These workers progressively diluted a slow oxidizing fuel with Exxsol D-80 and measured the oxidation profiles at 185°C. They observed that as the fuel was diluted to a 1:1 fuel:solvent ratio, that oxidation slowed. Upon further dilution the oxidation rate increased. We have previously argued that the dilution of a slow oxidizing fuel, i.e., one which contains a significant quantity of naturally occurring antioxidants, is effectively the same as lowering the concentration of these antioxidants.[7] Thus, the present modeling predicts that at relatively high concentrations of antioxidant, increases in the oxidation rate will be observed relative to lower, more optimum levels. Indeed, the blending experiments showed such behavior, implying the slow oxidizing fuel contained a concentration of antioxidant greater than optimum. Thus, dilution slows oxidation until the optimum concentration is reached, and further dilution decreases the time to complete oxygen consumption due to a lower than optimum antioxidant concentration. This behavior, where there exists an optimum antioxidant concentration above and below which the oxidation rate increases, was also predicted by the previous modeling study.[4]

Figure 6 also shows that as the concentration of added antioxidant is varied over the range 0.5 to 8 x 10^{-4} M, the time at which complete oxygen consumption occurs appears to increase in approximately even increments as the antioxidant concentration is doubled. This behavior is remarkably similar to that observed in the blending of fuels.[8] Balster et al. observed an approximate even spacing in increasing oxygen consumption time as the dilution factor is doubled

for the blending of a fast oxidizing fuel with a slow oxidizing fuel. This occurred over the range 2.5 to 20% of the slow oxidizing fuel. This agreement lends further support to the validity of the chemical kinetic model. It also supports the view that dilution of a slow oxidizing fuel with a fast oxidizing fuel is, in effect, a dilution of the naturally occurring antioxidants present in the slow oxidizing fuel.

The good qualitative agreement observed between the chemical kinetic model employed here, and measurements of fuel and hydrocarbon oxidation, provides evidence of the correctness of the assumptions in the mechanism. In particular, the interception of peroxy radicals by the antioxidant species, reaction 5, and subsequent antioxidant product chemistry is successful in reproducing both the observed slowing in oxidation at short times and the subsequent increase in oxidation rate at long times. On the other hand, Jones et al.[5] have hypothesized that the primary mechanism for the relatively slow autoxidations observed in some jet fuels is the reaction of hydroperoxides with sulfur species to produce non-radical products, reaction 17. We have shown above that the presence of peroxy radical inhibiting species can provide significant slowing of oxidation and the modeling of these reactions shows excellent qualitative agreement to the measured oxygen profiles. In order to explore the role that hydroperoxide decomposers may play in the autoxidation process, we will set the AH concentration to zero and vary the concentration range of the SH over the range 0 to 2×10^{-2} M for oxidation at 185°C. In order to maximize the importance of reaction 17, we have used a "fast" A-factor and an activation energy of zero for the rate parameters of this reaction. The results are shown in Figure 7. The figure shows that over the range of SH concentrations 2 to 200×10^{-4} M, significant delays in oxidation are predicted. Complete oxygen consumption is delayed to 670 seconds upon addition of 2×10^{-3} M of SH. No further changes in oxidation are predicted at higher concentrations of SH. With increasing SH concentration, the oxygen profiles appear to approach a limiting oxygen profile which is near linear in time. This is due to hydroperoxide consumption via reaction 17 completely preventing unimolecular hydroperoxide decomposition via reaction 11.

Can we now use these modeled oxygen profiles to determine if the observed laboratory oxygen behavior during fuel/solvent blending[8] is due to a peroxy radical inhibitor or a peroxide

decomposer? The behavior of the calculated oxygen profiles of Fig. 7 with increasing peroxide decomposer, SH, is different from those observed with increasing peroxy radical interceptor, AH (Figure 6), in three respects. First, the delays observed, a maximum of 670 seconds, are significantly smaller than for the addition of AH. Second, as the SH concentration is doubled over the range 2 to 16 x 10^{-4} M, the time for complete oxygen consumption is not evenly spaced. And third, at large SH concentrations the oxidation profile reaches a limiting rate. In contrast, the measured oxygen profiles of fuel blends of Balster et al. have oxygen consumption times greater than 1500 seconds, show evenly spaced consumption times with a doubling of the AH concentration, and do not reach a limiting profile. It is apparent that the predicted effects of a peroxide decomposer addition on oxidation are not similar to the laboratory measurements of Balster et al., while the peroxy radical inhibition mechanism does represent the data well.

In a separate work, Jones et al.[5] studied the effects of blending two jet fuels, one of which (the slower oxidizing fuel) is the same fuel as in the Balster et al. study. This study reports maximum oxygen consumption times of 840 seconds and the oxygen profiles do reach a limiting value at blends approaching 100% of the slow oxidizing fuel. But as the slow oxidizing fuel is added to the fast oxidizing fuel, as the slow oxidizing fuel is doubled the time to complete oxygen consumption does appear to be evenly spaced. Thus, it would appear that in this study the oxygen decay behavior has some, but not all, of the characteristics of the peroxide decomposer mechanism. Unfortunately, this study is complicated by the probable presence of naturally occurring (and possibly refinery added) antioxidants in the relatively fast oxidizing fuel. The blending of these two fuels is not a true dilution of the antioxidant concentration of the slow oxidizing fuel because the fast oxidizing fuel contains these additional inhibitors. Balster et al. point out that dilution of a jet fuel which contains approximately 20% aromatics with another jet fuel of similar aromatic content is different from dilution with a solvent which is devoid of aromatics. They posit that the initiation rate is proportional to the aromatic content and attribute the differences in the two studies to these changes in aromatic content.

This modeling study shows that the fuel/solvent blending behavior matches the behavior predicted by the peroxy radical interception mechanism and is therefore the most likely

mechanism for the observed oxygen profiles in these fuel blends. The fuel/fuel blending study exhibits behavior that has some of the characteristics of both the peroxy radical inhibition and hydroperoxide decomposition (reaction 17) mechanisms. As the slow oxidizing fuel is the same in the two studies, it is likely that the same oxidation slowing pathways are important in both studies. It must be emphasized that the mechanism used here is an oversimplification of the complex chemistry that occurs during the oxidation of real fuels. In particular, the peroxide decomposer reaction, reaction 17, is a simplification of a poorly understood mechanism in which oxidized sulfur species that are produced from the reaction may provide additional peroxide decomposition pathways.[17,18] Also, as jet fuel is a complex chemical mixture which likely contains both naturally occurring peroxy radical inhibitors and peroxide decomposer compounds, it is likely that both mechanisms occur in real fuels. To determine the behavior predicted for the simultaneous occurrence of the two inhibition pathways we have modeled the case at 185°C in which equal concentrations of the two compounds, AH and SH, are present at a concentration of 1×10^{-4} M. The results are shown in Fig. 8, along with the predicted oxygen profiles in the presence of the individual compounds at 2×10^{-4} M. It is apparent from the figure that the model predicts the two compounds acting together display a synergistic effect on the oxidation profile. The oxidation rate is drastically slowed by the presence of both species, much more than would occur from just the sum of the two effects. Indeed, this type of synergism between peroxy radical inhibiting antioxidants and peroxide decomposing species has been observed experimentally.[19] Apparently, the presence of the peroxide decomposer lowers the radical production rate enough to significantly slow the consumption of the peroxy radical inhibiting antioxidant. Thus, AH survives longer and the change to faster oxygen consumption occurs later. Another view is that the peroxy radical inhibiting antioxidant slows the production of hydroperoxides and thus the peroxide decomposer is able to survive longer. These processes occur simultaneously as both SH and AH are removed simultaneously during the run.

Conclusions

This study has utilized the QCM/Parr bomb system with a headspace oxygen sensor to simultaneously measure oxidation and deposition during thermal oxidative stressing of jet fuel. We find that rapid increases in oxidation will occur upon consumption of an added antioxidant to a fast oxidizing fuel. The antioxidant appears to be consumed by reaction, presumably with alkylperoxy radicals. We find that MDA is consumed during thermal oxidative stressing, and this consumption results in large increases in the oxidation rate in metal containing fuel. Mechanisms for MDA consumption have been hypothesized. The consumption of antioxidants and MDA have important implications in the design of jet fuel thermal stability improving additive packages, particularly in the additive concentration optimization process. We also used chemical kinetic modeling to simulate the autoxidation of jet fuel including the chemistry of peroxy radical inhibiting antioxidants and hydroperoxide decomposing species. Recent experimental measurements of oxygen concentration during autoxidation of jet fuel were used to "calibrate" the rate parameters of the mechanism. The model shows excellent agreement for oxygen profiles of static measurements at 140°C. At this temperature the model predicts large increases in oxidation rate upon peroxy radical inhibiting antioxidant consumption to below 1×10^{-5} M. At 185°C we have shown that peroxy radical inhibiting antioxidants and hydroperoxide decomposers both slow and/or delay oxidation, but the resulting oxygen profiles display different characteristics. We have shown that comparison of these profiles with fuel blending measurements has the potential to differentiate between the two types of oxidation slowing species. The modeling predicts that the presence of both types of species in a fuel results in a synergistic slowing in the oxidation rate.

References

(1) Hazlett, R. N. *Thermal Oxidation Stability of Aviation Turbine Fuels*; ASTM: Philadelphia, 1991.
(2) Heneghan, S. P.; Zabarnick, S.; Ballal, D. R.; Harrison, W. E. *J. Energy Res. Tech.* **1996**, *118*, 170-179.
(3) Edwards, T. *Prepr.-Am. Chem. Soc., Div Pet. Chem.* **1996**, *41*, 481-487.
(4) Zabarnick, S. *Ind. Eng. Chem. Res.* **1993**, *32*, 1012-1017.
(5) Jones, E. G.; Balster, L. M.; Balster, W. J. *Energ. Fuels.* **1996**, *10*, 509-515.
(6) Zabarnick, S.; Whitacre, S. D. "Aspects of Jet Fuel Oxidation," ASME 97-GT-219, 1997.
(7) Zabarnick, S.; Zelesnik, P.; Grinstead, R. R. *J. Eng. Gas Turbines Power.* **1996**, *118*, 271-277.
(8) Balster, L. J.; Balster, W. J.; Jones, E. G. *Ind. Eng. Chem. Res.* **1996**, *10*, 1176-1180.
(9) Zabarnick, S. *Ind. Eng. Chem. Res.* **1994**, *33*, 1348-1354.
(10) Zabarnick, S.; Grinstead, R. R. *Ind. Eng. Chem. Res.* **1994**, *33*, 2771-2777.
(11) Striebich, R. **1996**, unpublished results.
(12) Whitbeck, M. *Tetrahedron Comput. Methodol.* **1990**, *3*, 497-505.
(13) Zabarnick, S. *Energ. Fuels.* **1997**, submitted.
(14) Downing, F. B.; Clark, R. G.; Pedersen, C. J. *Oil & Gas J.* **1939**, *38*, 97-101.
(15) Clark, R. H., Presented at the 3rd International Conference on the Stability and Handling of Liquid Fuels, London, 1988.
(16) Clark, R. H.; Delargy, K. M.; Heins, R. J. *Prepr.-Am. Chem. Soc., Div. Fuel Chem.* **1990**, *35*, 1223-1230.
(17) Holdsworth, J. D.; Scott, G.; Williams, D. *J. Chem. Soc.* **1964**, 4692-4699.
(18) Denison, G. H.; Condit, P. C. *Ind. Eng. Chem.* **1945**, *37*, 1102-1108.
(19) Scott, G. *Chem. and Ind.* **1963**, 271-281.

Table 1
Reaction Mechanism for Chemical Kinetic Modeling

Reaction	Arrhenius A-Factor (moles, liters, and secs units)	Activation Energy (kcal/mole)	Reaction Number
$I \Rightarrow R\cdot$	1×10^{-3}	0.0	(1)
$R\cdot + O_2 \Rightarrow RO_2\cdot$	3×10^{9}	0.0	(2)
$RO_2\cdot + RH \Rightarrow RO_2H + R\cdot$	3×10^{9}	12.0	(3)
$RO_2\cdot + RO_2\cdot \Rightarrow$ termination	3×10^{9}	0.0	(4)
$RO_2\cdot + AH \Rightarrow RO_2H + A\cdot$	3×10^{9}	5.0	(5)
$AO_2\cdot + RH \Rightarrow AO_2H + R\cdot$	3×10^{5}	10.0	(6)
$A\cdot + O_2 \Rightarrow AO_2\cdot$	3×10^{9}	0.0	(7)
$AO_2\cdot + AH \Rightarrow AO_2H + A\cdot$	3×10^{9}	6.0	(8)
$AO_2\cdot + AO_2\cdot \Rightarrow$ products	3×10^{9}	0.0	(9)
$R\cdot + R\cdot \Rightarrow R_2$	3×10^{9}	0.0	(10)
$RO_2H \Rightarrow RO\cdot + \cdot OH$	1×10^{15}	42.0	(11)
$RO\cdot + RH \Rightarrow ROH + R\cdot$	3×10^{9}	10.0	(12)
$RO\cdot \Rightarrow R_{prime}\cdot$ + carbonyl	1×10^{16}	15.0	(13)
$\cdot OH + RH \Rightarrow H_2O + R\cdot$	3×10^{9}	10.0	(14)
$RO\cdot + RO\cdot \Rightarrow RO\cdot$ termination	3×10^{9}	0.0	(15)
$R_{prime}\cdot + RH \Rightarrow$ alkane $+ R\cdot$	3×10^{9}	10.0	(16)
$RO_2H + SH \Rightarrow$ products	3×10^{9}	0.0	(17)

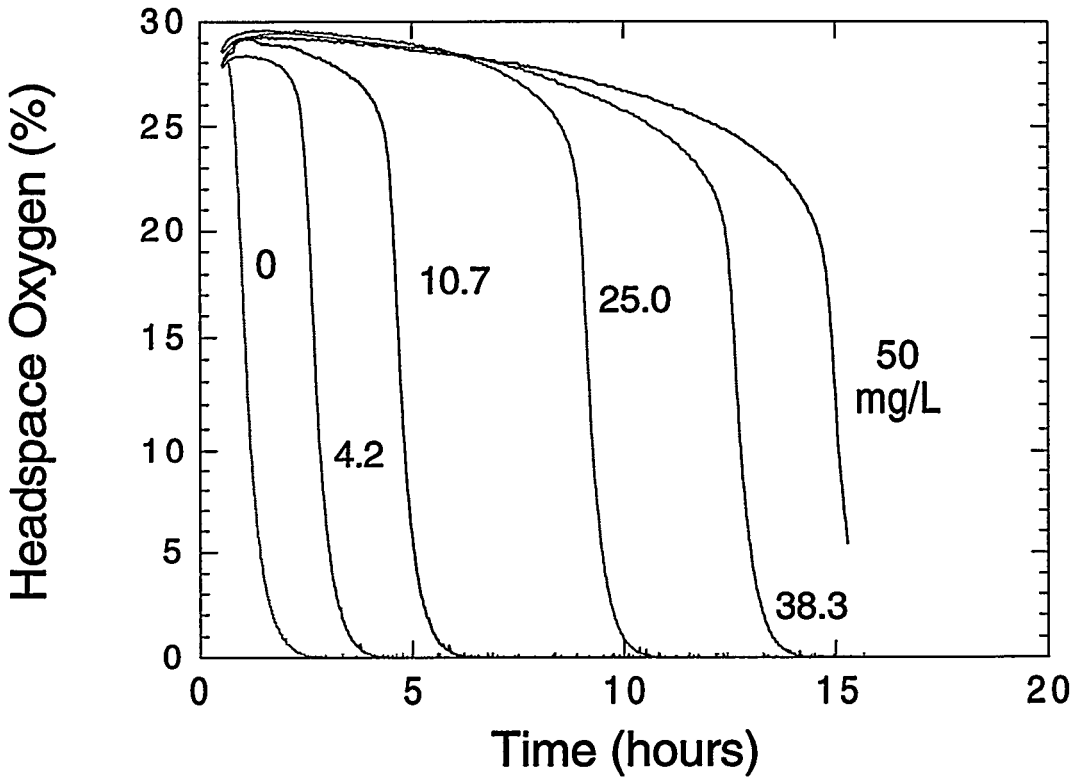

Figure 1. Plots of headspace oxygen concentrations versus time for Exxsol D-110 at various concentrations of added BHT at 140°C.

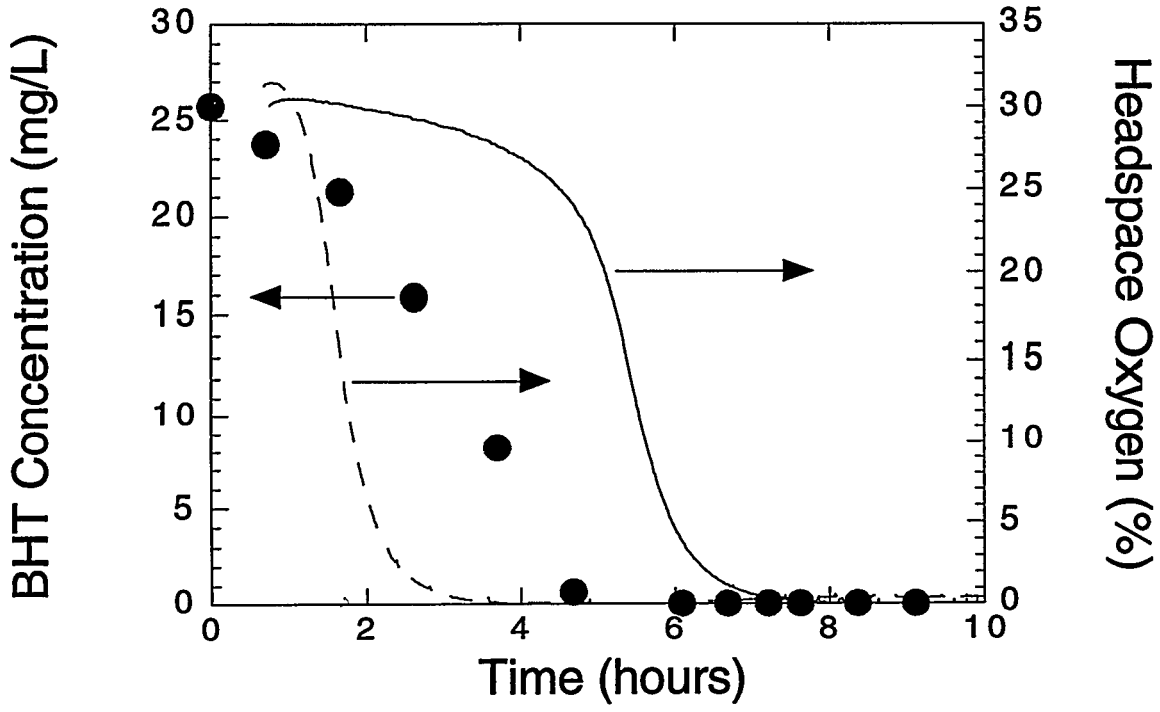

Figure 2. Plots of BHT (●) and headspace oxygen concentrations versus time for fuel F-3139 neat (dotted line) and with 25 mg/L BHT (solid line) at 140°C.

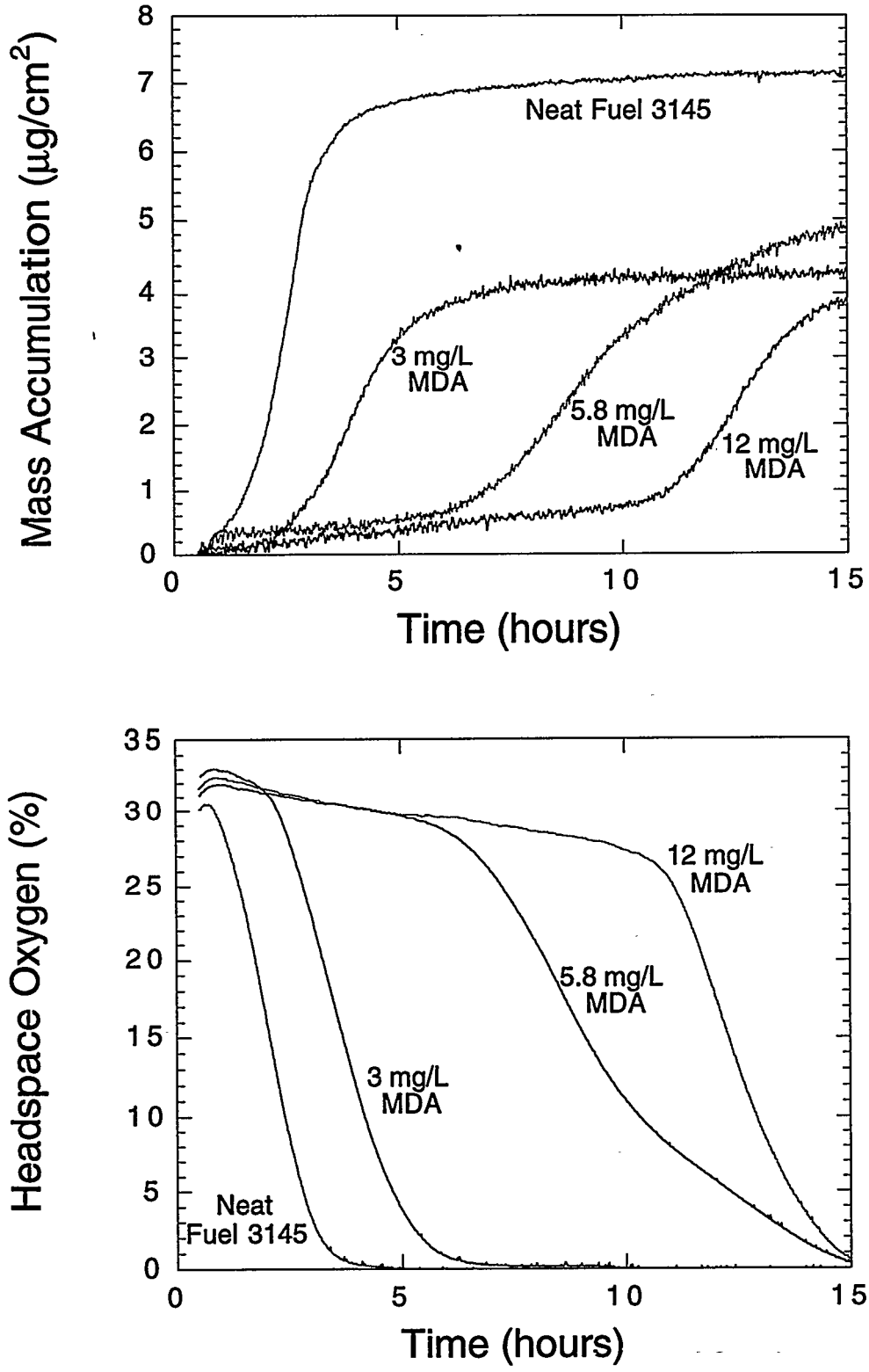

Figure 3. Plots of mass accumulation (a, top) and percent oxygen (b, bottom) for fuel F-3145 at various concentrations of added MDA at 140°C.

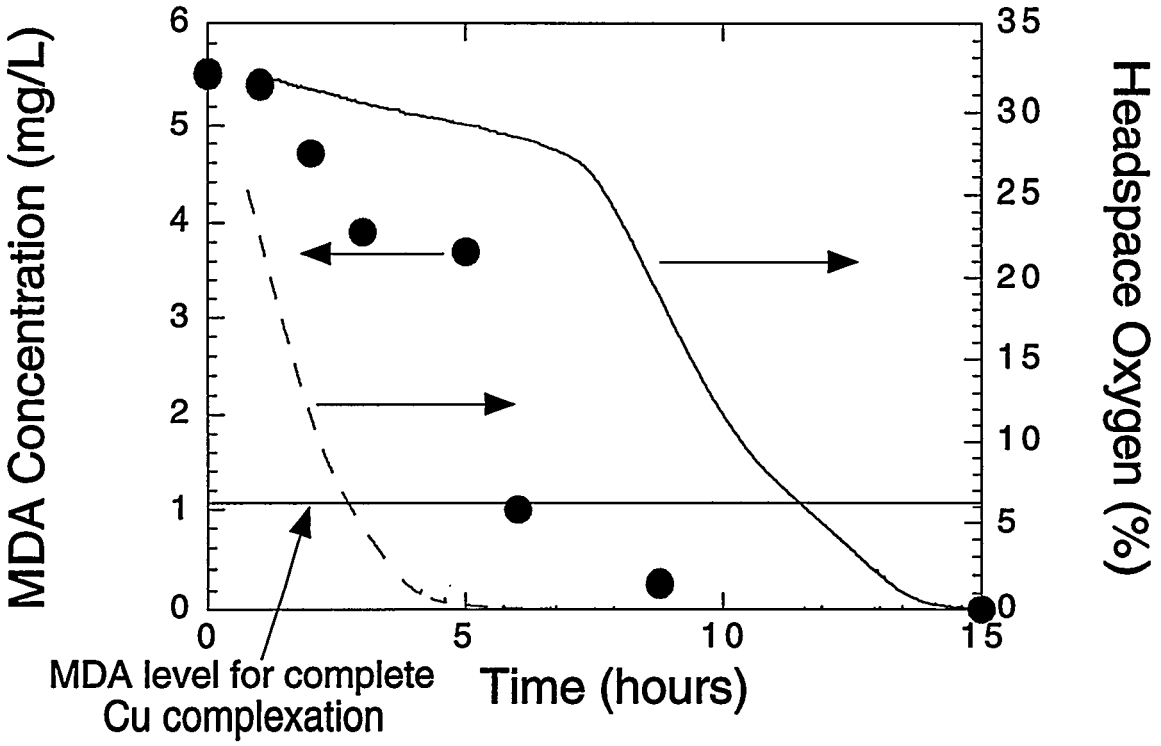

Figure 4. Plots of MDA (●) and headspace oxygen (line) concentrations versus time for fuel F-3145 with 5.8 mg/L MDA at 140°C.

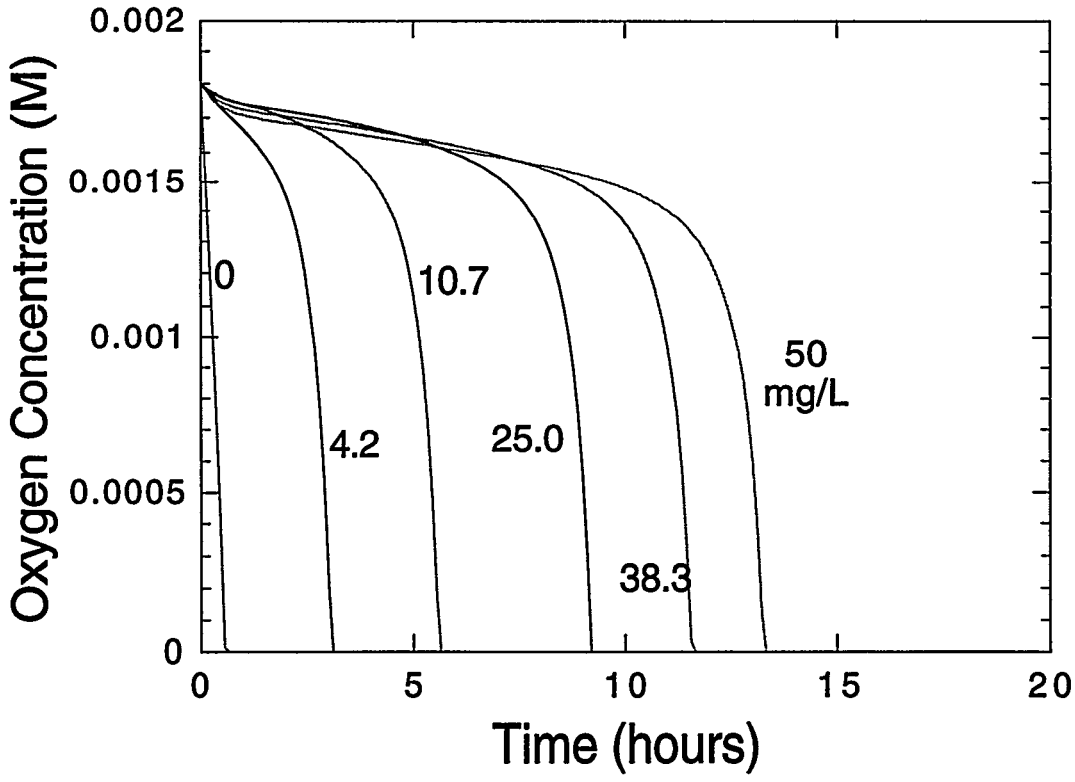

Figure 5. Plots of calculated oxygen concentration versus time at various concentrations of added antioxidant BHT at 140°C.

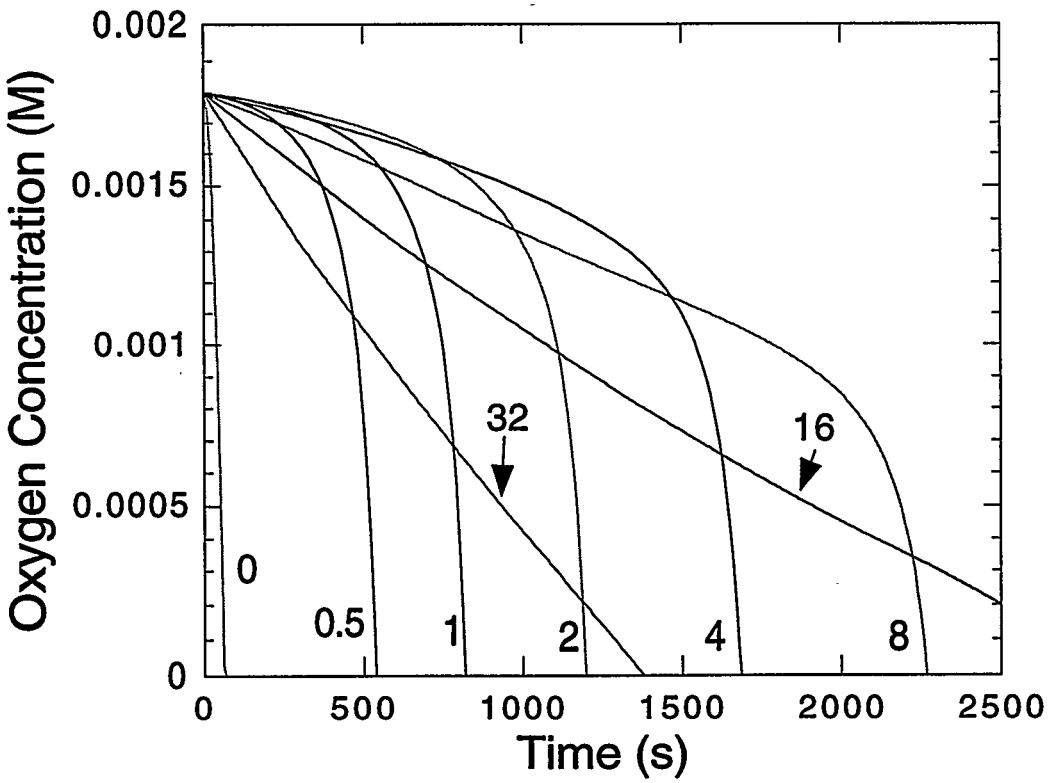

Figure 6. Plots of calculated oxygen concentration versus time for various concentrations of added antioxidant AH (x 10^{-4} M) at 185°C.

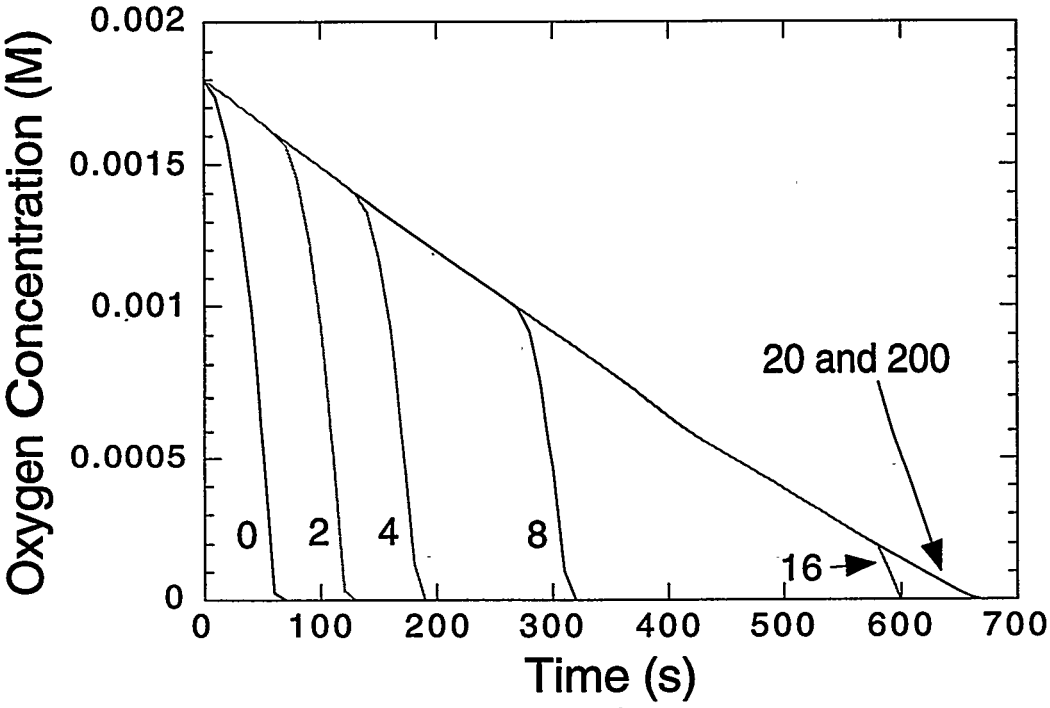

Figure 7. Plots of calculated oxygen concentration versus time for various concentrations of hydroperoxide decomposer, SH (x 10^{-4}) at 185°C.

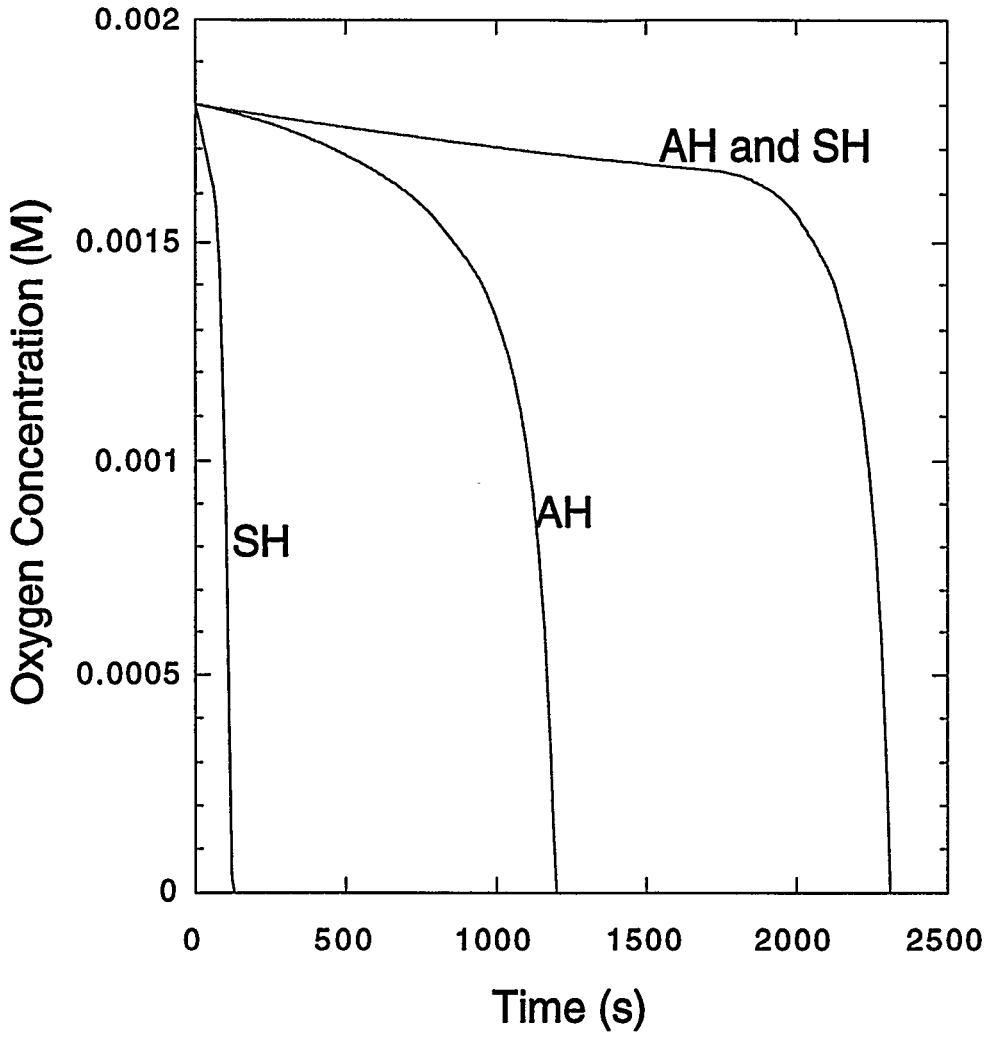

Figure 8. Plots of oxygen concentration versus time at 185°C for AH and SH both at 1×10^{-4} M and each compound individually at 2×10^{-4} M.

6th International Conference
on Stability and Handling of Liquid Fuels
Vancouver, B.C., Canada
October 13-17, 1997

NUMERICAL SIMULATIONS OF JET FUEL OXIDATION AND FLUID DYNAMICS

J.S. Ervin* and S. Zabarnick
University of Dayton Research Institute, Dayton, OH 45469-0210

A pseudo-detailed kinetics model which considers antioxidant chemistry was employed in a computational fluid dynamics code, and concentration profiles of various species along a stainless-steel tube were calculated for both nearly isothermal and non-isothermal flowing systems. Flowing experiments were performed with both a severely hydrotreated fuel and a straight-run fuel, and the predicted dissolved oxygen and hydroperoxide profiles agreed well with the measured profiles over a range of bulk fuel temperatures and flow conditions. Favorable comparison was also found between model predictions and measurements taken from the literature. The model was found to be capable of simulating a synergistic reduction in the oxidation rate that is sometimes observed among different fuel antioxidants. The present model offers an improved understanding of jet fuel oxidation, antioxidant chemistry, and the involved fluid dynamics.

Introduction

Jet fuel is circulated in military aircraft as a coolant. In the presence of heat and dissolved O_2, jet fuel degrades through a complex sequence of chemical reactions forming oxidized products and fouling surfaces. Fouling can disrupt normal fuel flow within fuel system components and may potentially lead to catastrophic failure.[1] Since the reactions in which dissolved O_2 is consumed comprise a portion of the fouling process, an understanding of dissolved O_2 removal is imperative for aircraft design.

Computational simulations which use the mass, momentum, energy, and species conservation equations along with an appropriate chemical kinetics model can be used to predict O_2 consumption for different flow conditions. However, jet fuels are mixtures of numerous compounds and, thus, it is impractical to model the chemical changes of all components. To add to the complexity of numerically simulating O_2 removal, military jet fuels come from many different geographical sources and their compositions change while in storage. Since fuel oxidation is complex, global-chemistry kinetics have been used in previous computational

simulations.[2,3,4,5] The global mechanisms used in computational fluid dynamics simulations generally employ one reaction to represent fuel autoxidation:

$$\text{Fuel} + O_2 \rightarrow \text{Products} \quad (1)$$

The underlying assumption of equation 1 is that the overall reaction of a mixture of compounds can be represented by a single rate equation that is comprised of a rate constant multiplied by concentrations with simple order dependence.[6] It is further assumed that the rate constant is defined by the product of an Arrhenius A-factor and an activation energy term.

The approach taken here is to model the oxidation of hydrocarbon fuels by means of pseudo-detailed chemical kinetic modeling. The model is pseudo-detailed in the sense that the chemical kinetics of O_2 consumption are described using several reactions which represent the dominant chemistry rather than using hundreds of reactions as might be found in a detailed model or a single oxidation reaction as found in previous studies. The current work employs the first computational fluid dynamics code which uses pseudo-detailed kinetic modeling of dissolved O_2 consumption and antioxidant chemistry in jet fuel. The numerical model permits the study of the effects of naturally occurring antioxidants and antioxidant additives. It is highly desirable to have the capability to predict the effects of additives on fuels because experiments involving the additive testing of fuels are costly.

Two groups of antioxidants are considered. The first, denoted by AH, represents hindered phenols which slow oxidation by removing alkyl peroxy free radicals from the autoxidation chain.[7,1] Hydroperoxide decomposers, represented by SH, comprise the second group. SH is thought to be some sulfur (or other) species which provide alkyl hydroperoxide (ROOH) decomposition pathways as an alternative to unimolecular ROOH decomposition reactions.[7,8,9] The objective of this paper is to study jet fuel oxidation and the behavior of these two groups of antioxidants in flowing systems using computational fluid dynamics and pseudo-detailed chemical kinetic modeling.

Experimental

For model verification, experiments were conducted using a heat exchanger which simulated a complex thermal and flow environment approaching that of an aircraft. Profiles of dissolved O_2 and ROOH concentrations along the tube length for both a rapidly-oxidizing

hydrotreated fuel and a slowly-oxidizing straight-run fuel were compared to numerical predictions which used a pseudo-detailed kinetic model. Table 1 lists characteristics of neat F2827 and F2747 jet fuels used in the experiments. F2827 produces relatively low hydroperoxide concentrations and oxidizes relatively slowly when heated in the presence of dissolved O_2. On the other hand F2747, which has very low sulfur and naturally occurring antioxidant components and produces relatively high concentrations of ROOH, oxidizes relatively rapidly when oxidatively stressed. Based on the measurements of Striebich and Rubey,[10] the dissolved O_2 concentration (air saturated value) at the flow rig inlet was 65 ppm (w/w) for F2827 and 73 ppm for F2747.

Fuel at ambient temperature enters the heated tube[11] at a pressure of 2.48 MPa. At this pressure level, the fuel remains as a liquid everywhere within the system. Bulk dissolved O_2 levels were measured on-line at the flow inlet and exit by means of a modified gas chromatograph.[12] The ROOH concentrations of the aged fuel were measured by cyclic voltammetry techniques.[13]

A heated copper block envelopes the 316 stainless-steel tubing (45.8-cm long by 2.16-mm ID by 3.18-mm OD) through which the fuel passes. Calibrated thermocouples (20 gage) are welded to the outer surface of the stainless-steel tubing to provide the outer tube wall temperatures with an uncertainty of ± 2 °C. The bulk fuel temperature at the exit of the heated tube was also measured, and the uncertainty in its measurement was $\pm$ 10 °C. The stainless-steel tubes (ASTM grade A269/A213) have a surface roughness (arithmetic average) of 8 to 15 micro inches and are cleaned with Blue Gold alkaline solution in an ultrasonic bath, rinsed with deionized water, and dried with flowing laboratory-grade nitrogen gas prior to use.

The tests conducted in the present apparatus are usually conducted under conditions of relatively high flow rates and temperatures. In the present work, with a volumetric flow rate of 16 ml/min, the flow was laminar at the entrance of the heated block but became turbulent. Buoyancy forces normal to the flow direction increased the heat and mass transport, rendering the flow turbulent.[4] The study of turbulent flow is important because it is normally encountered in the fuel systems of military aircraft.

Fluid dynamics and heat transfer strongly influence jet fuel oxidation, but the nature of this influence is not well understood.[1] For this reason, numerical simulations of dissolved O_2

consumption were performed for the present flow conditions as well as for the flow conditions reported by Jones et al.[8,14] in a near-isothermal flowing test rig (NIFTR). In contrast to the conditions of our apparatus, the NIFTR experiments are conducted at lower temperatures and flow rates in order to attain near-isothermal conditions in a minimum length of tube. In both experiments, the temperature of the copper block used to heat the tube and the flow rate are varied to produce different oxidation rates and residence times, respectively. Figure 1 shows calculated bulk fuel temperature and measured tube wall temperature profiles along the heated tube length for both the present experiments and the NIFTR experiments. The NIFTR experiments use a 81.3 cm-long heated tube, whereas the current experiments use a 45.8 cm-long heated tube. The maximum wall temperature for both experiments of Figure 1 is near 200 °C. Figure 1 shows that for a flow rate of 16 ml/min and a maximum tube wall temperature near 200°C, the calculated bulk fuel temperature increases along the entire heated tube length, never reaching the wall temperature. Although not shown, similar experiments performed at greater wall temperatures were characterized by bulk temperature profiles which also never attained the wall temperature. In contrast in the NIFTR for a flow rate of 0.125 ml/min, the fuel temperature reaches the tube wall temperature near the flow entrance.

Numerical Simulations

Pseudo-detailed chemical kinetic modeling was performed using the mechanism of Table 2 which is based on the mechanism of Zabarnick.[7] It is extremely difficult, if not impossible, to model the multitude of compounds present in jet fuel. Thus, the fuel is represented by the single compound RH. The initiation step (reaction 1 of Table 2) is assumed to occur by unimolecular decomposition of an initiating species, I. Reaction 1 is a simple representation of complex process that initiates the autoxidation chain with a low production rate of $R^{\bullet}$ radicals.[7,15] Reactions 1 through 4 and reaction 10 represent a simple chain mechanism for the oxidation of a hydrocarbon fuel. Reactions 5 through 9 represent the antioxidant chemistry associated with AH, which is a species with an easily abstracted H atom. Reactions 11 through 16 are associated with ROOH decomposition which occurs at sufficiently high temperatures and is believed to play an important role in accelerated O_2 consumption.[9,15] Reaction 17 is used to model the effects of hydroperoxide-decomposing species (SH). Zabarnick[7,15] estimated the rate parameters

(Arrhenius "A-factors" and activation energies) for the pseudo-elementary reactions largely by comparison with measured rate constants and Benson style "thermochemical kinetics" analysis.[16]

With the exception of three rate parameters, those listed in Table 2 are taken from Zabarnick[7] where a similar mechanism was used to study the antioxidant chemistry of hydrocarbon fuels in a non-flowing isothermal system. In the present study, the pre-exponential factor for the initiation reaction (Reaction 1) is 1×10^{-10}, whereas in Zabarnick[7] this pre-exponential factor is given as 1×10^{-3}. A smaller pre-exponential factor is used here such that the production rate of $R^{\bullet}$ becomes negligible once the chain begins. In the current work, the activation energies of reactions 11 and 17 are different from those originally given in Zabarnick.[7] For reaction 11, Zabarnick[7] used an activation energy of 42 kcal/mole, which is a representative value for a homogeneous ROOH decomposition reaction. However, metals have long been suspected of being involved in catalytic decomposition of hydroperoxides.[1,8,9] Thus, in the presence of a metal surface and/or dissolved metals, it is reasonable for the activation energy for the ROOH decomposition reaction to be less than 42 kcal/mole. In the present work, the activation energy for reaction 11 was taken as 37 kcal/mole. This value provided predictions of O_2 consumption which agreed well with flowing experiments which used fuel F2747 over a large temperature range. Fuel F2747 has very low concentrations of AH and SH and is nearly a pure solvent. Thus, Fuel F2747 was chosen for the "calibration" of the activation energy corresponding to reaction 11 because it is desirable to make the "calibrated" activation energy independent of the AH and SH concentrations. The activation energy for reaction 17 was chosen to be zero in Zabarnick.[7] In the present work, the activation energy for reaction 17 is selected to be 16 kcal/mole. It was observed here that an activation energy less than 16 kcal/mole removed ROOH too rapidly at lower temperatures for various concentrations of AH and SH. As a result, for activation energies less than 16 kcal/mole, the predicted dissolved O_2 concentration was nearly always greater than the measured concentration at the exit of the heated tube for the straight-run fuel (F2827). In the modeling performed here, it is assumed for simplicity that all fuels have the same initiating species concentration (I) of 4×10^{-8} moles/liter. With the activation energies and pre-exponential factors of Table 2, it is then possible to define different fuels in terms of their initial AH and SH concentrations.

The species concentrations were found numerically by a finite difference solution[4,18] of the coupled equations that arise from the mechanism of Table 2 and the transport equations. The following were input to the numerical code: the activation energies and pre-exponential factors of Table 2, concentrations (O_2, AH, RH, SH, and I) for each species at the entrance of the heated tube, tube wall temperature profile, and the grid resolution. Individual jet fuel samples are known to possess a range of oxidation and deposition characteristics which results from varying source petroleum and refinery processing. To provide the range of oxidation properties that a fuel may possess, we have chosen to modify the antioxidant, AH, and hydroperoxide decomposer, SH, concentrations for individual fuel samples. In simulations of fuel oxidation, two kinds of computations were performed: those for a naturally inhibited system (F2827 fuel) and those for a relatively non-inhibited system (F2747 fuel). For the inhibited fuel, AH and SH concentrations were chosen to match experimentally determined oxidation rates and measured hydroperoxide concentrations. The initial AH concentration was assumed to be 1.62×10^{-3} moles/liter which is a reasonable value for jet fuels,[7] and the initial SH concentration was assumed to be 1.21×10^{-3} moles/liter. For the completely uninhibited case, both the AH and SH concentrations were set equal to 0 moles/liter. For both the severely hydrotreated fuel (F2747) and the straight-run fuel (F2827), an identical initial I concentration was used for simplicity. The normal air saturation concentration was used for the initial O_2 concentration. Table 3 summarizes the initial O_2, AH, SH, and I concentrations used in the simulations. Ultimately, this model will be most useful if an analytical chemistry test could be used to determine an "effective" AH and SH concentration for individual jet fuel samples. Thus, a measure of the "effective" AH and SH concentration could be measured in the laboratory and entered into the model to provide a method to predict the oxidation properties of the fuel over a range of temperature, residence times, and flow properties.

Results and Discussion

Simulations of Flowing Fuel F2747. Figure 2 shows measured and predicted fractions of remaining dissolved O_2 at the exit of the heated tube for F2747 fuel (zero AH and SH concentrations) flowing at 16 ml/min for different bulk temperatures. Figure 2 shows that as the temperature approaches 170 °C, the dissolved O_2 concentration decreases rapidly until near 210

°C where the O_2 is nearly depleted. This rapid increase in oxidation rate with increasing temperature has been observed previously[17] for similar flow conditions and different fuel types.

The rate of ROOH decomposition has been shown to be important in understanding jet fuel oxidation.[1,9,15] Figure 3 shows measured and predicted ROOH concentrations at the heated tube exit for F2747 fuel for the same range of bulk temperatures described in Figure 2. Figure 3 shows a maximum in both the predicted and measured hydroperoxide concentrations at 210 °C, which is near the temperature associated with the dissolved O_2 depletion of Figure 2. In addition, the ROOH concentration of Figure 3 increases to levels near the initial dissolved O_2 concentration. This means that the initial dissolved O_2 concentration reacts nearly entirely to form ROOH. After the dissolved O_2 is fully consumed and as the bulk temperature continues to rise, ROOH decomposition by unimolecular reaction (Reaction (11) of Table 2) becomes increasingly significant. Figure 3 shows a relatively large maximum concentration of ROOH for fuel F2747 in contrast to the ROOH concentration produced with fuel F2827 (described later) for otherwise identical conditions. This was expected as the hydrotreating process removes heteroatomic species which may decompose hydroperoxides.

Simulations of Flowing Fuel F2827. Figure 4 shows predicted and measured dissolved O_2 fractions at the exit of a heated tube for fuel F2827 flowing at 0.125 ml/min (laminar flow) and for different constant wall temperatures. The experimental measurements[8,14] are for fuel F2827 passing through stainless-steel tubes. At a constant mass flow rate, any position along the tube may be directly related to the reaction time through the average velocity which, in turn, can be found from the known inner tube diameter, mass flow rate, and fuel density. Thus, Figure 4 shows the dissolved O_2 fraction as a function of residence time. Figure 4 shows that as the tube wall temperature is increased, the reaction time required for complete O_2 depletion decreases. The initial AH and SH concentrations were adjusted to give an O_2 consumption history which followed the O_2 measurements at 185 °C. Oxygen consumption histories of F2827 at the other temperatures and in our experiments were then predicted reasonably well using these initial concentrations of AH and SH.

In contrast to the constant wall temperatures associated with Figure 4, the imposed wall temperatures vary along the tube length for the present experiments (fuel F2827 flowing at 16 ml/min). The bulk fuel temperature (275 °C) at which the O_2 is fully consumed is greater than

that observed with fuel F2747 (210 °C) for similar flow conditions. This depletion of O_2 at the greater temperature for F2827 might be expected because F2827, unlike F2747, contains relatively large concentrations of AH and SH. After heating of the fuel, the ROOH concentrations measured for F2827 were much smaller than those produced with F2747. Calculated ROOH concentrations at the exit of the heated tube lie in a range between 0 mole/liter and 0.0004 mole/liter and agree reasonably with measured values.

Figure 5 shows the simulated consumption of dissolved O_2, AH, and SH together with the ROOH concentration for turbulent, non-isothermal flowing F2827 fuel at 300 °C maximum wall temperature. The O_2, AH, and SH concentrations drop slowly until near 0.28 m, where there is increased O_2 consumption. As a result of increased fuel oxidation, the ROOH concentration begins to rise. Consequently, the rate of disappearance of SH increases due to the increase in the ROOH concentration. In addition at 0.28 m, the fuel temperature (251 °C) is relatively high which means that reaction 17, based on its activation energy, will proceed more readily than at lower temperatures. Beyond 0.28 m, the ROOH concentration profile rises rapidly to a maximum at a location of 0.33 m, which coincides with the location of O_2 depletion. There, $RO_2^{\bullet}$ is no longer produced by means of reaction 2. Later in the tube as the $RO_2^{\bullet}$ concentration decreases to zero (reactions 3 and 5), the AH concentration profile becomes flat because AH is no longer consumed (reaction 5). The ROOH concentration profile decays by both the unimolecular decomposition reaction (reaction 11) and the ROOH-SH decomposition reaction (reaction 17) beyond the location of 0.33 m. For the initial conditions of Figure 5, the acceleration in O_2 consumption is controlled by ROOH decomposition rather than by depletion of the antioxidants. Although occurring later in the tube, similar behavior in consumption profiles for O_2, AH, and SH was observed at lower wall temperatures of 270 °C and 265 °C.

Temperature Effects. Using a flow rate of 16 ml/min and the heated copper block of the present experiments, the fuel temperature continuously rises along the tube. Thus, the interpretation of AH and SH concentration changes is complicated by the fact that the increasing temperature decreases the fuel density and increases the rates of reactions with high activation energies. Thus, to further explore the antioxidant chemistry associated with F2827 fuel, the more simple conditions of isothermal walls and laminar flow are used. Figures 6 and 7 show simulations of the consumption of dissolved O_2, AH, and SH together with the depletion of

ROOH for F2827 fuel flowing at a rate of 0.125 ml/min and an imposed constant tube wall temperature. For reference, O_2 removal profiles are also shown for the situation where there are no initial antioxidants present in the fuel. At 175 °C (Figure 6), the O_2 and SH profiles are parallel over much of the tube length, until the O_2 is depleted. At this location, the AH is no longer consumed, and the AH profile is horizontal. As the ROOH concentration approaches 0.0001 moles/liter, SH is consumed at an accelerated rate by means of reaction 17 until the ROOH concentration is sufficiently decreased by both reactions 11 (unimolecular ROOH decomposition reaction) and 17 (SH-ROOH decomposition reaction). Once the available ROOH is consumed, Figure 6 shows that there is negligible consumption of SH. Figure 7 shows that with a wall temperature of 205 °C, the AH and O_2 profiles appear less linear than those observed at 175 °C. Again, as with the wall temperature of 175 °C of Figure 6, Figure 7 shows an increased rate of consumption of SH as the ROOH concentration approaches 0.0001 moles/liter. As the tube wall temperature is increased from 175 °C to 205 °C, the location of dissolved O_2 depletion moves in the upstream direction.

Simulations of Flowing Fuel in Which the Concentration of AH or SH Is Individually Varied. As the proposed mechanism of Table 2 has been shown capable of predicting measurements of dissolved O_2 consumption for real fuels under conditions of laminar and turbulent flow over a wide temperature range, it is reasonable to use the mechanism to explore the effects of varying the initial concentration of one antioxidant while the initial concentration of the other is zero. For these simulations, it was decided to use the well-defined conditions of laminar flow with the tube walls held at constant temperature. Two tube wall temperatures (185 °C and 205 °C) and a flow rate of 0.125 ml/min were chosen.

For a constant wall temperature of 185 °C (not shown), O_2 concentration profiles were calculated for different initial concentrations of AH and zero SH. In the initial portion of the heated tube (upstream of 0.0025 m), the O_2 concentration decreases because of changes in fuel density associated with heating. As the AH concentration at the entrance of the tube is varied from 0 moles/liter to 16.2×10^{-4} moles/liter, the location of dissolved O_2 depletion moves downstream. This downstream shift in the location of complete O_2 removal with increasing AH concentration demonstrates that the predicted oxidation rate decreases significantly with increasing AH. For the same initial AH concentrations but at a higher wall temperature of 205

°C (Figure 8), the locations of complete O_2 removal are upstream from those calculated using a wall temperature of 185 °C. As the temperature is increased, the rates of reactions which have non-zero activation energies tend to increase. Reactions (reactions 3, 6, 11, 12, 13, 14, and 16) which either directly or indirectly produce R• and propagate the oxidation chain have greater rates at 205 °C. Thus relative to 185 °C, there is increased oxidation prior to O_2 depletion at 205 °C.

Figure 9 shows O_2 consumption along the heated tube length for a wall temperature of 205 °C. Here the initial SH is varied between concentrations of either 0 or 16.2 x 10^{-4} moles/liter in the absence of AH. As the initial SH concentration is increased above zero, the location of complete O_2 removal moves slightly further from the tube entrance. The profiles of dissolved oxygen removal corresponding to the nonzero inlet SH concentrations (0.81 x 10^{-4}, 8.1 x 10^{-4}, and 16.2 x 10^{-4} moles/liter) essentially overlay each other. At a tube wall temperature of 185 °C (not shown), the dissolved oxygen profiles again nearly lie on each other, but the individual curves are less distinguishable near the tube inlet than those observed for an imposed wall temperature of 205 °C. For the same flow and temperature conditions, a comparison of Figures 8 and 9 reveals that SH is significantly less effective in delaying dissolved O_2 depletion for identical initial concentrations of SH and AH. Similarly at a lower tube wall temperature of 185°C (not shown) and with the same initial concentrations of SH and AH, AH is substantially more effective in delaying dissolved O_2 removal.

Synergistic Effects. Although the pseudo-detailed model presented here is an oversimplification of the complex chemistry that occurs during the oxidation of fuels, the model has been shown to correctly predict measured O_2 consumption and ROOH production and, as a consequence, may be used to further study the simultaneous presence of both AH and SH antioxidants. To this end, autoxidation under conditions of a constant wall temperature of either 185 or 205 °C and a flow rate of 0.125 ml/min has been modeled. Figure 10 shows that the presence of both AH and SH, each at a concentration of 8.1 x 10^{-4} moles/liter and at a wall temperature of 185 °C, is much more effective in delaying O_2 consumption than that occurring from the sum of the two effects of the antioxidants acting individually. The synergism between peroxy radical inhibiting antioxidants and peroxide-decomposing species shown in Figure 10 and

with a wall temperature of 205 °C (not shown) has been observed experimentally[9] and in an isothermal non-flowing model.[7]

Conclusions

A pseudo-detailed kinetics model has been incorporated into a computational fluid dynamics code to predict species concentrations for both non-isothermal and isothermal flows. With this pseudo-detailed model, experimental measurements such as hydroperoxide measurements in addition to dissolved oxygen measurements are used to characterize fuels over fairly wide temperature ranges. No assumption of a value for the over-all reaction order for oxygen consumption needs to be made with the current model. Since pseudo-detailed kinetic modeling relies on rate parameters which are more physically realistic than simpler global parameters, it is believed that pseudo-detailed kinetic modeling offers more promise to extend current simulation capabilities to include the effects of fuel additives. Experiments were conducted using a heat exchanger which simulated a complex thermal and flow environment. Oxygen consumption and the production of hydroperoxides were measured for a rapidly oxidizing hydrotreated jet fuel and for a slower oxidizing straight-run jet fuel. The predictions from the numerical simulations compared well with the experimental measurements.

Acknowledgments

This work was supported by the U.S. Air Force, Fuels and Lubrication Division, Aero Propulsion and Power Directorate, Wright Laboratory, WPAFB, under Contract Numbers F33615-92-C-2207 and F33615-97-C-2719 (Technical Monitor: C.W. Frayne). The authors would like to thank V.R. Katta of Innovative Scientific Solutions, Inc. for many helpful comments.

References

(1) Hazlett, R. N. *Thermal Oxidative Stability of Aviation Turbine Fuels*; ASTM: Philadelphia, 1991.

(2) Krazinski, J. L; Vanka, S. P.; Pearce, J. A.; Roquemore, W. M. *ASME Jour. Eng. Gas Turb. Power.* **1992**, *114*, 104-110.

(3) Chin, L. P.; Katta V. R.; Heneghan, S. P. *Am.Chem. Soc., Div. Pet. Chem. Preprints.* **1994**, *39*, 19-25.

(4) Katta, V.R.; Blust, J.; Williams, T.F.; Martel, C.R. *J. of Thermophysics and Heat Transfer.* **1995**, *9*, 159-168.
(5) Ervin, J.S.; Williams, T.F.; Katta, V.R. *Ind. Eng. Chem. Res.* **1996**, *35*, 4028-4032.
(6) Ervin, J.S.; Heneghan, S.P. International Gas Turbine Institute Turbo Expo: Orlando, Florida, 1997; Paper No. 97-GT-224.
(7) Zabarnick, S. Chemical Kinetic Modeling of Antioxidant Chemistry for Jet Fuel Applications, Submitted *Energy and Fuels.*
(8) Jones, E.G.; Balster, L.M.; Balster, W.J. *Energy and Fuels.* **1996**, *10*, 509-515.
(9) Scott, G. *Chem. and Ind.* **1963**, 271-281.
(10) Striebich, R.; Rubey, W. *Am.Chem. Soc., Div. Pet. Chem. Preprints.* 1994, *39*, 47-50.
(11) Heneghan, S.P.; Williams, T.F.; Martel, C.; Ballal, D.R. *ASME J. Eng. Gas Turb. and Power.* **1993**, *115*, 480-485.
(12) Rubey, W.A.; Striebich, R.C.; Tissandier, M.D.; Tirey, D.A.; Anderson, S.D. *J. Chromatogr. Sci.* **1995**, *33*, 433-437.
(13) Kauffman, R.E. *Am.Chem. Soc., Div. Pet. Chem. Preprints.* 1994, *39*, 42-46.
(14) Jones, E.G.; Balster, W.J.; Post, M.E. *ASME J. Eng. Gas Turb. and Power.* **1995**, *117*, 125-131.
(15) Zabarnick, S. *Ind. Eng. Chem. Res.* **1993**, *32*, 1012-1017.
(16) Benson, S.W. *Thermochemical Kinetics*; Wiley: New York, 1976.
(17) Heneghan, S.P.; Martel, C.M.; Williams, T.F.; and Ballal, D.R. *ASME J. Eng. Gas Turb. and Power.* **1995**, *117*, 120-124.
(18) Katta, V.R.; Jones, E.G.; Roquemore, W.M. 81st AGARD Symposium on Fuels and Combustion Technology for Advanced Aircraft Engines: Colliferro, Italy, May 1993; Paper No. PEP-19.

Table 1. Characteristics of F2747 and F2827 Jet Fuels

	F2747	F2827
fuel type	Jet A-1	Jet A
refinery treatment	hydrotreated	straight-run
total sulfur (%)	0.004	0.079
mercaptan sulfur (%)	0.000	0.001
aromatics (vol %)	19	19
JFTOT breakpoint (°C)	332	266
copper (ppb)	< 5	< 5
iron (ppb)		8
zinc (ppb)	18	<5

Table 2. Pseudo-Detailed Reaction Mechanism for Chemical Kinetic Modeling[7]

Reaction	Arrhenius A-factor (mol, L, and S)	Activation Energy (kcal/mol)	Reaction No.
$I \rightarrow R^{\bullet}$	1×10^{-10}	0	(1)
$R^{\bullet} + O_2 \rightarrow RO_2^{\bullet}$	3×10^{9}	0	(2)
$RO_2^{\bullet} + RH \rightarrow R\,O_2H + R^{\bullet}$	3×10^{9}	12	(3)
$RO_2^{\bullet} + RO_2^{\bullet} \rightarrow$ termination	3×10^{9}	0	(4)
$RO_2^{\bullet} + AH \rightarrow R\,O_2H + A^{\bullet}$	3×10^{9}	5	(5)
$AO_2^{\bullet} + RH \rightarrow AO_2H + R^{\bullet}$	3×10^{5}	10	(6)
$A^{\bullet} + O_2 \rightarrow AO_2^{\bullet}$	3×10^{9}	0	(7)
$AO_2^{\bullet} + AH \rightarrow A\,O_2H + A^{\bullet}$	3×10^{9}	6	(8)
$AO_2^{\bullet} + AO_2^{\bullet} \rightarrow$ products	3×10^{9}	0	(9)
$R^{\bullet} + R^{\bullet} \rightarrow R_2$	3×10^{9}	0	(10)
$RO_2H \rightarrow RO^{\bullet} + {}^{\bullet}OH$	1×10^{15}	37	(11)
$RO^{\bullet} + RH \rightarrow ROH + R^{\bullet}$	3×10^{9}	10	(12)
$RO^{\bullet} \rightarrow R_{prime}^{\bullet}$ + carbonyl	1×10^{16}	15	(13)
${}^{\bullet}OH + RH \rightarrow H_2O + R^{\bullet}$	3×10^{9}	10	(14)
$RO^{\bullet} + RO^{\bullet} \rightarrow$ termination	3×10^{9}	0	(15)
$R_{prime}^{\bullet} + RH \rightarrow$ alkane + $R^{\bullet}$	3×10^{9}	10	(16)
$RO_2H + SH \rightarrow$ products	3×10^{9}	16	(17)

Table 3. Initial Concentrations of Species

Species	Initial Concentration (moles/liter)
I	4.0×10^{-8}
RH	4.4
AH	Varied, 0-16.2 x 10^{-3}
SH	Varied, 0-16.2 x 10^{-3}
O_2	1.8×10^{-3}
remaining species	0

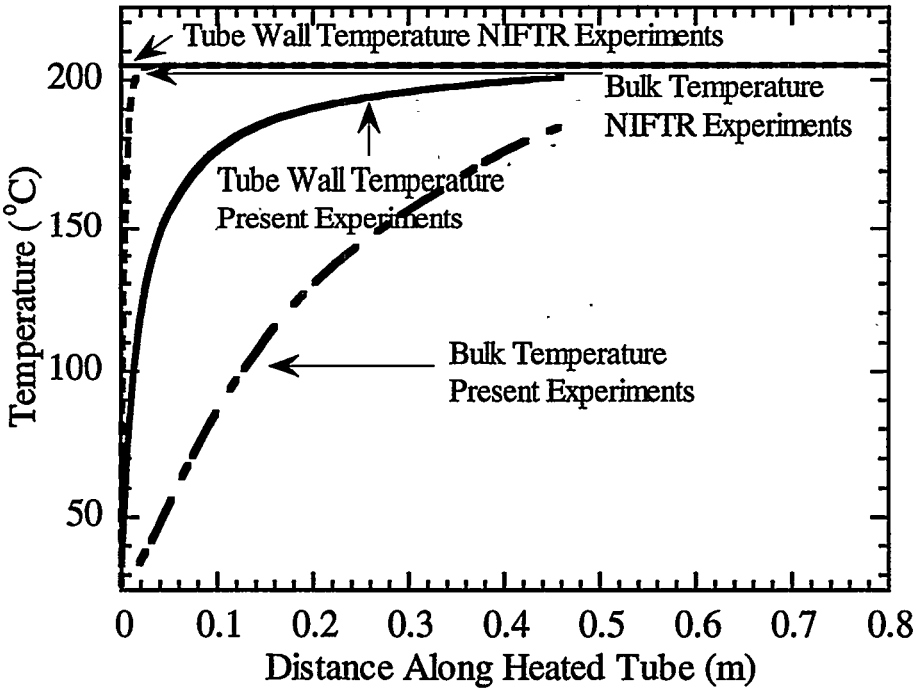

Figure 1. Bulk and tube wall temperature profiles along heated tube length. Present experiments (16 ml/min & 0.46 m length) & NIFTR experiments[14] (0.125 ml/min & 0.8 m length).

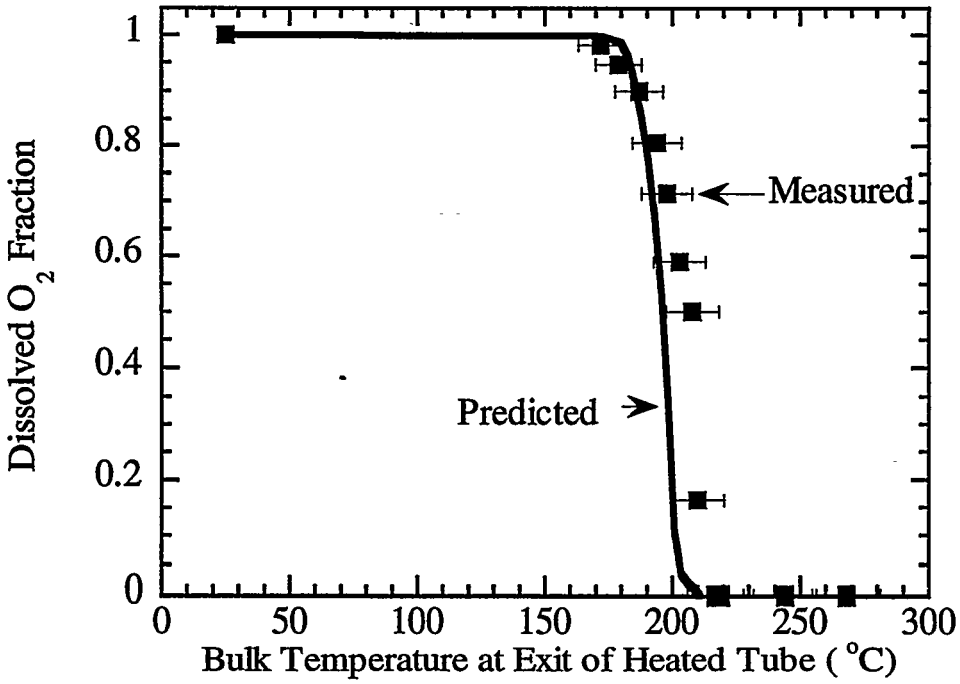

Figure 2. Dissolved O_2 concentration at tube exit. 16 ml/min & F2747 fuel.

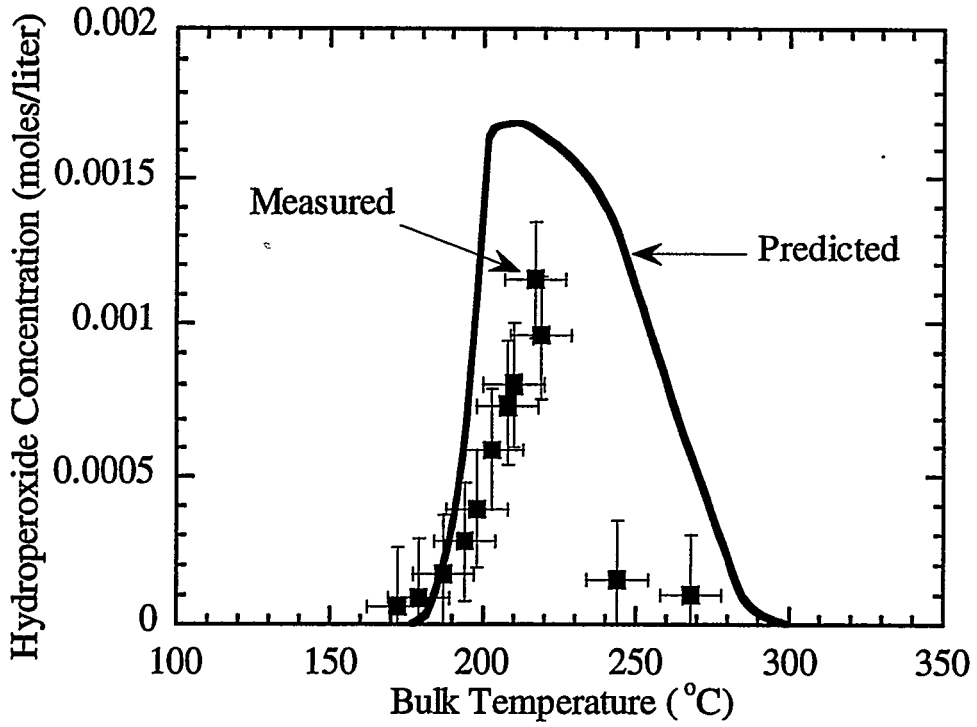

Figure 3. Hydroperoxide concentration at tube exit. 16 ml/min & F2747 fuel.

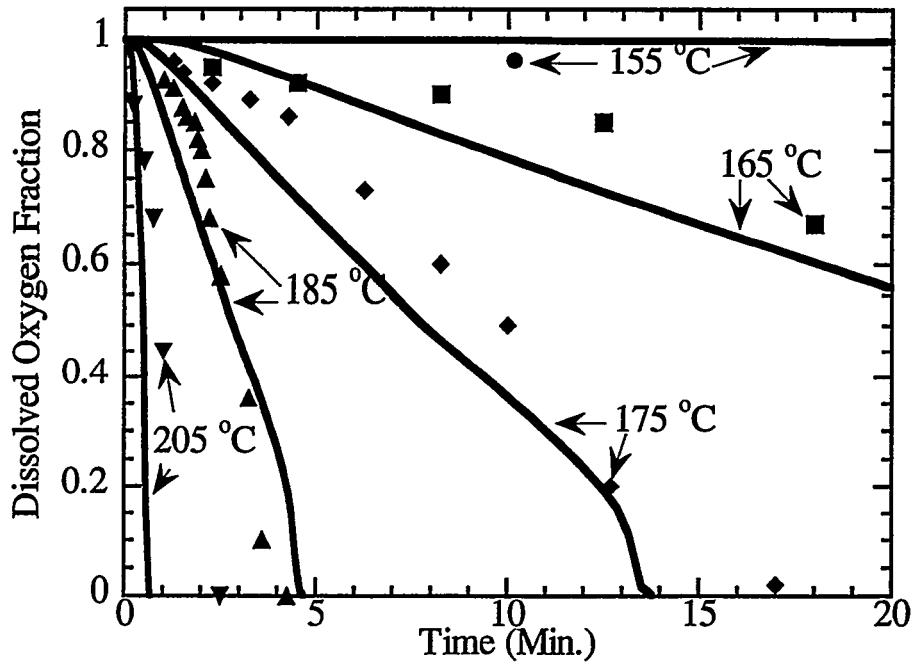

Figure 4. Predicted & measured[8,14] dissolved O_2 removal for nearly isothermal flow. 0.125 ml/min & F2827 fuel. Curves represent predictions.

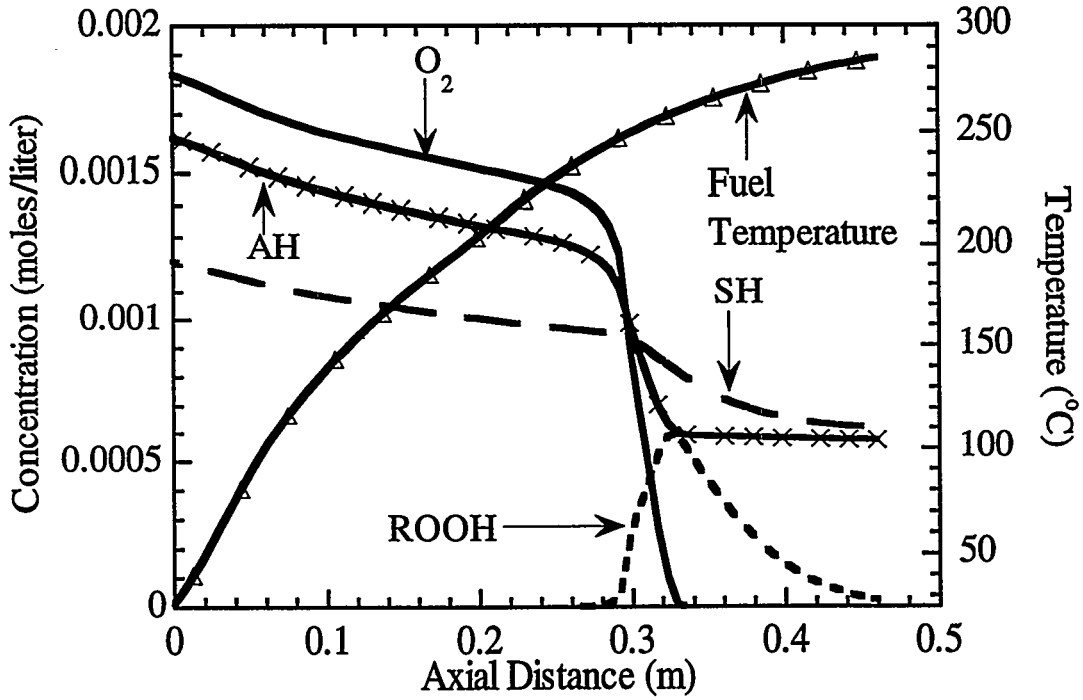

Figure 5. Calculated profiles of dissolved O_2, ROOH, AH, SH, & fuel temperature for F2827 fuel. 16 ml/min & 300 °C wall temperature.

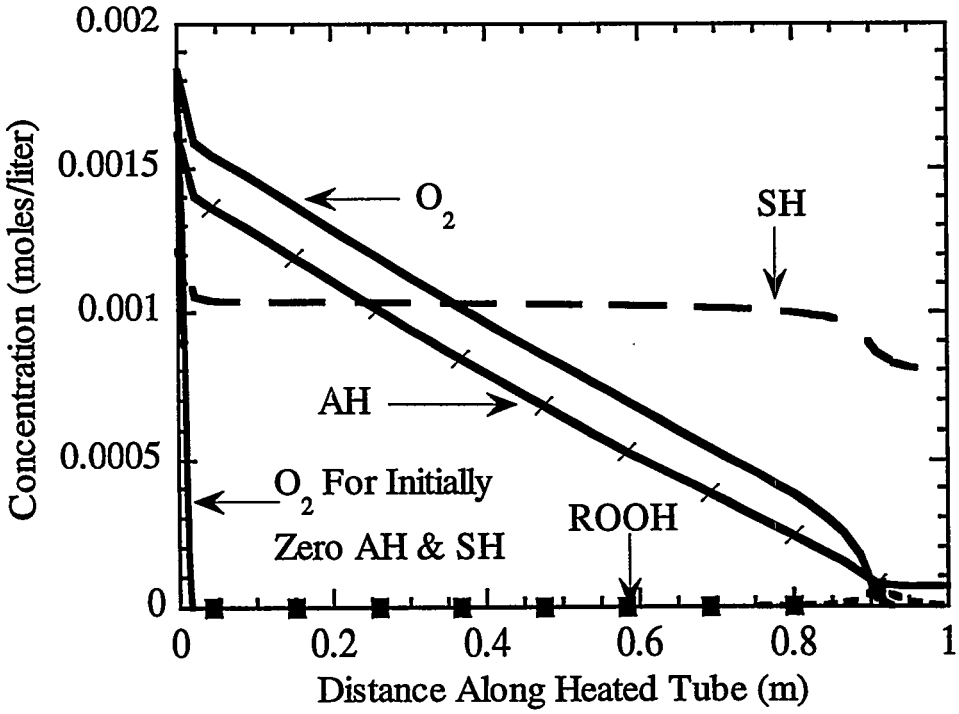

Figure 6. Calculated profiles of dissolved O_2, ROOH, AH, & SH. F2827 fuel, 0.125 ml/min, & 175 °C wall temperature.

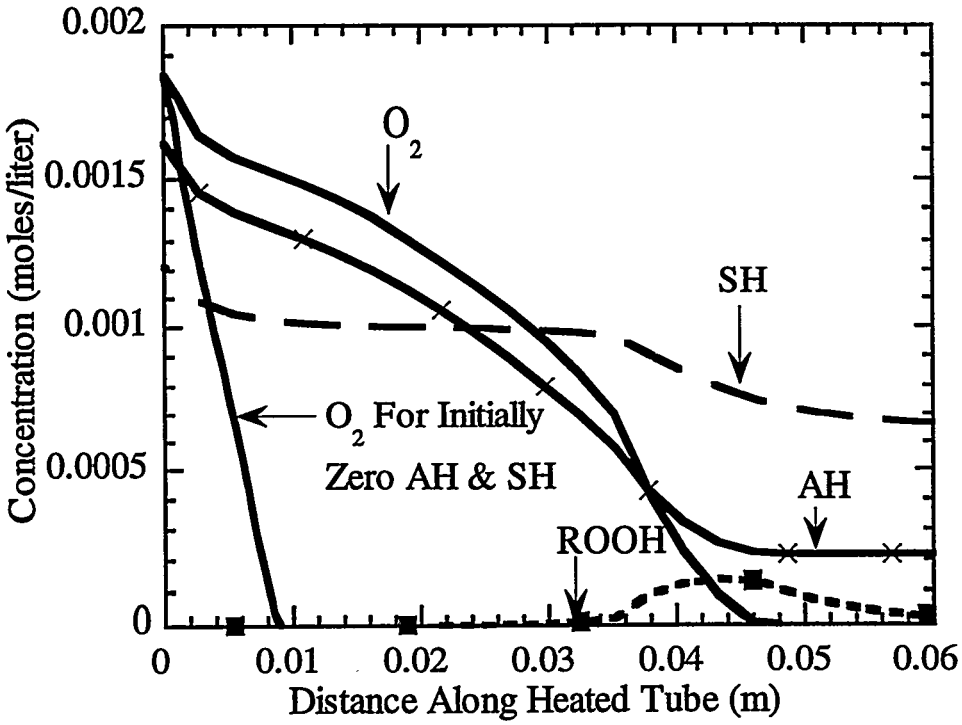

Figure 7. Calculated profiles of dissolved O_2, ROOH, AH, & SH for F2827 fuel. 0.125 ml/min & 205 °C wall temperature.

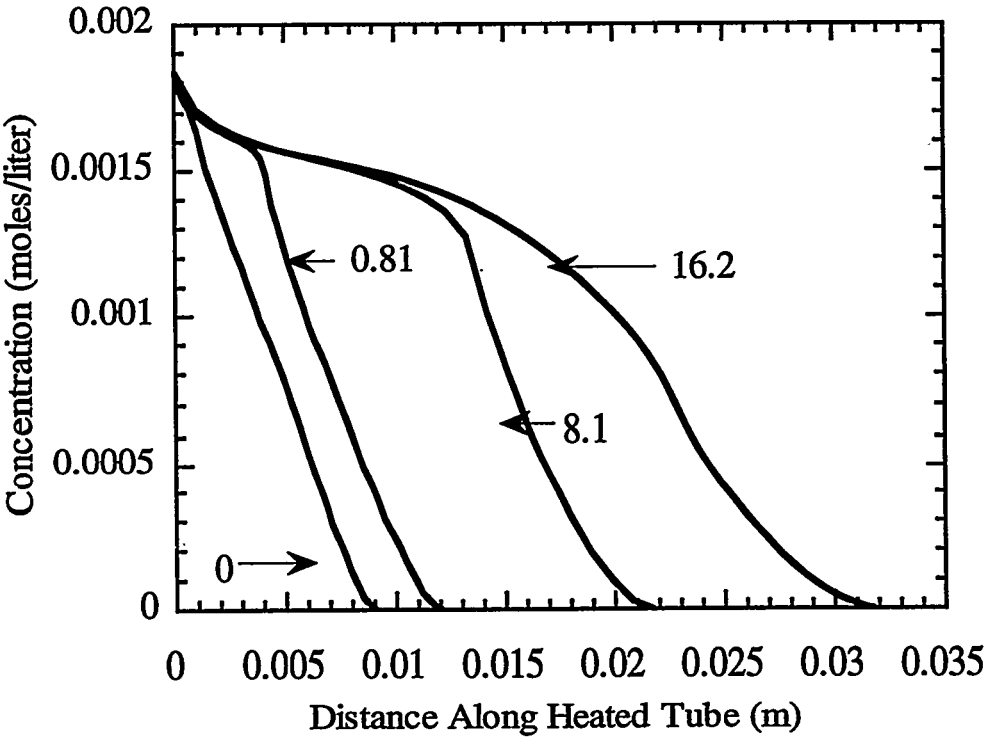

Figure 8. Calculated O_2 concentration profiles for different inlet concentrations of AH (x 10^{-4} moles/liter) in the absence of SH. 0.125 ml/min & 205 °C wall temperature.

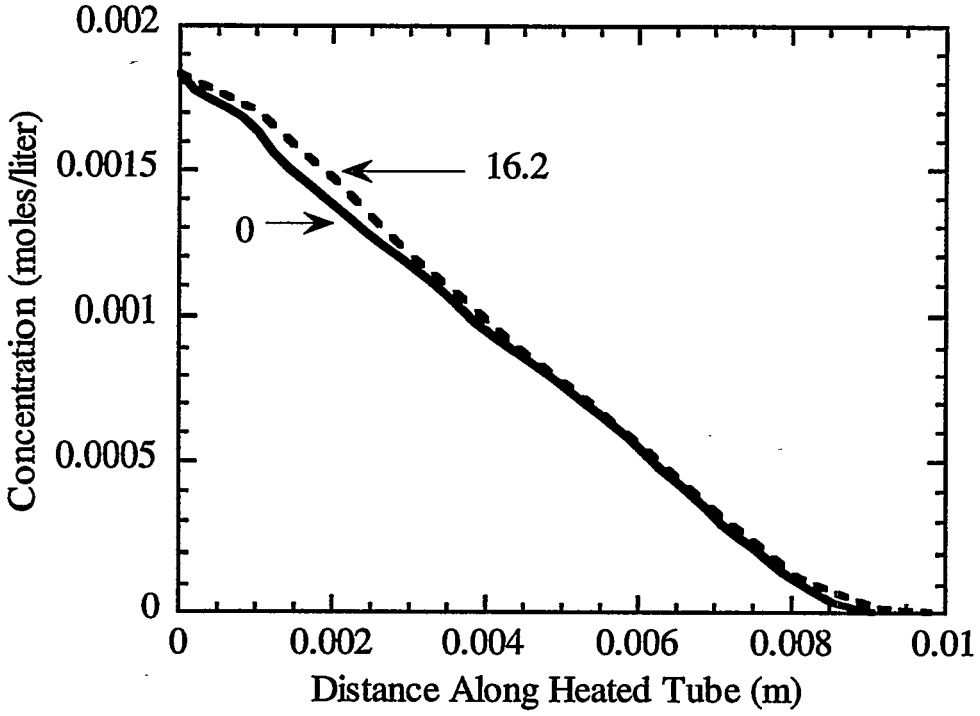

Figure 9. Calculated O_2 profiles along tube for different inlet concentrations of SH (x 10^{-4} moles/liter) in the absence of AH. 0.125 ml/min & 205 °C wall temperature.

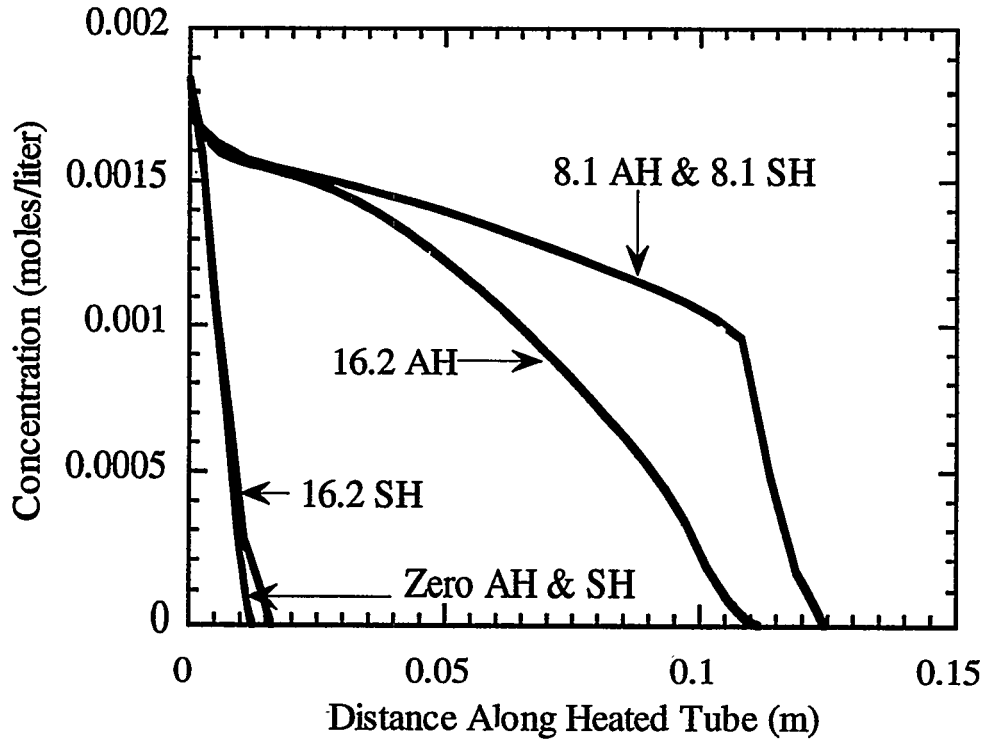

Figure 10. Synergism between AH & SH antioxidants. Calculated O_2 profiles for different initial concentrations (x10^{-4} moles/liter) of AH & SH. 0.125 ml/min & 185 °C wall temperature.

6th International Conference

on Stability and Handling

of Liquid Fuels

Vancouver, Canada October 13-17, 1997

Eighteen Years of EBV's Handling and Quality Experience

J.W. Joachim Koenig
ERDÖLBEVORRATUNGSVERBAND
(German Strategic Petroleum Reserve)
Jungfernstieg 38
20354 Hamburg, Germany

Chairman, Ladies and Gentlemen,

It is hard to imagine an oil company to report on spectacular handling events over the last 18 years of her existance, as those events are probably mainly problems and in the competitive business it can be quite damaging to talk about ones past difficulties.

As an entity of public law we do not have competitors to watch out for and thus can talk more frankly about the difficulties conducting our business, of which the main is the handling of oil and its quality maintenance, as well as the financing. Though we will not talk about the latter today.

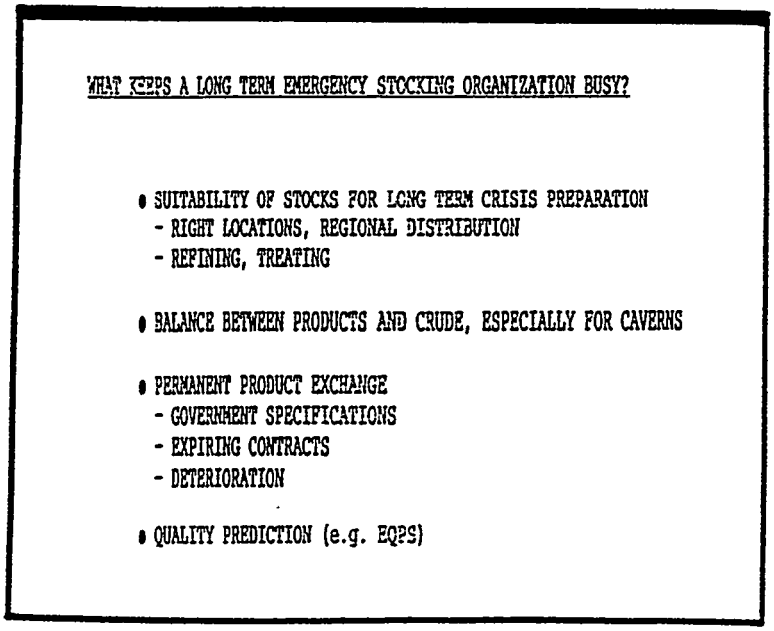

Let us first define what we mean by handling: handling comprises transport to our (own or rented) tankage facilities, storage in tankage while the oil is in our responsibility, turnover of the oil due to the end of the oil's natural lifetime or ending of a storage contract requiring to exchange, sell off or move the oil from the storage vessel, and finally the efficient release of oil in a minor/or major oil shortage period or crisis, for which the reserve has been created.

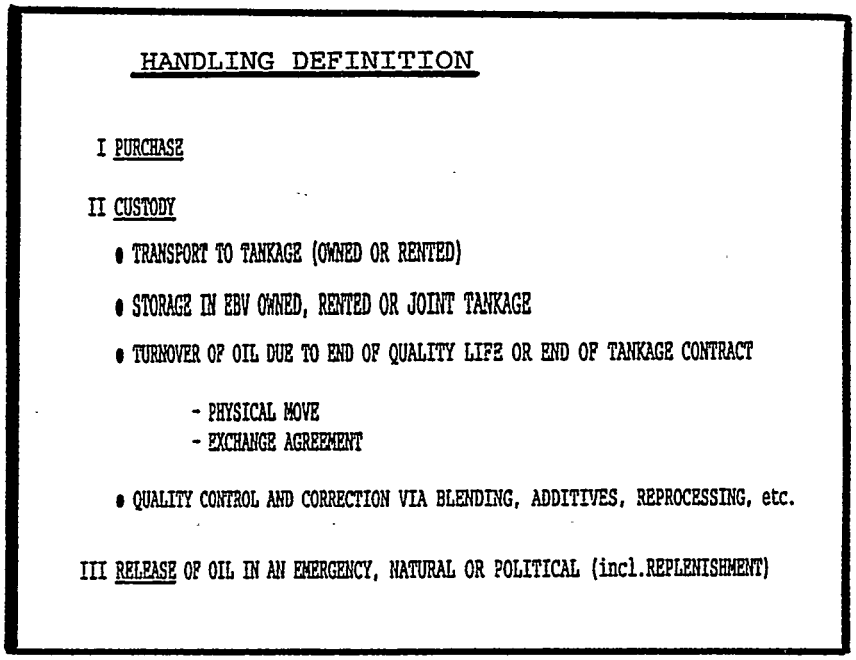

In a wider sense I would like to include even the oil purchase and quality surprises at a later date. The law allows the purchase of various products in three category groups like aviation and motor car gasolines, naphthas and naphtha based jet fuel as category I, all diesel, heating oils, kerosenes, kerosene based jet and gasoils as category II and all residual fuels, vaccum gasoils (incl. cat cracker feeds) and heavy oils as category III. Besides this, crude oil can substitute for product in a typical previous year manufacturing ratio, thus the internal flexibility to economize the mix is enormous. As a result EBV found itself with off-spec naphthas and gasolines, poor gasoils and home heating oils, practically no diesel or jet fuel, very high sulfur and high metal resids and heavy cheap Arabian Gulf crude oils, at the outset when after official foundation by law it had to take over all the left-overs companies wanted to get rid of fast.

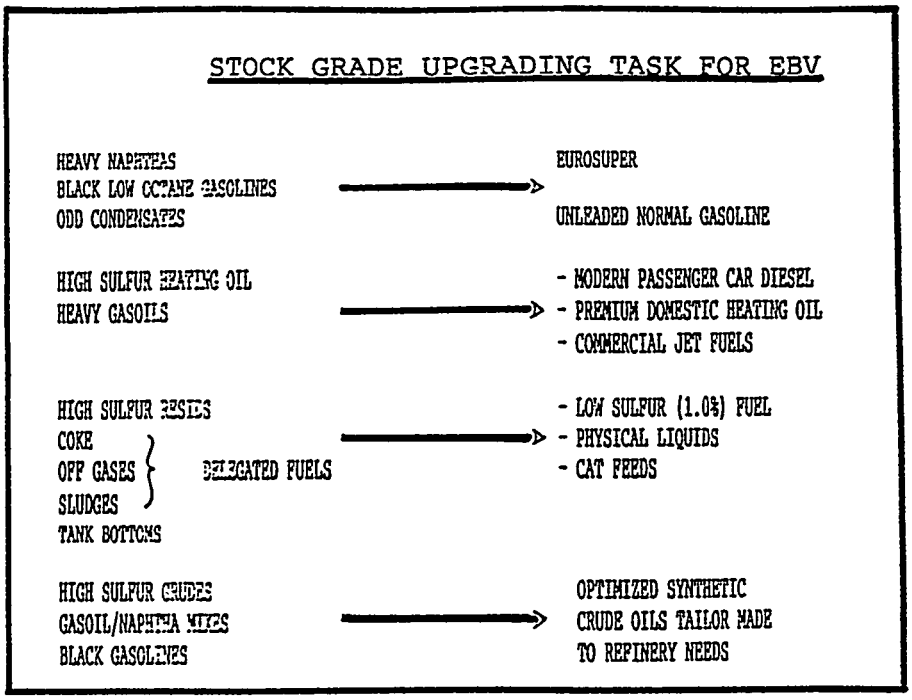

A joke of the time was that EBV harbours dangerous chemicals to be disposed of by special environmental permit. EBV has struggled ever since to improve its mix to a quality customers would expect from us in a crisis.

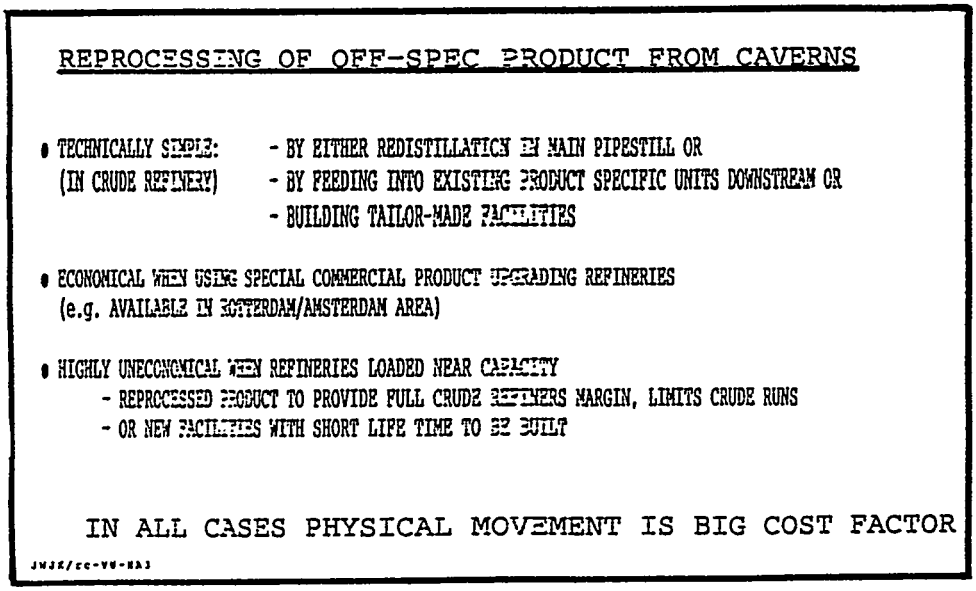

At the outset it was assumed that reprocessing in refineries would be a realistic option for off-spec gasolines and gasoils, it proved to be extremely costly and logistically difficult. In order to get rid of ca. 400 000 m^3 of crude

oil contaminated low octane gasoline, a special distillation tower had to be erected at a member's refinery site and a crude oil pipeline to be used to get it there. Neither EBV nor the refinery were happy with this handling and the contract was terminated prematurely.

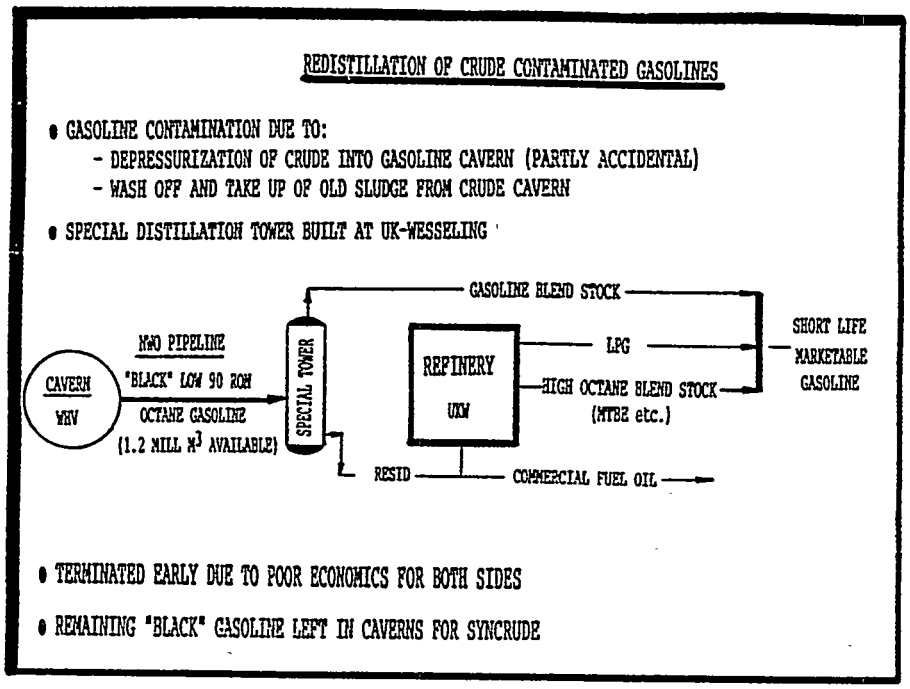

Left over black gasoline volumes were integrated into the syncrude concept. Care had to be taken to avoid the overloading of syncrude with gasoline, which had seen catalytic reformers and thus contained aromatics, which would starve the reformers after re-distillation and a second go-through of hydrogen partial pressure. The syncrude concept has many advantages.

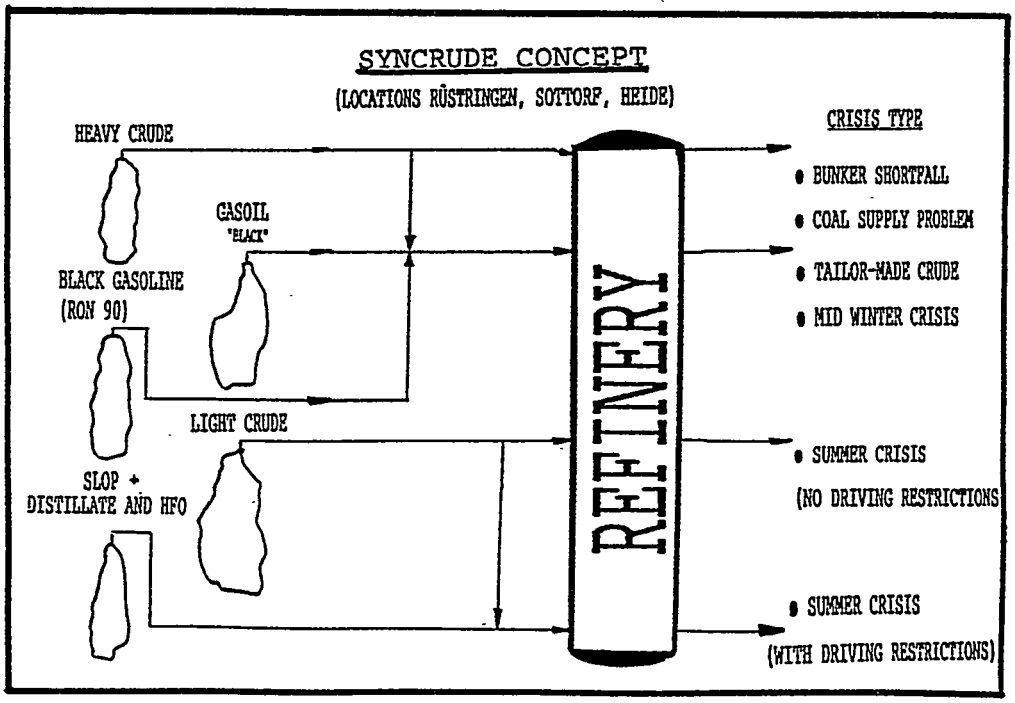

holds crude oils, contaminated naphthas and gasoils as well as cavern slop at several cavern sites. If all is available at one site including tanks for blending, any kind of "synthetic" tailor-made crude oil can be manufactured to suit the refinery type and a specific oil crisis situation.

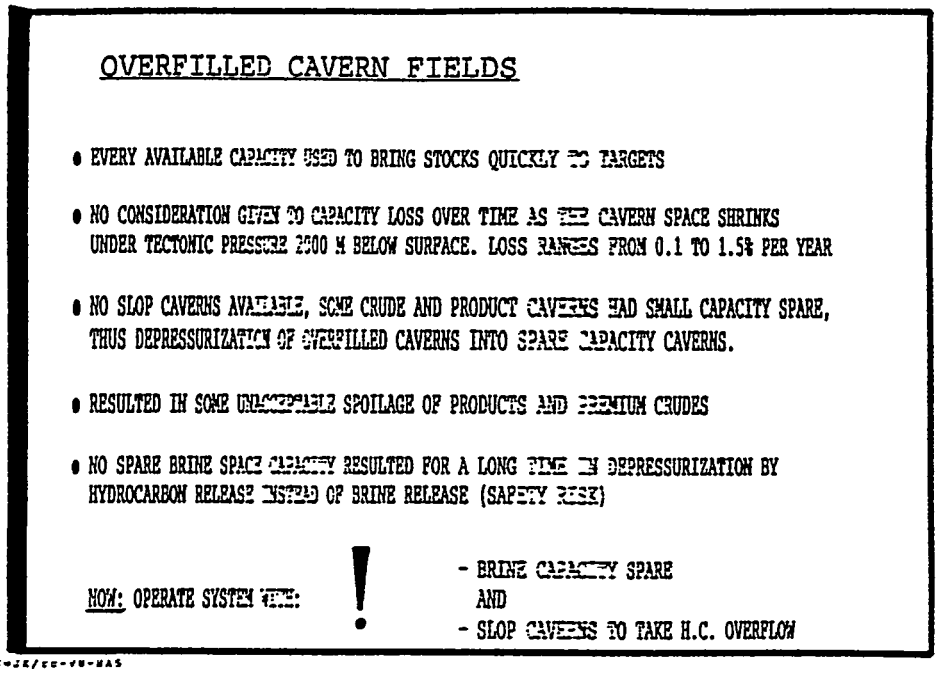

When EBV started product storage in caverns, clean new caverns were not always available. When large quantities of low octane Romanian gasoline (so called RON 90) were purchased, they had to be stored in caverns which previously contained crude oil, thus they turned quickly black and at the time no one seemed to worry about the fact that this gasoline would not only be too low in RON and MON for German cars but would also block carburators and/or injection nozzles. Gasoils were generally purchased into caverns previously used to store naphthas, jet and middle distillate components by adjacent refineries, but when in stock, accidental decompression of crude caverns into the gasoil caverns caused again spoilage resulting in dark distillates.

The cavern fields had been overfilled in order to use every available capacity to reach EBV's stock targets as quickly as possible. No spare slop caverns were left aside nor built-in cavern spare by leaving substantial amounts of brine at each cavern bottom was provided for; so decompression, for each cavern in Rüstringen more than once a year required, had to use above ground tankage at the jetty tank terminal or accidental spare in a few large caverns. Now the system has been relieved by slop cavern spare, tank terminal capacity and a brine margin in each cavern for up to 5 years.

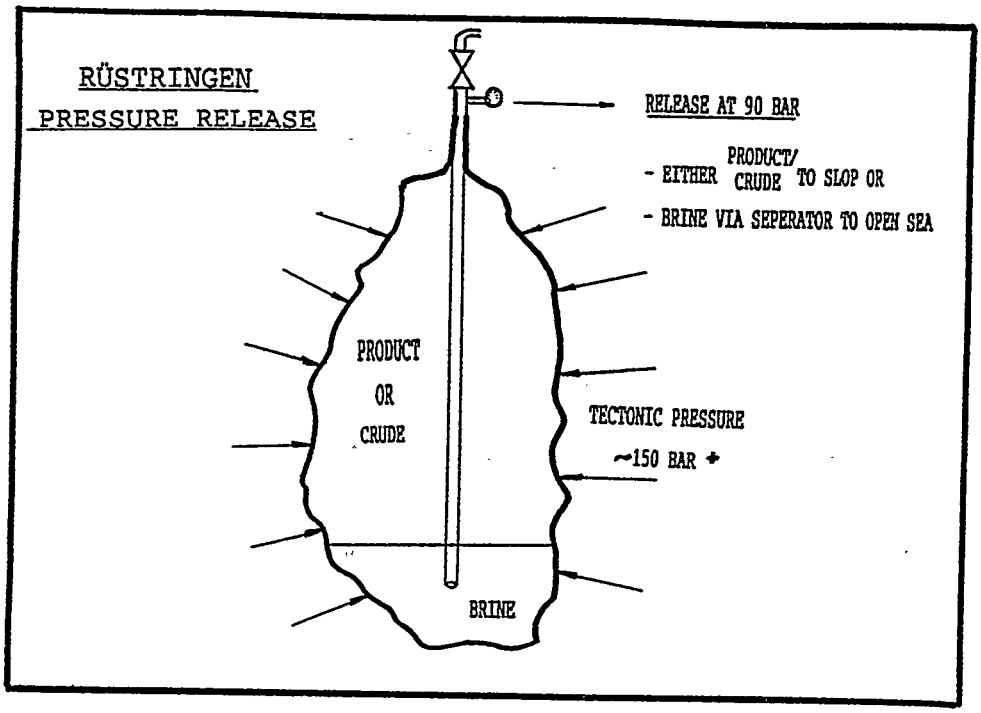

OTHER EBV EXPERIENCED HANDLING ISSUES WITH CAVERNS

- VAPOR PRESSURE OF DIESEL SPOILED BY PREFILL WITH GASOLINE
  - NEEDED IN BETWEEN WASH STEP WITH GASOIL
- PRODUCT QUALITY TO BE SUPERVISED LOW COST
  - PRODUCT TO STAY IN CAVERN 10 YEARS
  - INSPECTION LOW COST AT ANY TIME NECESSARY
  - LOST INSPECTION TUBES BY ROCK FALL IN ONE OUT OF THREE BLEXEN CAVERNS
- PRODUCT ADDITIVATED AGAINST
  - OXYDATION
  - METAL CATALYTICS
  - CORROSION

  ACHIEVE STILL 10 YEARS IN SPITE OF HIGH CONVERSION CRACKERS
- AROMATICS AND LIGHT H.C. WASH-OUT FROM GASOLINE INTO BRINE
  - BENZENE WASH-OUT ALSO FROM CRUDE
- CAVERN TURNOVER
  - SIZE INCREASE
  - LOGISTICAL PROBLEMS

JWJE/cc-VU-HA6

But also diesel fuel at one time had to use an old gasoline cavern. The vapor pressure of the diesel would have become unacceptable so that an expensive wash-out step with gasoil returned to a nearby refinery for stabilization had to be taken before the low sulfur diesel could enter. In spite of early spoilage experience when starting product storage in caverns, the low cost option for large volumes being totally environmentally sound was further explored with some great success.

At Heide we managed to empty two gasoline caverns after 7 and 9 years of storage directly into DEA's retail system without any quality problems. Admittedly there are precaution steps necessary to achieve such storage results. Today we plan for 10 years at least, for both middle distillates and gasolines. Special additivation and tight quality restrictions when purchasing the fuel are employed to avoid surprises. Although the old Heide gasoline caverns could not be inspected on a routine basis, we bought all the

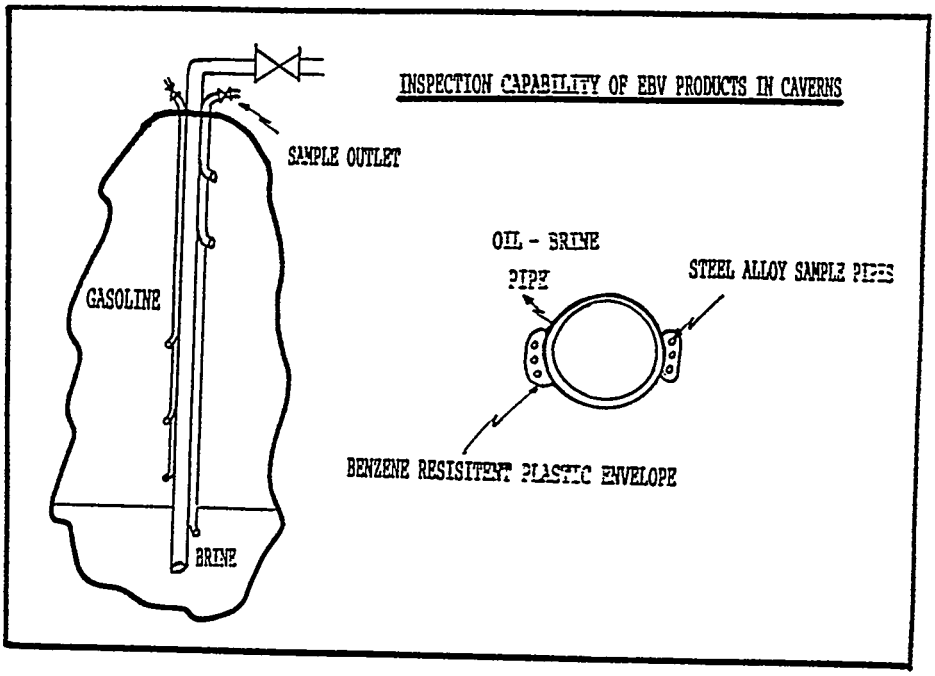

gasoline to cover the new eastern territories after German unification for storage in caverns at Blexen (Wintershall). We equipped three caverns of 350 000m^3 each with inspection tubes, which allow to test the product quality at various cavern horizons at any time. Normally 6 inspection tubes of ca. 1/2 inch diameter are flanged to the main pipe and are open at different levels. Ball valves on top of the cavern prevent the product outflow. When opened the cavern overpressure ejects the samples automatically. Before we had this device the main pipe had to be pulled out first at a cost of >100 000 US $ prior to sampling. Unfortunately we lost the device in one Blexen cavern due to a major rock fall sheering off the main pipe.

The only draw back of product storage over brine is the loss of benzene and toluene as well as some other light H.C. into the brine, whose solubility is higher than in sweet water. In the lower zone near the oil/brine interface normally about one RON number is lost due to the aromatics drain. Logistically a major problem of product storage in salt caverns is the mere size of those cavities. As the fill is part of EBV's reserves which by law have to be available at all times, product in large volumes has to be stored in above ground tankage temporarily when a cavern is emptied.

Such stand-by storage - especially for gasoline - is difficult to find in Germany and definitely not near the caverns. Therefore a complex system of delegations has to be activated with refineries and bulk plants elsewhere in the country.

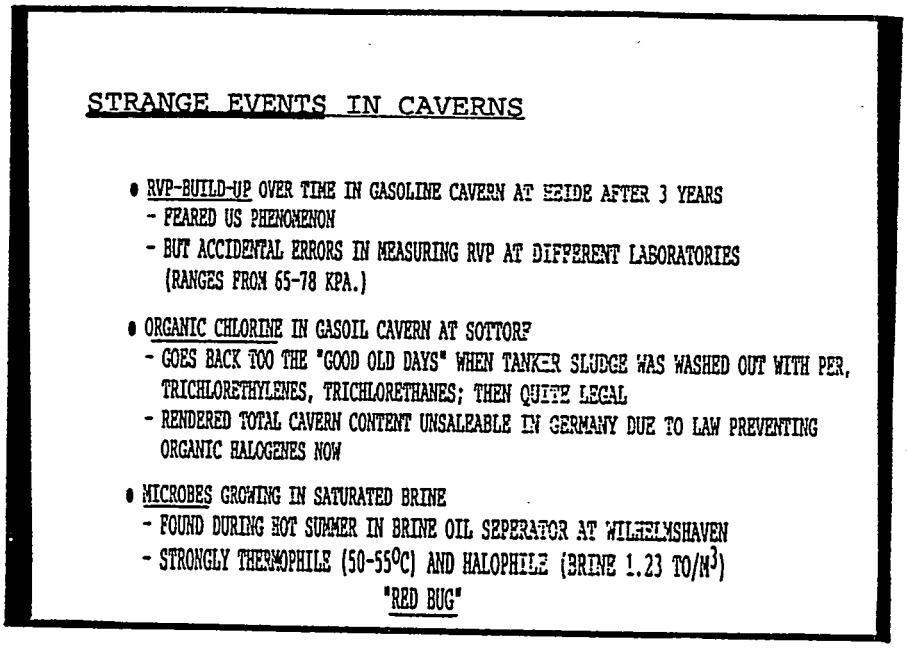

We also had our share of "strange events" with cavern storage. We observed a gradual increase of RVP-pressure in gasoline at Heide over the last 3 years. Since this was almost a straight line increase since filling time from 65 - 78 kpa we suspected intrusion of gas through the salt like it happened with the SPR in the USA. In the end it turned out to be a laboratory problem, a coincident of obviously wrong RVP measurements.

Another spectacular event, which unfortunately proved real was the organic chlorine content in one of our Sottorf gasoil/diesel caverns. Halogenated H.C. in middle distillates are strictly forbidden in Germany on environmental/health grounds. But 15 years ago when the gasoil was purchased it was quite common - and still legal - to wash tankers and vessels with PER, trichlorethylene, trichlorethane or tetra chlorcarbon and similar agents. A final definite explanation was never found, disposal was not without problems and loss of market value.

Since we use caverns for crude and products we have worried about the possibility of microorganisms not only entering but growing deep down in the caverns. It was shown by others (e.g. NIPER for SPR) that sludge in caverns contains microbes which will actively start multiplying again once conditions on the surface are right; no evidence was found that real metabolism takes place at the oil/brine interface at high cavern temperatures. In the hot summer of 1995 we found a rich biomass in the brine/oil seperator at Wilhelmshaven cleaning our brine before discharge into the sea, obviously very viable.

When exposing/adapting those bacteria to cavern conditions, we isolated a "red bug" which is strongly halophile and thermophile. It dies at low temperatures (e.g. 20°C) and low salinity. The biosurfactance and biomass capabilities are still being investigated.

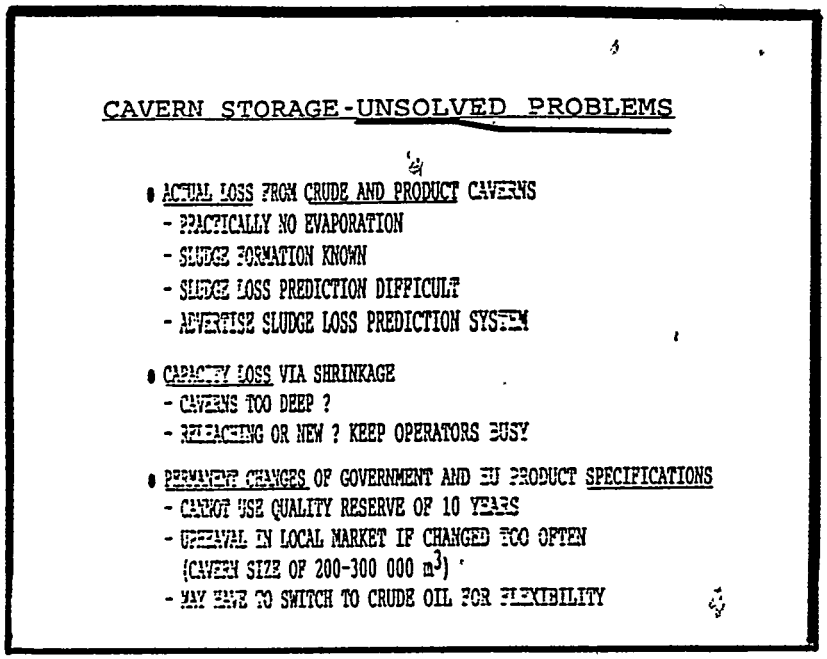

Some cavern storage problems remain unresolved for EBV. While product losses through leakages and/or evaporation are negligible, we still do not have a clear understanding how much oil can be recovered when finally emptying caverns. Cavern losses are a function of:

- the cavern shape (oil lost in traps)
- the type of material stored:
  - o solubility
    (e.g.: benzene losses in brine)
  - o occluded waxes/asphaltenes at cavern walls
  - o sludge formation capability
- the type of technical equipment at the cavern head (e.g. pumps etc.)

EBV is conducting an active research programme in this field and fosters a sludge prediction technology development, of which we report elsewhere in this conference.

Further, the continuous loss of cavern capacity through shrinkage and the balancing of it through additional leaching of existing or new caverns in the same field still requires economic optimization. The questions of depth and type of salt are important influencing factors. While in some of our cavern fields the capactity loss is minimal, in deep fields like WHV-Rüstringen it is a real headache keeping an operating organization pretty busy.

Finally the biggest issue however is influenced by government regulations. While we are quite capable and successful to extend a normal 2-3 years product life time towards 10 years in caverns, the ever changing mainly environment driven product spec alterations since about 5 years (and expected to last at least until the year 2010) render the technical ageing control almost nonsensical. So far we were not successful to get permission to keep our products in stock until the end of their natural storage life and then sell under a special licence into the local markets.

Since German caverns are built to allow in average about 7-8 turnovers only until the size gets too big and danger exists that one dissolves the support pillars between them, a too frequent exchange can ruin the whole cavern field. We do not operate brine lakes but displace the oil with sea water. The logistical cost of frequent changes also become quickly prohibitive, so that we actively consider to terminate product cavern storage in favour of crude oil or syncrude stocks. This would be a most unfortunate result of the wrongly understood environmental consciousness.

AGE QUALITY DEFINITION PARAMETERS (TYPICAL TESTS)

GASOLINES	DIESEL/GASOILS/DOMESTIC HEATING OIL
EXISTENT GUM	OXYDATION IN AIR } GUM
POTENTIAL GUM/INDUCTION TIME	OXYDATION IN OXYGEN }
UV-LIGHT STABILITY	- AMBIENT TEMPERATURE
BROMINE NUMBER	- RAISED TEMPERATURE
DIENE NUMBER	- OVERPRESSURE
	- W/W.O. CATALYSTS
	COLOR
	EXISTENT GUM
	UV-LIGHT STABILITY
	THERMAL STABILITY
	SEDIMENTS (ORGANIC/UNORGANIC)
	ACIDITY
	NITROGEN (TOTAL AND BASIC)

Lets now say a few words about quality. Manufacturers and consumers are mainly interested in performance and/or environmental specifications. While this must be of course also the basis for a strategic petroleum reserve, there are however additional considerations of susceptability to ageing, previous ageing, quality reserves etc. Since the age of an oil is not in itself a quality parameter, age and longevity can be characterized by sets of indicators like the ones in this vu-graph. Measurements of this kind on their own do not allow any predictions of how long the fuel may still be fit for use, but the results of such measurements can be used in ageing prediction models or

expert systems. EBV and its European sisters of the ACOMES group have built such an ageing predicton system called EQPS, which was presented at the Rotterdam IASH conference 3 years ago. The main difference between performance/environmental specifications and those for ageing/life prediction is the change over time, a phenomenon one finds generally with biological deterioration/degradation only. However the oil product is like a living organic system, which changes chemically and physically over time. This change effects seldom the performance unless one approaches "fit-for-use" limits and filters start plugging or deposits occur.

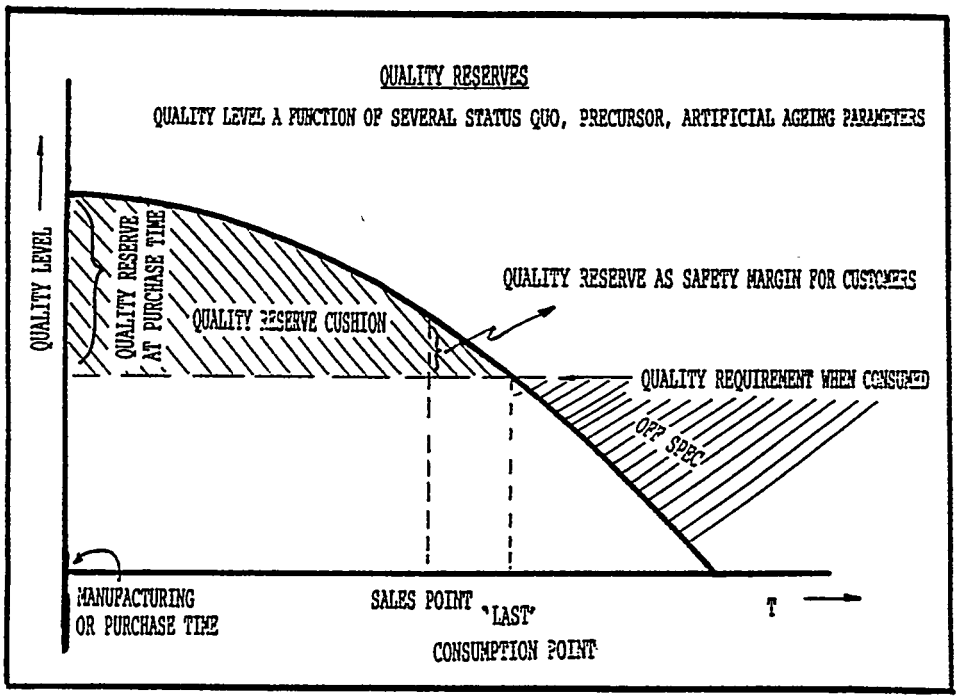

Since this change can be detected and predicted, there is a need to build a quality reserve, which is being consumed over time. This reserve often means special manufacturing and thus additional cost. The art of course is to quantify the quality reserve need and to sell the product into consumption before "fit-for-use" limits are approached, keeping in mind that most products spend a fair amount of time still in bulk/retail terminalling and customer tanks. These quality control and ageing predictions are major efforts of long term storage organizations holding finished or blend products. The problem does not really present itself when storing crude oil, other than the unpleasant crude oil sludging issue.

EBV EXAMPLES OF HISTORICAL PROBLEMS ARISING FROM LONG TERM STORAGE

- WAX FALL-OUT IN COLD WINTERS, EFFECTING MAINLY SMALL TANKS
  - WAX CRYSTALS TAKE OUT COLD PROPERTY ADDITIVES IN GASOIL
  - BUT ALSO AS HEAVY EMULSIONS IN CRUDE OIL TANKS
- TANK CONTENT CONTAMINATIONS
  - UNAUTHORIZED CHEMICAL DISPOSALS
  - SALT CARRY-IN FROM CAVERNS
  - ORGANIC CHLORINE FROM WASTE OILS (WRONGLY UNDERSTOOD SLUDGE CONCEPT)
  - BIODIESEL BLENDING
  - BIOLOGICAL INFECTIONS
- DEBLENDING
- SLUDGE FORMATION AND SLUDGE AGEING IN CRUDE OILS
- AGEING PROMOTION AND PERFORMANCE DETERIORATION CAUSED BY ENVIRONMENTAL IMPROVEMENTS
  - LOW SULFUR LUBRICITY
  - PEROXYDE PROBLEM THROUGH HYDROCRACKING/LOW SULFUR
  - BY-BLENDING OF OXYGENATES, MAINLY RME
- ADDITIVE 'POISONING'
  - BIOCIDES, - OVERADDITIVATION, - BIOLOGICAL FERTILIZATION

Allow me now to point out briefly also some typical long term storage issues for above ground steel tank storage. Strong winters occur in Germany about twice in 10 years. If the cold period is short, it mainly affects small tanks, if in very rare cases temperature stays below freezing point for more than 4 months even medium (>20 000 m^3) and large tanks (70 000 - 120 000 m^3) may be affected. The main problem is a fall-out of waxes, which in theory improves the cold properties of the fuel, in reality however it takes with the waxes most of the cold property improver additives (like WASA: wax antisettling additive) out as well, leaving behind a rather poor winter diesel or home heating oil. The fallen out waxes are hard to reblend back even in warm summers and often have to be sold under value as slop. As temperatures decrease water will also fall out and together with existing condensation water at tank bottoms and in pipes causes all sorts of damage in lines and pumps. In too cold crude oil tanks heavy emulsions at tank bottoms may solidify to permanent sludge prematurely, which then can be removed by physical "mining" methods only.

Great headaches have caused accidental or illegal contaminations like disposals of chemicals, waste oils, salt carry-ins from caverns or tankers and biological infections - mainly from poor house keeping in Eastern Europe. A static tank in a tank farm used by others seems to attract all sorts of junk; we once found the disposal of a whole gas station including rubber, nuts and bolts, stones wood, tools etc. in one of our naphtha tanks. Somebody tried to avoid polluting the environment by giving all this to us without permission.

As of recently the "trace contaminations" of the logistics system play a major role in handling and quality control. Luckily the "lead poisoning" gradually disappears, but biodiesel oxygenates and dozends of additives appear, many of which are detrimental to long term storage.

Also "smart blending" by Rotterdam "harbour artists" have bothered us in the past. They not only left unorganic acids from so called "tax crackers" in the product but used incompatible components to "tailor-meet" specifications. Unfortunately deblending in tanks occured after some time so that one customer got the front end, the other the back end octane. In gasoils it can be even more pronounced than in gasolines.

Not quite fully understood is the phenomenon of crude sludging in steel tanks, which we try to tackle by a special research programme. It sometimes even happens in gasoils, where in most cases however it is a wax shedding.

Even the blessing of improved environmental products proved often to create additional performance problems. A typical example is the poor lubricity of very low sulfur fuels or the peroxyde problems of hydrocracked blend stocks or the combustion improvement by oxygenates, which trigger off microbial spoiling in middle distillates.

Finally, cost pressures and competition forces companies more and more into joint terminalling of base stock products and brand differentiation by numerous additives at the loading racks prior to delivery into retail stations. Some of those additives at the time find their ways into cargoes offered to EBV, which then contain biocides dangerous to human health, or fertilize microbes in tanks or accumulate at lower tank parts after long term storage and form deposits in engines or burners, problems which do seldom occur if sales go immediately into consumption.

SPECTACULAR MICROBIAL CASES

- RUSSIAN GASOIL AND OVERADDITIVATION
- WRONG BIOCIDES, ESSO CASE, KICK-OUT OF KATHON
- CONTAMINATED JOINT BULK PLANTS, RHINE BARGE CASE
- RME ISSUE, BIOVULNERABILITY TEST
- ALCOHOL AND MTBE VULNERABILITY OF GASOLINE
- WATER DECLINE IN EBV-INSPECTED TANKAGE

Let me close my historical review of long term storage problems with a few important case studies of microbial spoilage, which occured in recent years in Germany, with direct or indirect influence on EBV. Microbiological problems - especially in kerosenes and diesel/home heating oils have been gradually increasing over the years in Germany with a major boost after the fall of the iron curtain, when large volumes from poor housekeeping tank farms - often in military hands - flooded western Europe. EBV was thought to be overexposed due to its normally high average storage times. However experience showed, that joint terminals and trading/transfer bulk plants are much more vulnerable due to continuous reinfection and carry-in of nutrition for microbes and water.

When the first highly infected Russian and East German cargoes arrived, traders used biocides at almost every trading step even before import into Europe, so that the German logistics system continued for quite some time a biocide level of at least 20 ppm or more. As a result this was delivered to end-consumer tanks, where sometimes even today thousand ppm of biocides can be found. (note that end-consumer tanks have no water drainage point by government order and thus biocides concentrate there over time with every refill). Even EBV in an overall survey found traces of biocides in almost every one of its tanks then, in spite of EBV's policy not to use them on a routine but rather in severe exceptional cases only.

A major oil company case excited everybody in North Germany and danger existed, that some of the highly contaminated Russian oil would also be traded to EBV. In the end, in desperation the company used the wrong emulsifying biocide which prevented the biomass to settle to tank bottom, and the oil was delivered with this biocide to retail customers. In their tanks the biocide emulsified the bottom water, carried all the deposits into the oil which then ruined the burners. Over one thousand customers had a heating
system failure and had to be "tank-cleaned", an enormous economic damage.

We had cases where barges stalled on the river Rhine and police boats failed when trying rescue operations, all had refuelled at the same "lousy" diesel tanks.

With biocides gradually on the decline (Kathon, the world's most popular was declared illegal in Germany) now gradually the logistics systems gets contaminated with biodiesel - mainly Rape Methyl Ester - an oxygenate which strongly heats up biomass production and speeds up biodeterioration, with start of major biological growth reduced from 2 years to 2-4 weeks.

We have evidence that alcohols and MTBE render unleaded gasolines vulnerable to microbial attack, even though any major outbreak has not been observed yet. With the historical biocides of TML/TEL lead and halogen-containing scavangers now gradually leaving the logistics system, the small amount of normal heptane, a strong biocide (as it dissolves the cell walls of microbes), still offers some protection. But as nc, as a low octane blendstocks is being converted to better components, this will not last long any more.

Finally a dramatic decline of water in tanks has resulted from an educational EBV-programme (naturally helped by spectacular incidents) at all of our contractual tank farms keeping microbial spoilage at bay.

HANDLING AFFECTS AGEING OF PRODUCTS

HOUSE KEEPING	DIRT AND RUST: CATALYTIC, MICROBIAL FOOD
	WATER: LEAKAGES OF ROOF, STARTS MICROBIAL SPOILAGE, DEWATERING A MUST
	SECURITY: AVOIDS DUMPING
CLIMATE	DEEP AND HIGH TEMPERATURE AS WELL AS SUDDEN TEMPERATURE SHOCKS PROMOTE AGEING REACTIONS
QUALITY OF TANKAGE	MODERN COATED, CLOSED CIRCUIT TANKS ARE BASIS FOR AGEING PREVENTION
CARE WITH BLENDING AND MIXING, TRANSPORT, DUMPING AND OVERADDITIVATION	INCOMPATIBILITY, DEBLENDING, FALL-OUTS, DEPOSITS BLOCKING OF FILTERS, UNCONTROLLED CHEMICAL AND PHYISICAL REACTIONS

→ ADDITIVES MAY HELP PERFORMANCE BUT MAY RUIN STABILITY AND LONGEVITY

As any long term storage organization has to worry about product ageing, the main message I would like to leave with you is, that not only the products chemistry, but to a very large extent the handling of products may contribute or prevent or at least slow down ageing processes significantly.

Poor housekeeping, lack of protection from an extreme climate, the overall quality of the tankage (underground is by far better than above ground) and wrong product blending, mixing, improper transport and by-blending/additivation play a major role precursing ageing reactions.

And please note that many additives good for performance may ruin stability and longevity.

Thank you ladies and gentlemen for your patience and attention.

6th International Conference on
Stability and Handling of Liquid Fuels
Vancouver, B.C., Canada
October 12-17, 1997

LONG-TERM STORAGE STABILITIES OF CRUDE OIL RESERVED BY JAPAN NATIONAL OIL CORPORATION

Takao Hara*[1], Naoyuki Hinata[2], Yutaka Imagawa[2], Masataka Kawai[3], Yoshiyuki Imai[3], Yoshihiko Kon[3] and Tatsuo Seiki[3]

[1]Department of Chemical Engineering, Faculty of Engineering, Yokohama National University, 79-5, Tokiwadai, Hodogaya-ku, Yokohama Japan 240

[2]Japan National Oil Corporation, 2-2-2, Uchisaiwaicho, Chiyoda-ku, Tokyo, Japan 100

[3]Japan Marine Surveyors & Sworn Measurers' Association, 1-9-7, Hachoubori, chuou-ku, Tokyo, Japan 104

Japan National Oil Corporation has been practicing the long-term strategic stockpiling of crude oil since 1978. The total amount of reserved crude oil now exceeds 48 million kl, corresponding to near 80 days' suply in Japan. Storage stabilities of crude oil, including formation of organic sludge, have been surveyed on four kinds of stockpiling systems (on-ground tank system, in-ground tank system, floating tank system and under-ground cavern tank system). Depositing sludge formed during stockpiling is removed periodically by the particular sludge sampler to clarify the physical and chemical properties. Depositing sludge is found to form W/O type oil-water emulsion and to be composed of crystalline n-paraffins of substantially higher carbon numbers. The amount of depositing sludge settled on the bottom of the tank has been carefully monitored during stockpiling for emergent dischaging. The efficiency of operational control against sludge accumulation is evaluated for various mixing device adopted in the on-ground and in-ground tank systems. In some occasional case, a slight amount of residual sludge is recovered after crude oil washing procedure (COW) during tank cleaning inspection. The residual sludge forms quite stable W/O emulsion, water content of which reaches 33 wt%. Minimum pour point of the sludge is found to be 52.5 ℃. In such case, hot water washing should be necessary in addition to the ordinary COW procedure. The mechanism of sludge formation is discussed and numerical analysis is applied to the relationship between amounts of accumulated sludge and stockpiling period. In further investigation, the coefficients of the assumed function could be expressed as variables of storage system, crude source, storage temperature, temperature drop, experienced condition on previous tank storage and so on.

1. INTRODUCTION

Japan National Oil Corporation (JNOC) has been practicing the long-term strategic stockpiling of crude oil since 1978. The total amount of reserved crude oil now exceeds 48 million kl, corresponding to near 80 days' suply in Japan. Four kinds of storage systems, namely on-ground tanks, in-ground tanks, floating tanks and under-ground caverns, have been adopted by JNOC. National oil srorage bases are located in ten places in Japan and most suitable storage system is adopted in each base, in keeping with the characteristics of the site location. It is, therfore, indispensable that the stability of the stored crude oil should be known to identify appropriate quality assurance after a certain period of storage. There are only few compilatory comprehensive informations on the long-term storage stabilities of crude oil either in Europe or in USA (1-5). The strategic stockpiling being in progress in Japan is the very unique and specific experience for the comprehensive understanding of chemistry involved in long-term storage of crude oil.

2. EXPERIMENTAL

2-1. Crude-Oil Source

The crude oil is basically stockpiled as pure base and the residual content in the pipeline is carefully replaced when the crude oil is transferred. JNOC reserves 31 kinds of crude-oil sources, as shown in Table 1. The densities of crude-oil sources vary in wide range from super light to super heavy (Fig. 1). The storage stabilities of the marked crude-oil sources in Fig.1 are carefully monitored throughout the storage period in this investigation. In the earlier stage of stockpiling project, some mixed crude oil were transferred in the on-ground storage system for the reason of the limitation of the storage vessels. The composition of mixed crude oil for stockpiling reserved by JNOC is listed in Table 2. The storage stabilities of these mixed crude oil are monitored in particular interest as well.

2-2. Stockpiling Systems Adopted by JNOC

Four kinds of storage systems are adopted by JNOC and the characteristic of each system is summarized in Table 3 with percent share of reserved crude oil among four systems.

2-3. Measurement of Depositing Sludge and Sludge Sampling

A steel tape and specified bob (disk-type weight) are used to determine the oil/sludge interface when the bob is grounded on the bottom deposit. The depositing sludge is defined in this investigation as the bottom deposit formed below the interface. Three-dimensional graphic aspect of depositing sludge formed on the bottom of the tank system can be drawn by use of the 20-200 inspection holes. The amount of depositing sludge is estimated for the contour-line aspect by the aid of computer. The depositing sludge is removed from the storage systems periodically and is subjected to determine the physical and chemical properties. The sludge sampler is designed and developed by Japan Marine Surveyors & Sworn Measurers' Association, as shown in Fig.2.

Table 1 Crude-Oil Sourse Reserved by JNOC

Classification		Kind of crude oil	Symbol	Number	Average Density
Light	Super Light	Marib Light	MR	2	0.8055
		Attaka	AT		0.8096
	Light	Qatar Dukhan	QD	5	0.8262
		Qatar Land	QL		0.8266
		Lower Zakum	LZ		0.8269
		Murban	MB		0.8273
		Zakum	ZK		0.8308
Medium	Light Medium	Umm Shaif	UM	6	0.8418
		Qatar Marine	QM		0.8485
		Arabian Light Berri	ALB		0.8494
		Mexican Crude	MC		0.8497
		Champion	CP		0.8508
		Oman	OM		0.8515
	Medium	Kirkuk	KC	9	0.8546
		Mexican	MX		0.8549
		Upper Zakum	UZ		0.8552
		Isthmus	IS		0.8577
		Arabian Light	AL		0.8600
		Iranian Light	IL		0.8602
		Hout	HT		0.8607
		Basrah	BS		0.8613
		Orient	OR		0.8638
Heavy	Heavy	Dubai	DB	7	0.8691
		Mexican Light	ML		0.8693
		Iranian Heavy	IH		0.8713
		Kuwait	KW		0.8733
		Suez Blend	SB		0.8735
		Arabian Heavy	AH		0.8764
		Khafji	KF		0.8784
	Super Heavy	Mexican Heavy	MH	2	0.8955
		Maya	MY		0.9085
		Total		31	0.8545

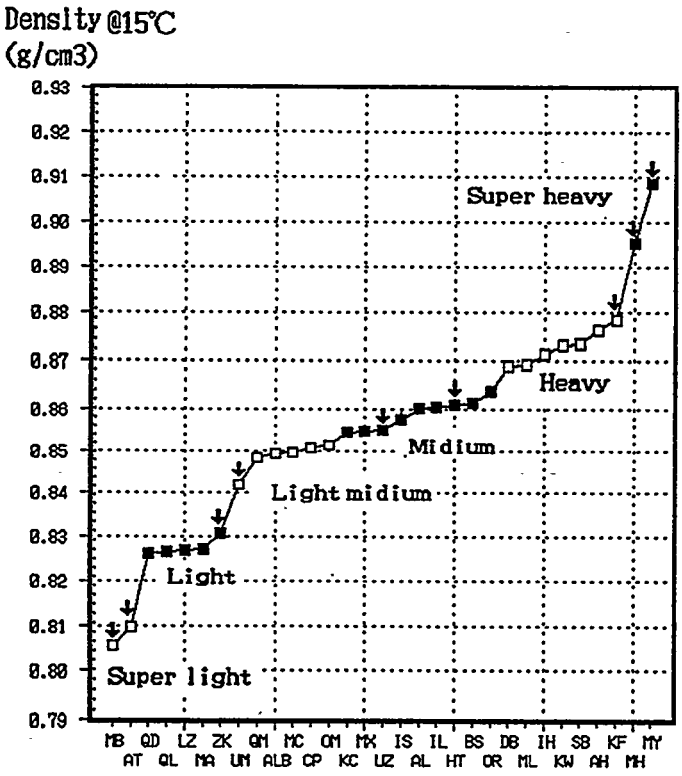

Fig. 1 Density of Crude Oil Reserved by JNOC

Table 2 Composition of Mixed Crude Oil for Stockpiling by JNOC

Crude Oil	Composition (vol%)
HT : AL	99.7 : 0.3
HT : AL: ZK : KF	78.8 : 17.2 : 2.4 : 1.6
KF : UM: ZK	16.7 : 47.5 : 35.8

HT: Hout, AL: Arabian Light, ZK: Zakum,
KF: Khafji, UM: Umm Shaif

Table 3 Stockpiling Systems Adopted by JNOC

Storing System (percent share of reserved oil)	Outline
On-Ground Tank System (60.5 %)	Floating Roof Tank (FRT) Capacity: 110,000-120,000 kl Equipped with a center-mount type of stirring device or side mixer.
In-Ground Tank System (11.7 %)	Under-ground FRT (diameter 97m, oil depth 48m) Capacity: 300,000-350,000 kl A submerged type pump is adopted for discharging. A center-mount type of stirring devise is equipped for agitation
Floating Tank System (11.6 %)	Dimensions of a floating vessel: (390m in length, 97m in width and 27.6m in height) Capacity: 880,000 kl Each vessel is divided into 9 compartments. An agitaion line and nozzle is equipped as mixing device.
Under-Ground Cavern System (16.2 %)	Each unit of artificial cavern tank consists of 2-4 tunnels, dug in the bedrock and each tunnel has 555m in length, 18m in width and 22m in height. Capacity of each unit: 350,000-740,000 kl Natural and/or artificial underground water is stored on the tank bottom, sealing the crude oil by groundwater pressure. A submerged type pump is adopted for discharging and for agitation as well.

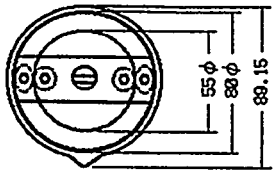

Material : Brass
Spring : SUP4
Surface : Crome
Redused scale : 1/2

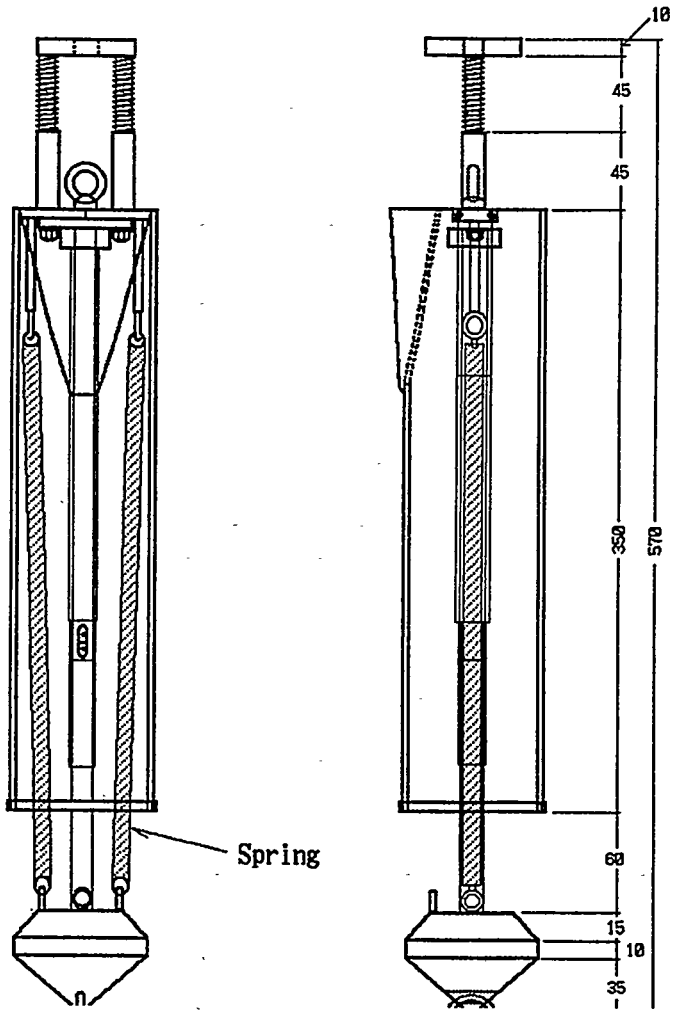

Fig. 2 Sludge Sampler

The sludge samples can be removed from the storage systems at the desirable positions by this sophisticated instrument.

2-4. Chemical Composition of Crude Oil and Sludge

The removed sample of crude oil as well as sludge from the storage systems is separated into volatile, saturates, wax, aromatics, resin and asphaltene by the conventional method, as shown in Fig.3.

3. RESULTS AND DISCUSSION

3-1. Formation of Depositing Sludge during Stockpiling

The formation of depositing sludge can be observed during stockpiling period among three storage systems (on-ground tank system, in-ground tank system and floating tank system), whereas, in under-ground cavern system, the substantial formation of sludge can not be detected even in the oil/water interface so far. The three-dimensional aspect of depositing sludge is sensitively influenced by the storage period, the seasonal change, the presence or absence of agitation and/or heating operation, the regional site of location, the crude oil source, the historical conditions (if the crude oil is transfered from one storage base to another because of the tank safety inspection), and so on. The typical aspect of depositing sludge is shown in Fig.4, where newly imported Kahfji crude oil (heavy-density: 0.8784) is stockpiled in on-ground floating-roof tank of 81.5 m in diameter at Mutsu-Ogawara storage base, located in northern Japan. The amount of depositing sludge is gradually increased along with the storage period, where agitation and heating operation is not carried out in this storage period. After two years of storage period, the maximum height of depositing sludge reachs to 2.97 m from the bottom of the tank. The surface of the accumulated sludge is quite complecated and shows mobile structure along with the seasonal change.

The maximum amount of depositing sludge reported from each storage base in the period of 1990-1992 is summarized in Fig.5. In general, the sludge amount is larger in the northern storage sites than in southern sites and is not necessarily larger along with the increase of density of crude source.

3-2. Physical and Chemical Properties of Depositing Sludge

Kinetic viscosity of crude oil and depositing sludge removed from the storage systems is shown in Fig.6. The usual depositing sludge is found to be so-called soft sludge. The kinetic viscosity of the soft sludge at 30 ℃ is quite similar with that of crude oil itself, but along with the decrease of temperature the kinetic viscosity of soft sludge increases substantially, as shown in the case of sample 4 and 5 in Fig.6. In quite occasional case, the depositing sludge is found to be so-called hard sludge, as shown in the case of sample 3 in Fig. 6. The kinetic viscosity of hard sludge reaches 31,000 cSt at 30 ℃. The optical microscopic photograph of both soft and hard sludge shows the formation of W/O-type oil-water emulsion, in which crystalline structure of n-paraffins can be observed. The difference between soft and hard sludge is only dependent on the degree of emulsification.

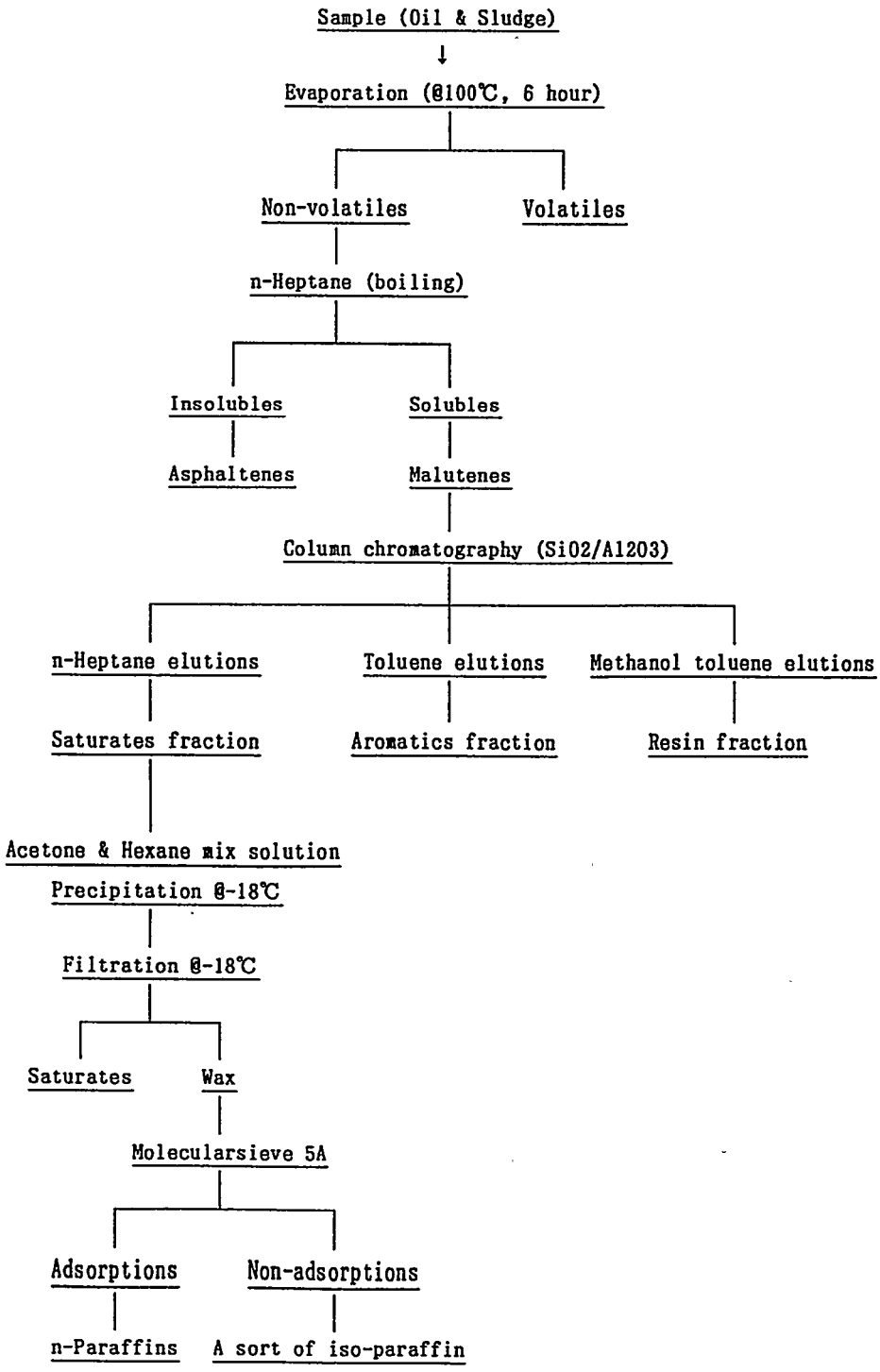

Fig. 3 Separation Scheme for Hydocarbon Composition

FRONT VIEW

JULY 1989

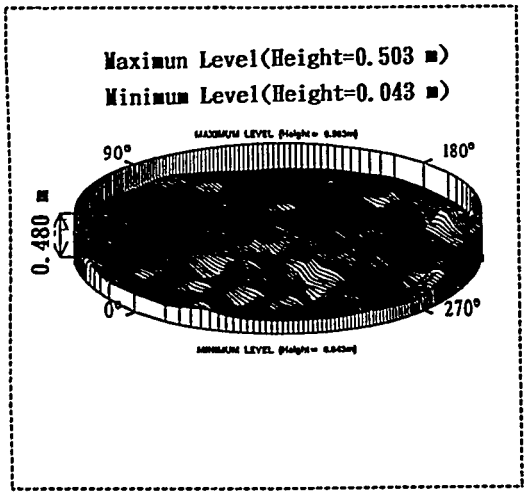

NOVEMBER 1989

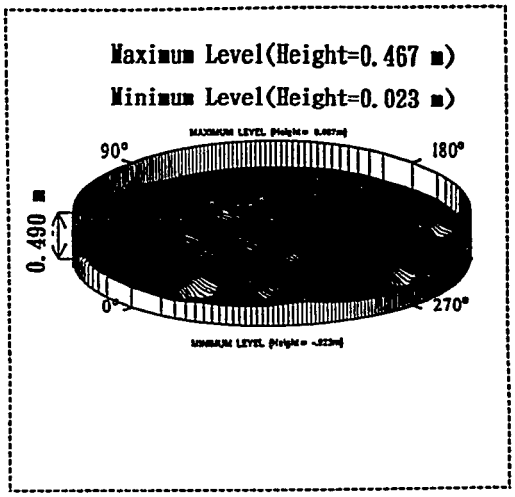

JULY 1990

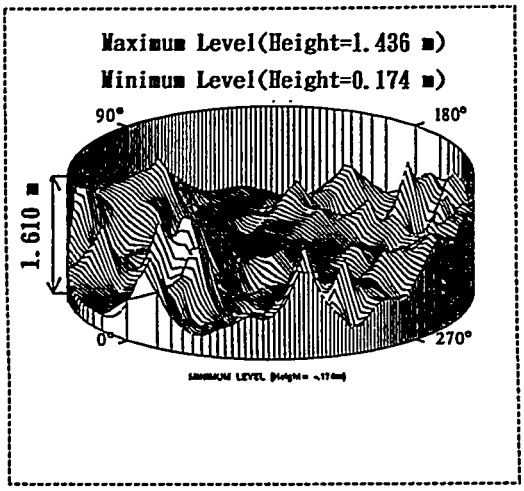

NOVEMBER 1990

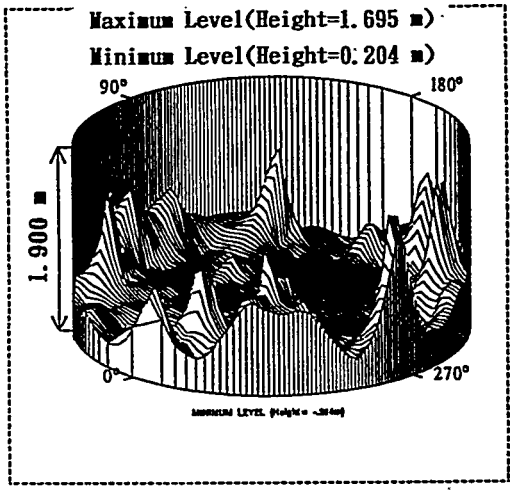

JULY 1991

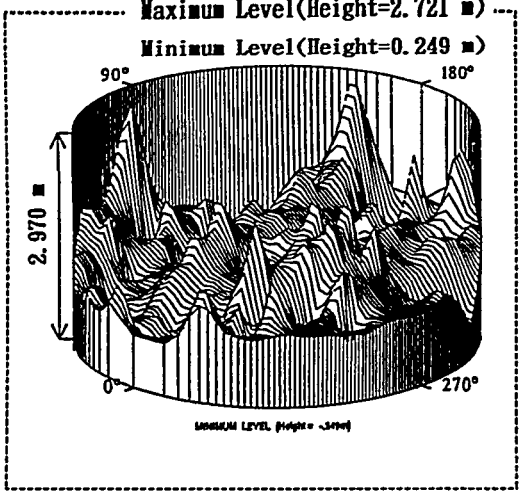

Fig. 4 Three-Dimensional Aspect of Depositing Sludge

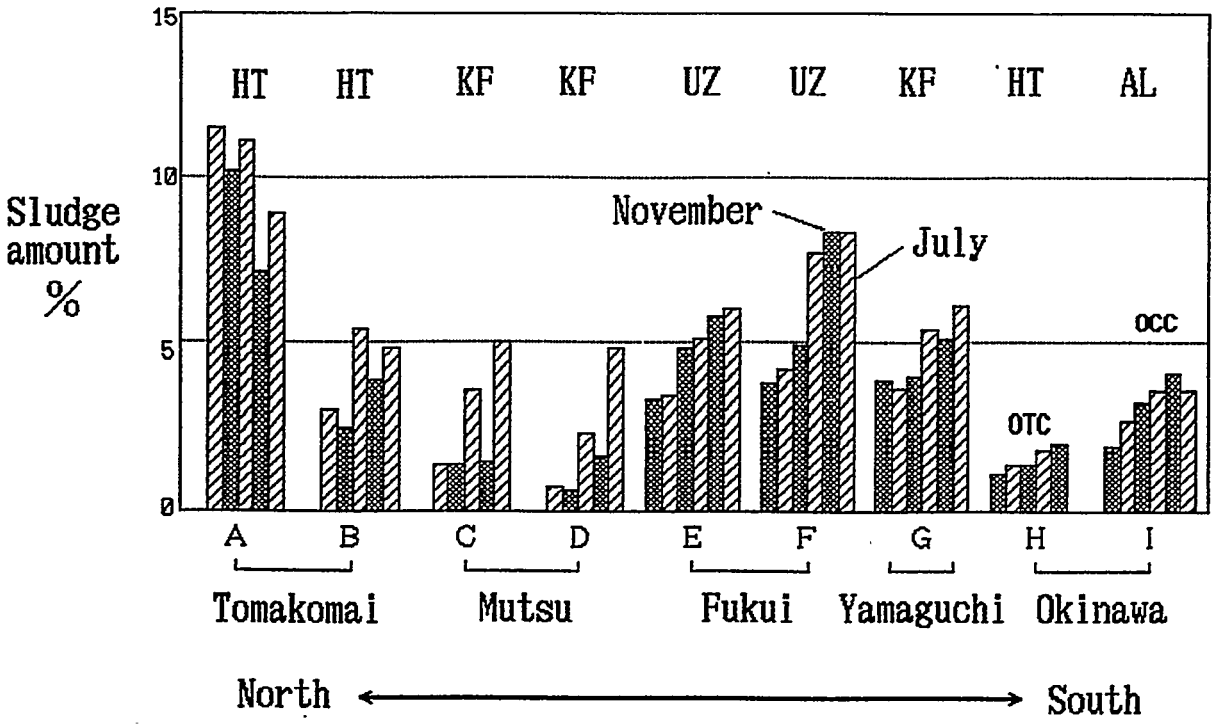

Fig.5 Maximum Amount of Depositing Sludge Reported by Each Storage Base during Stockpiling Period from 1990 to 1992

1. Zakum (Mutsuogawara No.23) ····· Bottom sample

Temperature		5℃	10℃	20℃	30℃
when received		—	—	—	—
Crude	upper	13.41	8.360	5.118	3.936
	midle	13.60	8.736	5.163	3.956
	lower	12.91	8.129	5.011	3.860
Sludge	upper	12.83	8.259	5.097	3.922
	lower	15.25	10.15	5.569	3.987

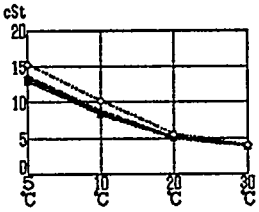

North

2. Hout (Tomakomaitobu No.ST-T24) ··· Bottom sample

Temperature		5℃	10℃	20℃	30℃
when received		—	—	—	10.34
Crude	upper	35.23	23.50	14.30	10.52
	midle	34.93	23.36	14.28	10.36
	lower	35.73	23.69	14.36	10.66
Sludge	—	32.73	22.74	14.62	10.70

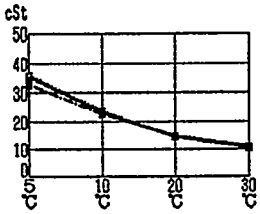

North

3. Hout (Shibushi No.40D-17) ····· hard sludge

Temperature		5℃	10℃	20℃	30℃
when received		—	—	—	33.56
Crude	upper	84.47	62.83	38.97	24.35
	midle	81.07	59.86	37.47	23.55
	lower	79.70	58.75	36.55	23.43
Sludge	upper	—	—	—	5,700
	lower	—	—	—	31,000

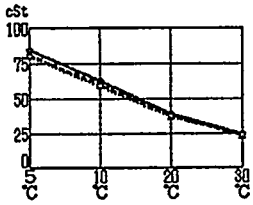

South

4. Khafji (Mutsuogawara No.04) ·····soft sludge

Temperature		5℃	10℃	20℃	30℃
when received		—	—	—	17.54
Crude	upper	50.23	41.16	25.89	19.39
	midle	55.27	38.81	25.84	17.83
	lower	55.87	40.33	25.33	18.50
Sludge	upper	97.12	60.71	28.25	18.44
	lower	238.8	111.9	38.86	20.37

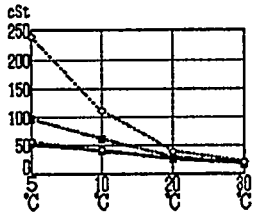

North

5. Kafji (Mutsuogawara No.46) ·····soft sludge

Temperature		5℃	10℃	20℃	30℃
when received		—	—	—	20.46
Crude	upper	62.49	48.94	31.26	23.71
	midle	63.03	48.66	31.17	23.83
	lower	64.48	50.30	32.15	22.27
Sludge	upper	175.1	90.53	36.03	23.28
	lower	65.08	48.29	30.53	21.08

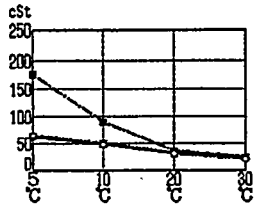

North

Fig.6 Kinetic Viscosity of Crude Oil and Depositing Sludge

In case of tank safety inspection, the whole researved crude oil is transferred from one storage system to another, accompanied by the crude oil washing (COW) procedure. The consecutive operation of COW procedure is shown in Fig.7. In some occasional cases, a slight amount of residual sludge (0.004 vol%) is recovered after crude-oil-washing in gas-phase (Fig.7), as shown in Table 4. The amount of sludge is estimated in each discharging step, as summarized also in Table 4. The properties of crude oil, depositing sludge (removed before mixing and heating operation) and residual sludge (recovered after COW in gas-phase) are clarified in Table 4. The residual sludge forms quite stable W/O emulsion as shown in Fig.8, water content of which reaches 33 wt%. Hydrocarbon composition (SARA components; saturates, aromatics, resin and asphaltene) is not changed substantially among three samples, whereas the content of wax component is quite larger in the residual sludge. According to the capillary GC profile of separated wax from three samples (Fig.9), the residual sludge is composed of crystalline n-paraffins of substantially higher carbon numbers including micro-crystal wax. The minimum pour point of the residual sludge is found to be 52.5 ℃, resulting in the complete disappearance of fluidity at ambient temperature. In order to avoid the formation of such residual sludge, hot-water-washing operation should be necessary in addition to the ordinary COW procedure, as shown in Fig.7. Moreover, the appropriate operational control against the excessive emulsification should be necessary during stockpiling period.

3-3. Operational Control against Sludge Precipitation

The efficiency of operational control against sludge precipitation is evaluated for various mixing devices adopted in the on-ground and in-ground tank systems. A center-mount rotary jet mixer is equipped in Shibusi (located in southern Japan) No.36 on-ground floationg roof tank. The effect of 24 hours mixing on the dispersion as well as on the dissolution of dipositing sludge is quantitatively investigated (Fig.10). The inspection hole 2 is located nearly in the center of the tank and the inspection hole A is in the side position. The distribution of temperature and the wax content along with the vertical position of the tank is measured before and after 24 hrs mixing operation. Before mixing operation, both distributions show quite large difference toward the bottom of the tank owing to the accumulation of depositing sludge. After mixing operation, both distributions are changed to uniform structure, indicating that the depositing sludge is effectively dispersed and dissolved in crude oil phase.

3-4. Mechanism of Sludge Formation

The amount of depositing sludge is quite sensitively influenced by various stockpiling conditions, as mentioned in 3-1. However, the sludge accumulation pattern can be classified into four types, as shown in Fig.11. Numerical analysis is applied to elucidate the relationship between sludge accumulation and stockpiled period (Fig.12). When the Gompertz function is applied, accumulation curves (Pattern I-Ⅲ) are well fitted with the calculated lines,

1. Transfering

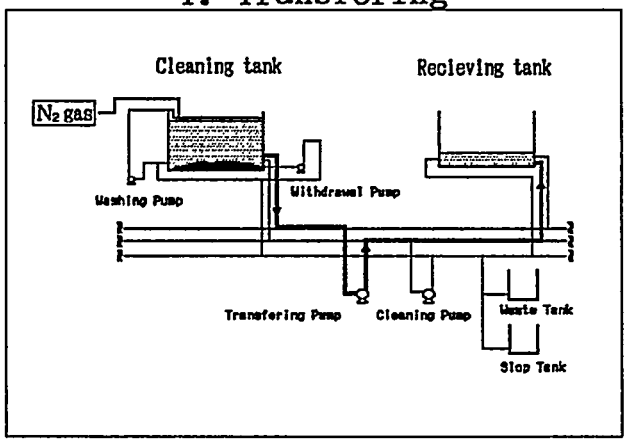

2. Circuration

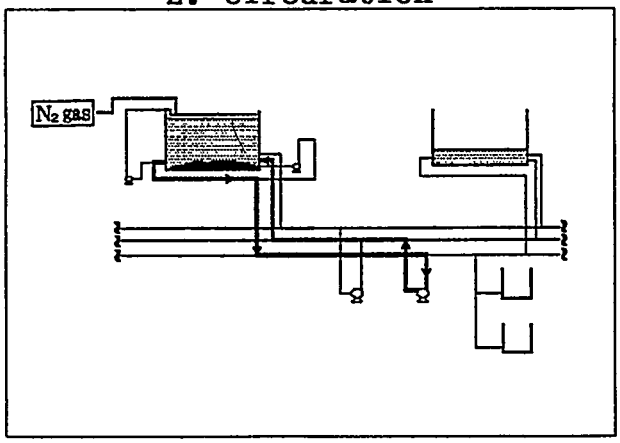

3. Crude Oil Washing
(In Oil phase)

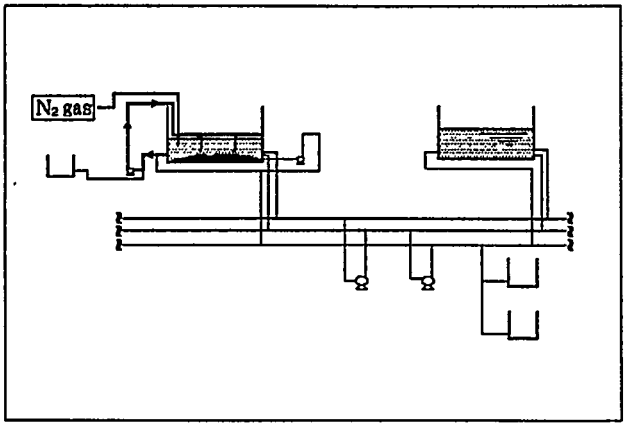

4. Stripping

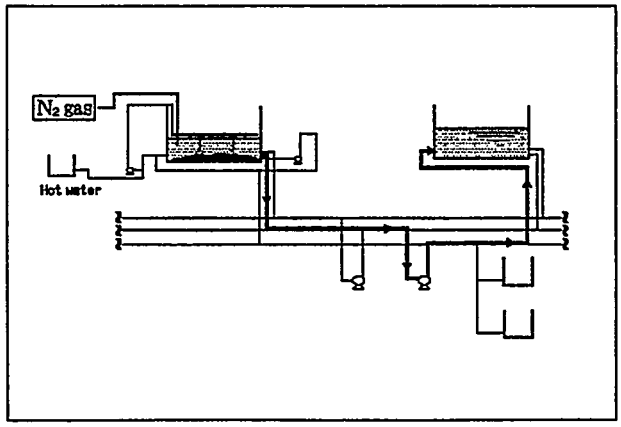

5. Crude Oil Washing
(In Gas phase)

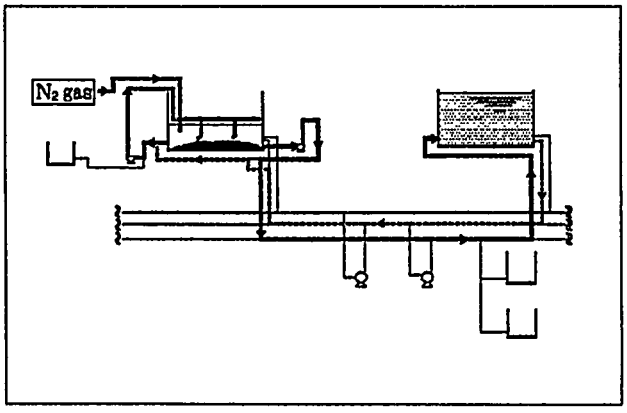

6. Washing by Hot Water

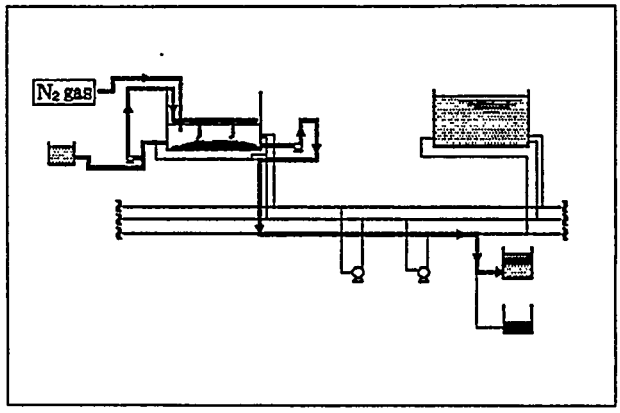

Fig.7 Procedure for Cdude Oil Washing (COW)

Table 4 Residual Sludge Recovered after COW Procedure

Crude oil: 97,800 kl (HT : KF = 95.8 : 4.2 vol%)

Step for Discharging		Amount of Sludge
Mixing and Heating	before	5,250 kl (5.4 vol%)
	after	2,230 kl (2.3 vol%)
COW	after	4 kl (0.004 vol%)

Properties of Crude oil, Depositing Sludge and Residual Sludge

Test Items	Crude Oil	Depositing Sludge	Residual Sludge
Water Content, wt%	0.75	1.70	33
Hydrocarbons, wt%			
Volatile	34.0	32.9	24.8
Saturates	28.4	25.7	26.9
Wax	3.1	6.8	13.1
Aromatics	24.8	24.5	24.3
Resin	7.7	8.2	8.4
Asphaltene	2.0	1.9	2.5
Density@15℃, g/cm³	0.8656	0.8678	0.9400
Fluidity Temp, ℃			
Minimun Point*1	<-20	<-20	52.5
Maximum Point*2	12.5	22.5	42.5
Kinetic @ 0℃, cSt	73.6	90,000	—
Viscosity @10℃	22.9	5,000	—
@20℃	15.6	1,300	—
@30℃	11.2	54	100,000

Depositing Sludge: Precipitated Sludge Settled on the bottom of the Tank before Mixing Procedure.

*1: Cooling down after heating at 80 ℃.

*2: Cooling down after heating at 45 ℃.

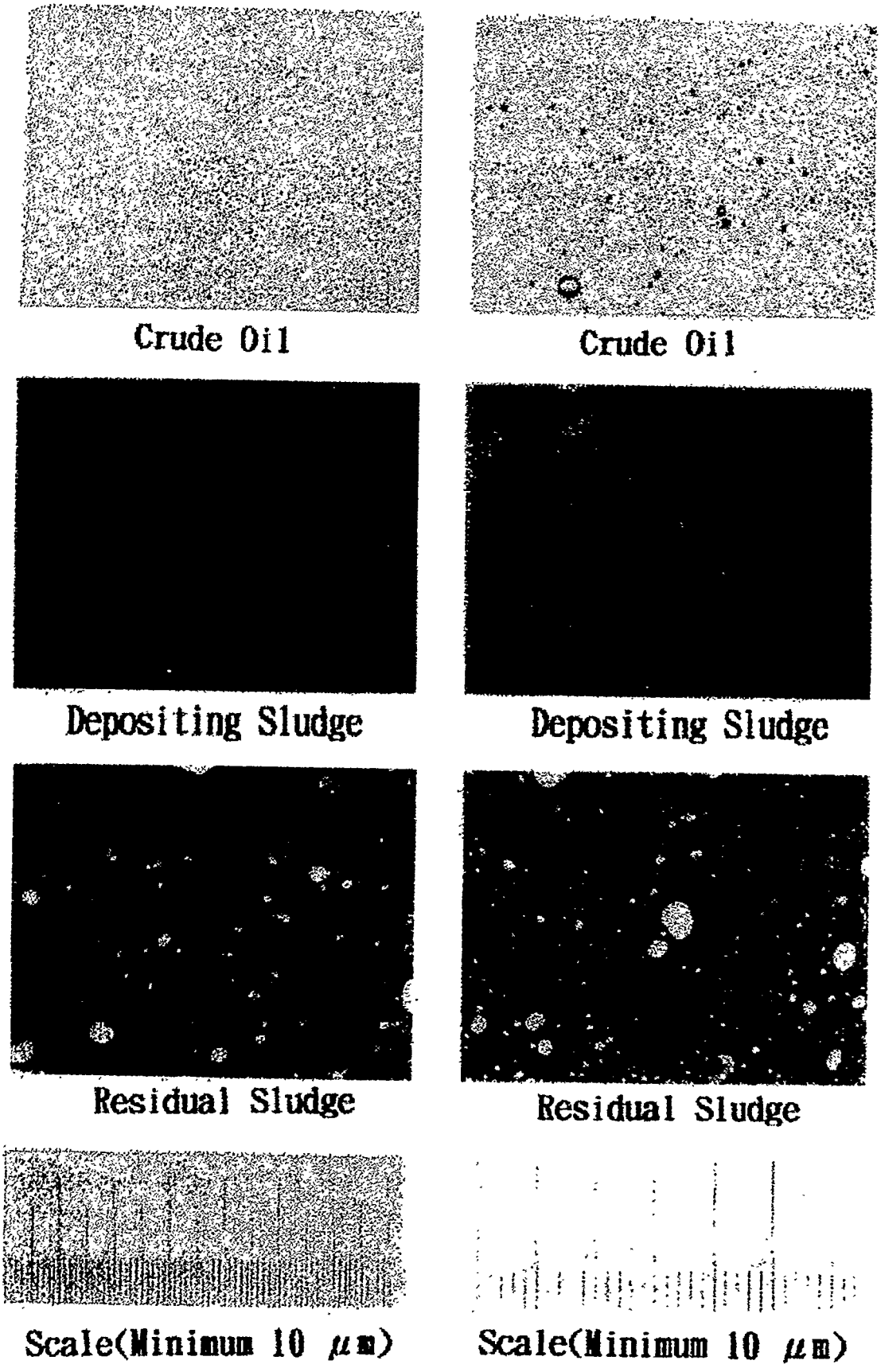

Fig.8 Optical Microscopic Photograph for Crude Oil, Depositing Sludge and Residual Sludge

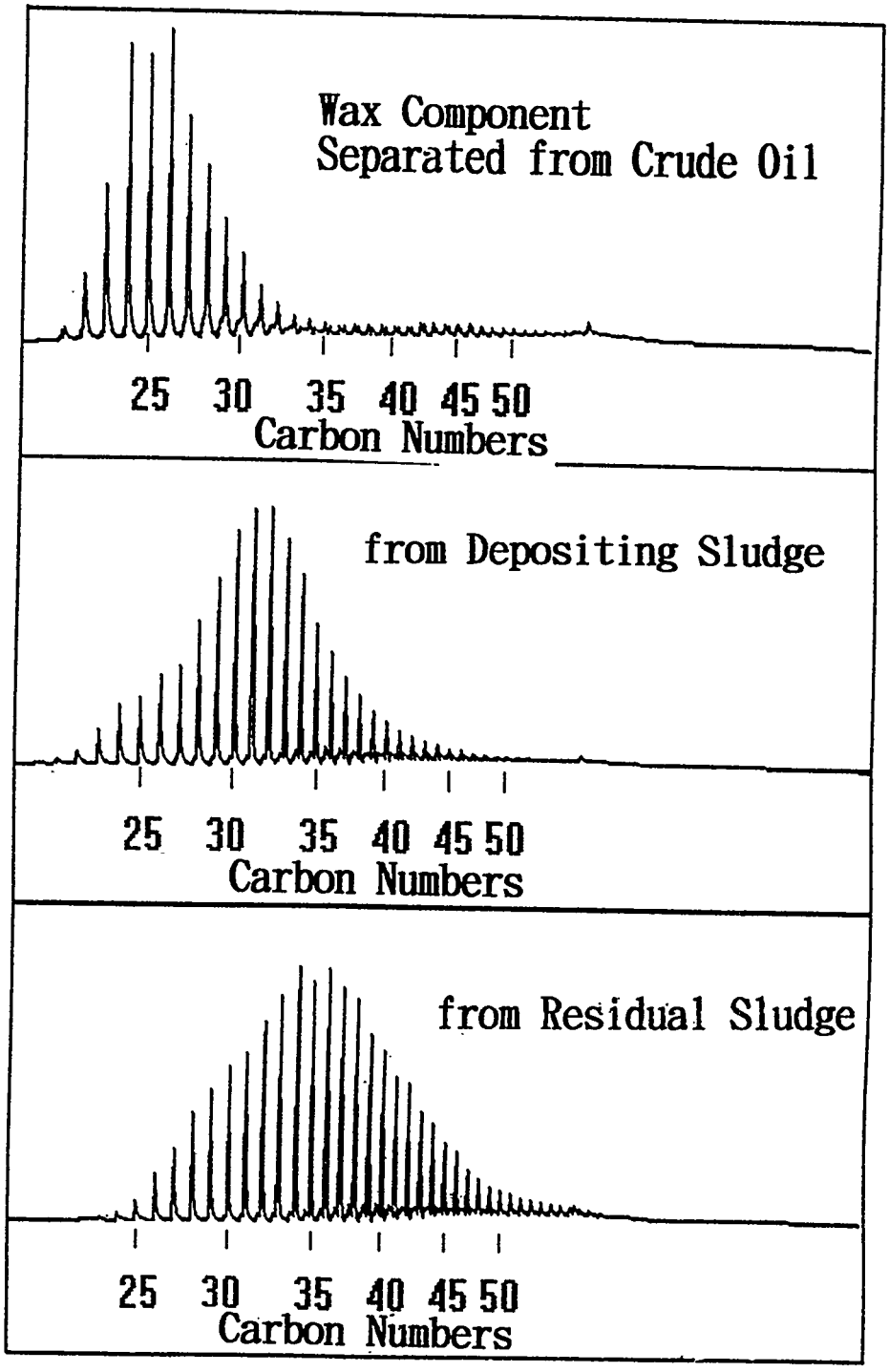

Fig.9 Capillary GC Profile of Separated Wax from Crude Oil, Depositing Sludge and Residual Sludge

Mixing Procedure: Center Mount Rotary Jet Mixer

Mixing Time: 24 hours

Crude Oil: Upper Zakum

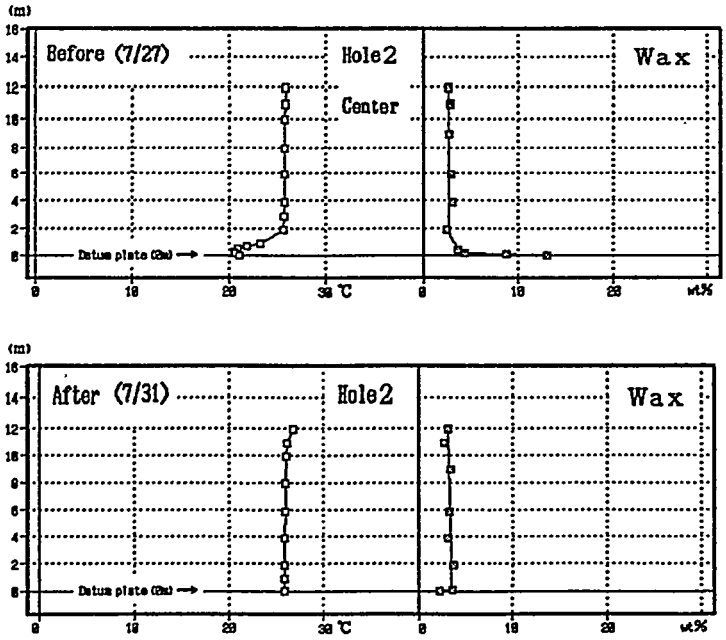

Shibushi No. 36 Tank Hole2(Center Location)

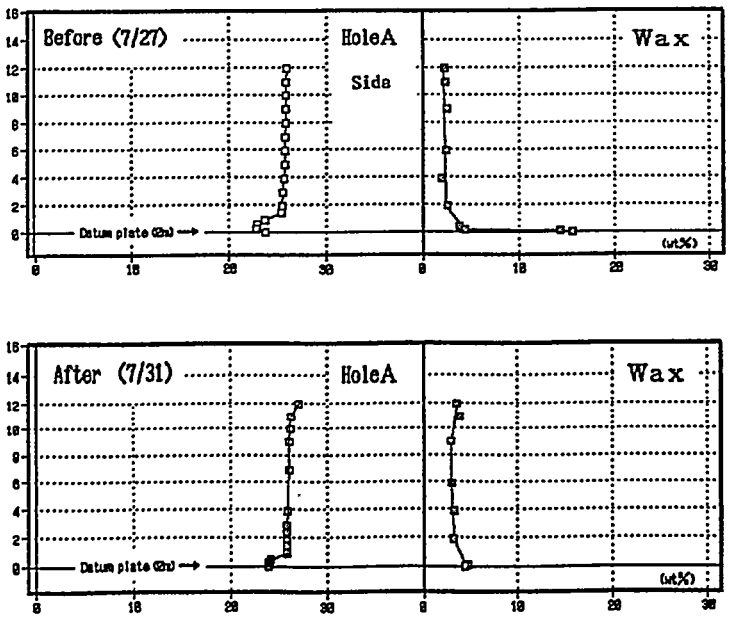

Shibushi No. 36 Tank HoleA(Side Location)

Fig.10 Evaluation of Operational Control against Sludge Accumulation

Pattern Ⅰ (some) : Generally, the sludging amount is some. (< 3 %)

Pattern Ⅱ (gradual increase) : The sludging amount increases gradually.

Pattern Ⅲ (rapid) : Sludge is deposited rapidly at the first stage of the storage, and then remains steady.

Pattern Ⅳ (gradual decrease) : Sludge is deposited rapidly at the first stage of storage, and the sludging amount decreases gradually afterwards.

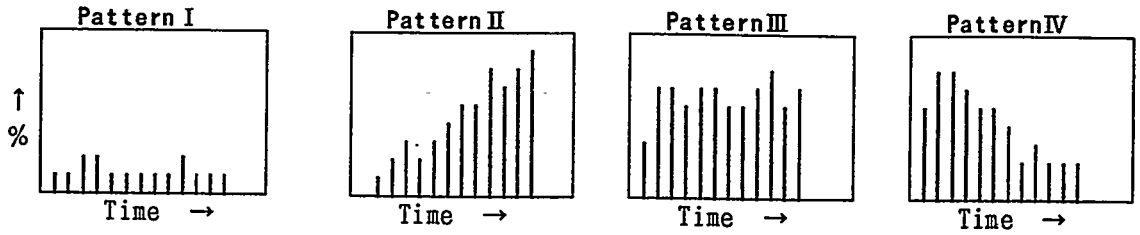

Fig.11 Accumulation Pattern for Depositing Sludge

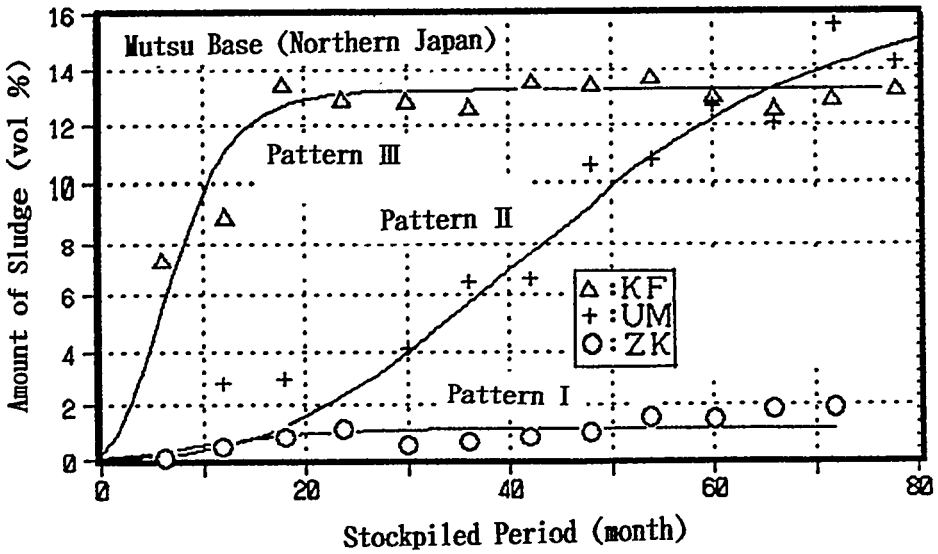

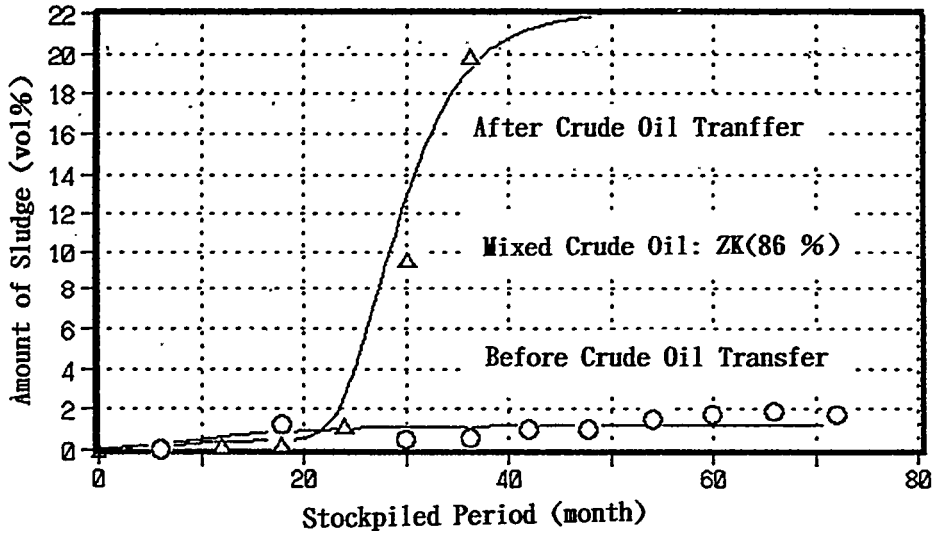

$$Y = K \times A^{b^t}$$

Y = Amount of Sludge t= Stockpiled Period

K, A and b = Coefficient

Variables: Properties of Crude Oil,
Method of Stockpiling System,
Temperature and Temperature Drop,
Operational Control for Sludge
Historical Stockpiling Condition
and so on.

Fig.12 Numerical Analysis for Relationship between Sludge Accumulation and Stockpiled Period

as shown in Fig.12. As for Pattern Ⅳ, a linear combination of Gompertz function can be applied. In the case of mixed crude oil mainly composed of light-density Zakum crude oil (86 vol%), accumulation curve shows typical Pattern I. After the mixed crude oil is transferred to another storage base, the pattern is changed into Pattern Ⅲ in the presence of certain induction period (Fig.12). The fact can be expressed as the dependence of coefficients A and b on storage conditions, namely temperature and/or temperature drop. Therefore, multi-variates analysis of three coefficients (K,A and b) should be necessary to clarify the dependence on storage variables, listed in Fig.12, in further investigation.

4. CONCLUSION

(1) Organic sludge formed during stockpiling is exclusively waxy sludge and is not asphaltic one.

(2) Any degradation reaction could not be detected throughout the stockpiling period, including oxidation, oxygenation, biochemical degradation and so on.

(3) Depositing sludge contains crystalline structure of waxy molecules and forms stable W/O type emulsion. In some case, the content of water reaches more than 30 wt% to decrease fluidity drastically.

(4) Operational control against sludge accumulation adopted by JNOC works effectively and efficiently, so far.

(5) Prediction system for accumulation of sludge should be developed to improve the eficiency of stockpiling operation.

References

(1) Hara,T.; 2nd Conference Proceedings on Long-Term Storage Stabilities of Liquid Fuels, p 39-50, San Antonio, Texas 1986.

(2) Stavinoha,L.L.; Bowden,J.N.; Westbrook,S.R.; Giles,H.N.; AFLRL Report No.121 (1979).

(3) Brinkman,D.W.; Bowden,J.N.; Giles,H.N.; BETC/RI-79 (1979).

(4) Report on "Long-Term Storage Stabilities of Crude Oil", by Fuel Society of Japan, 1984-1986.

(5) Proceedings of 1st Conference on Long-Term Storage Stabilities of Liquid Fuels, Tel Aviv, Israel (1983).

6th International Conference
on Stability and Handling of Liquid Fuels
Vancouver, B.C., Canada
October 13-17, 1997

LONG TERM GASOLINE STORAGE AT GEOSEL MANOSQUE SALT CAVERN FIELS

Emmanuel David[1] and Gilles Le Ricousse[2]

[1]SAGESS, Société Anonyme de Gestion des Stocks de Sécurité, 3, rue E. et A. Peugeot - BP 282 - 92505 Rueil-Malmaison Cedex, FRANCE
[2]GEOSTOCK, 7, rue E. et A. Peugeot - 92500 Rueil-Malmaison, FRANCE.

1 - INTRODUCTION

GEOSTOCK, an engineering company subsidiary of ELF, TOTAL, BP and TRACTEBEL, specialized in design, construction and operation of underground storages, has built the storage of Manosque. GEOSTOCK, on behalf of GEOSEL MANOSQUE the owner of the site, is now operating this storage in salt leached caverns in which a long term storage of gasoline was performed between 1989 and 1996.

2 - MANOSQUE

The site is located in southeastern part of France near Marseilles and the Mediterranean coast. The storage was created in Manosque area, which is very sensitive in the field of environmental protection, because of the existence of an underground salt deposit dated 35 million of years (Oligocene period) and rearranged during Alpine formation. The salt layer is 200 - 1,000 m thick.

The MANOSQUE underground storage complex consists of 28 salt leached caverns having an available capacity of 6,5 million m3 used for the storage of crude, diesel oil, premium and naptha.

The storage system includes pipelines for the supply of fresh water and the transport of hydrocarbons and brine, and two holding ponds at LAVALDUC and ENGRENIER (owned by Salins du Midi) where brine can be stored for the local salt and petrochemical industries and for destroying.

The whole complex is controlled by one operator at a central control station using a computer interfaced system.

The system is interlinked with three refineries, two chemical plants, the port of LAVERA and the S.P.L.S.E and S.P.M.R pipelines.

3 - CHARACTERISTICS OF THE STORAGE

The storage caverns were made by drilling a short distance into the top of the salt dome and cementing in a main casing over the whole length. The hole was then deepened to the required position for the bottom of the caverns, and two concentric wash pipes installed. Fresh water pumped down the center pipe dissolves the salt and brine is forced up the annular space to the surface. The shape of the resulting cavern can be controlled by moving the wash pipes upwards in steps while monitoring the progress of the solution mining by sonar.

The stability of the caverns is ensured by their shape and the fact that they are kept full of liquid - brine or hydrocarbons - at all times.

Containment of stored product is rigorously checked by Mines department inspectors. The storage method is entirely safe because the product is kept out of contact with the atmosphere, lightning cannot reach it, and there are none of the dangers of leakage from accidental holing or corrosion attendant on surface storage tanks.

4 - BRIEF STATISTICS ON MANOSQUE

- Cavities vary in capacity from 100,000 to 425,000 m3. They are approximately 300 m high (the Eiffel Tower is 321 m high) and have a maximum diameter of 80 m (Notre Dame Cathedral in Paris is 48 m wide). The cavities are 400 m to 1,200 m below ground level.

- Brine buffer ponds with a capacity of 100,000 m3 each are provided at the storage site

- The main pumping station at MANOSQUE has 23 pump groups

- About 100 million m3 of fresh water will be used to mine the designed 10 million m3 of storage capacity.
  This would be sufficient water to meet the annual needs of a town of 600,000 to 700,000 people.

- About 12 million tons of salt will be removed, two of three times the annual salt production in France.

- More than 20,000 tons of steel pipe were used.

- Products are pumped in at a speed of 2 m per sec.

- The MANOSQUE facility uses a ground area of only 8 hectares. An equivalent surface tank farm would require 300 hectares

- Operational power requirement is 24,000 kva.

5 - GEOSEL OBJECTIVES FOR MANOSQUE STORAGE

MANOSQUE storage, whose creation was initiated after the first SUEZ crisis in 1956, was first intended to face supply crises. Therefore, its first aim is strategic.

This objective, which was first restricted to crude oils, was recently extended to refined products (gas oil and gasoline).

The integration of this specific storage (operated on behalf of its shareholders) in the logistic chain of the refineries of the South of France makes it a very important part of the French network of strategic petroleum storages.

Running this facility, integrated into the interlinked refineries, enables to meet seasonal requirements of some petroleum products, such as gasoil, and besides to assure an emergency function, in case of problems on the proper storages of the refineries or on those of petroleum installations in the South of France area.

Finally, the important capacity of this storage enables to operate it as a buffer storage in the framework of adjustments made by petroleum companies on their stocks because of circumstances due to the current conjuncture.

6 - THE V CAVERN

The V cavern in which the long term storage was performed is located in a multiproducts (diesel oil, premium, naphta) branch of the storage.

Its capacity is 195,000 m3 and it is now dedicated to gasoline after having stored diesel oil and naphta before 1989.

The particular shape of this cavern is *(see attachment 1)* due to the presence of insoluble banks broken up into pieces scattered throughout the mass of the salt.

SAGESS EXPERIMENT OF LONG TERM GASOLINE STORAGE IN MANOSQUE SALT CAVERN

1 - BACKGROUND

SAGESS is a private company which holds and controls strategic reserves of petroleum products on behalf of the French Government authorities. SAGESS stocks -5,5 million m3 of gasolines, diesel and heating fuels, jet fuels and crude oils- represent one fourth of the French reserves *(see attachment 2).*

SAGESS found attractive the possibility to store gasolines, then distillates and crudes in the MANOSQUE salt caverns rent to GEOSEL. In 1989, a joint SAGESS-GEOSTOCK venture was decided to set aside cavern «V» with a view to experiment the effects, on gasoline ageing, of a long-term storage in a salt cavern.

2 - SAGESS INCENTIVES

From a technical point of view, the salt caverns should provide a better protection of gasolines than above ground tanks against ageing *(see attachment 3)* for the following reasons :

- the cavern is entirely filled, thus ensuring the absence of air and UV, responsible for most of ageing processes,
- this close structure does not allow any volatility losses,
- the temperature inside the salt cavern is kept very stable due to the thermal inerty of the salt mine and depth of the cavern. GEOSTOCK estimated it should be within the 30 to 35°C range.

In addition, GEOSTOCK forbids the preliminary incorporation of any additive, dye or oxygenates in the virgin gasoline before storage to prevent it from ageing side effects. This additivation/blending treatment which aims to tailor the product to the retail specifications takes place in the refinery where it is returned in any case after storage for unexpected but possible need of reprocessing.

On the overall, the balance of technical/economical factors for this experiment looked attractive to SAGESS, taking in account the more economical storage costs in caverns and the possibility contemplated to extend storage times due to lower ageing processes.

3 - CAVERN « V » FEATURES

The so-called cavern « V » is a typical pear-shape structure of 180,000 m3 capacity leached by water in salt dome in 1971, at a depth between 590 and 660 meters. Between 1971 and 1989, the cavern «V» contained successively diesel fuel, naphtha, base gasoline for leaded *(see attachment 4)*.

4 - FILL / DISCHARGE HISTORY

Between January 1989 and January 1991, the cavern was filled, on behalf of SAGESS, with 11 batches supplied from the three refineries for a total volume of 175,926 m3 of a lead-free virgin gasoline. The material was considered to be a base stock for the later production of a leaded premium containing 0,25 g/l lead. The different lots were pumped sequentially into the cavern over 2 years. Between January 1991 (end of cavern fill) and March 1996 (beginning of discharge), no gasoline was added or withdrawn from the « V » cavern.

Discharge history

The injection of brine into the bottom of the cavern has displaced the filled-in lots in reverse order. Between March and September 1996, a total volume of 175,926 m3 was pumped out of the cavern in 8 sequential lots with volumes ranging from 15 to 31,000 m3.

Each delivering refinery got about one third of the cavern fill for entering it into their own blending/additivating logistic system. As already noted by GEOSEL in their previous fill/discharge operations of cavern «V», a volume of about 5,000 m3 product is permanently kept in vertical traps.

Storage time

As shown by the histogram of cumulated volumes in the cavern *(see attachment 5)*, 88,5 % of the gasoline volume had a storage time between 7 years 5 months and 7 years 8 months. The remaining share (11,5 %) corresponding to the volume of 20,000 m3 introduced in January 1991 stayed for 5 years and 2 months.

The average storage time, calculated on weighted volumes, was found to be of 6 years and 9 months.

5 - QUALITY CONTROL ANALYSIS

There is no documentation on the control data issued by the 3 supplying refineries on their respective production batches (before cavern fill-in, and at receipt of the lots after cavern discharge) which were kept for internal use. The control data available were obtained from the external independent laboratory which inspected the cumulated samples obtained by GEOSEL in recipes fed from the cavern fill-in and discharge lines.

The present report could not include the detailed quality control results on individual lots of gasoline but retained the most significant ranges of values and averages in the *attachments 6 and 7* and the corresponding graphs *(attachment 8).* They can be commented as follows :

Analysis of fill-in qualities

The individual quality control results appear typical of a virgin product including cat cracked gasoline, with few abnormal values identified :

- one batch (4,004 m3) exceeded the max. spec. of density at 15°C (778 versus 720-770 kg/m3),
- two batches (totalling 24,643 m3) were noted with a yellow colour (all others were rated yellow pale),
- one batch (10,170 m3) was noted with a copper corrosion of 1 b for a spec. of 2 max (others 1 a) and an existent gum value of 6 mg/dl (spec. 10 max).

The reported RON and MON results are clear, lead-free octane values. They cannot therefore be compared to the specifications of 97 min for RON and 86 min for MON which pre-suppose TML addition of 0,25 g/l lead. However, the clear values indicate good potential.

The discrepancies of results noted between several sequential batches and noticeable on the attached graphs, must be considered normal taking in account the supply from 3 different refineries and the effect of seasonal refinery production (e.g. P.V.R. and distillation) since gasoline delivery spread over 2 years (Jan 89 to Jan 91).

Analysis of pump-out qualities

The ranges of values obtained on the samples of the 8 consecutive lots are considerably narrower. They indicate that a mixing of the original batches took place in the cavern probably due to mixes induced by the superposition of the gasoline layers during filling-in operations and also from the convection moves during the nearly 7 years storage time. A more uniform gasoline has evolved during storage :

All characteristics illustrate this, but more especially :

Density at 15° C		range	reduced	from	32	to	4	units,
Distillation	E100	„	„	„	19	to	4	„
	FBP	„	„	„	28	to	7	„
RON (clear)		„	„	„	4,2	to	1,1	„
MON (clear)		„	„	„	6,4	to	0,8	„

The control results on the 8 sequential lots of the discharged gasoline fully meet the quality specifications originally established for its intended application.
An increase of colour level and existent gum values point out a moderate ageing but within reasonable limits.

New outlets for base gasoline

During the 7 years storage period, the French market demand has moved towards unleaded gasolines and gasolines containing lower contents of lead (0.25 g/l grade replaced by 0.15 g/l grade). This brought the refiners to consider the possible use of the stored gasoline in these new outlets.

The gasoline quality was found suitable by the refiners to manufacture both the premium leaded grade and the 95 unleaded Europremium. It went into their respective blending processes and their retail systems without any reprocessing and raised no quality complaint. How and to what extent each company upgraded their batches is not known to SAGESS. The only indication received was that the sulfur content of the gasoline (≅ 600 ppm) required a preliminary dilution with another low-sulfur gasoline stock to meet the 500 ppm limit of the Europremium grade.

6 - STUDY OF AGEING CHARACTERISTICS

The determination of ageing characteristics aimed to appraise better the interest of the underground salt caverns for long term storage of gasolines and other petroleum products.

SAGESS requested EBV partner's help to analyse the Manosque experience and learn lessons for their own cavern stocks of gasoline in Blexen and Heide (North Germany).

- **Composite samples**

EBV obtained cumulated samples (remainder of quality control) which were pooled into 3 representative composite samples for the top, middle and bottom sections and analysed by a Dutch expert laboratory, leading to the following conclusions :

1. The product after storage is very uniform but a slight density increase can be identified towards the bottom.

2. There is an aromatic increase from top to bottom in line with the density increase. The bottom section shows reduced olefins content, possibly due to the reaction with oxygen from the brine : under ultra-violet light, the top and middle sections are more reactive than the bottom section, as there are more reactive olefins left.

3. The product has formed no additional gum over the storage period : the available gum is not resin-like and easily washed away by normal heptane. The little amount of washed gum is dry and of uncritical consistency for modern injection engines.

4. The potential gum values show that substantial further and possibly faster ageing could have occurred, had the product been stored in a less protected environment like above ground ' el tankage.

   The above measurements allow the conclusion that the original gasoline probably contained some 20-30 % of light cat crack naphta but definitely no pyrolysis material and was more reactive than normal hydroskimming type gasoline, but as a conversion gasoline very suitable for cavern storage and long residence time.

- **Spot samples / Cavern segment analysis**

Analysis of spot samples *(see attachment 9)* performed by ETS Mont-Saint-Aignan on behalf of SAGESS revealed the following :

1. The existing gum values show a very consistent picture from top to bottom of the cavern.

2. While induction periods reach generally times over 1,000 minutes, they fall dramatically for the last m3 before interface with a corresponding big increase in oxygen reactivity and thus potential gum formation.

3. The aromatic increase going in hand with density increase reaches a peak value then decreases again with density at the cavern bottom, due to wash-out effects of light aromatics (mainly benzene) into the brine. The last liters of gasoline show this drastically. The loss in benzene and other aromatics explains the loss of research/motor octane numbers by at least one point.

4. The brine analysis *(see attachment 10)* shows a significant content of benzene and other aromatics as well as some other light hydrocarbons ; no bacteria contamination was detected.

7 - EQPS ASSESSMENT

EBV have operated EQPS, an expert system based on artificial intelligence, they have designed to predict ageing processes in oil products and calculate a further storage time during which the product use is still possible without significant risk.

Although the relevant ageing data were available only for the discharge batches and not for the fill-in batches the computer system labelled the gasoline after the storage time of 6 years 9 months as :

« A normal average product which may be very suitable for consumption within 18 months. Not ideal (anymore) for long term storage but risk of surprise is low -You may plan (even) for 2 years- ».

There was no difference in the predictions between the top, middle and bottom sections for the gasoline in the cavern. Please note that EQPS does not comment on changes of performance data, e.g. loss of RON due to benzene wash-out.

This would mean to say that the material could have been stored at least 2 years more in the cavern and still have been suitable for sale on the retail market, without reprocessing.

8 - MAIN CONCLUSIONS

Batches of base gasolines, intended for manufacture of 0,25 g/l leaded premium, were supplied from three refineries located in Marseilles area, and stored for nearly 7 years on behalf of SAGESS, in a salt cavern of Manosque site, rent to GEOSEL.

The gasoline analysis carried out at fill-in and after discharge of the cavern led to the following conclusions :

1. A mixing of the gasoline batches has resulted from the combined effect of their superposition in layers together with temperature convection moves. At discharge, the discrepancy of control values noted on original batches has disappeared to give a more uniform product.

2. An organized distribution of hydrocarbon families was noted from top to bottom of the cavern supported by a correlation of densities. The content of aromatics increases steadily to reach a max. peak at 130,000 m3 pumped, then followed by a fall until gasoline-brine interface. The balance of aromatics is made by olefins and isoparaffins. The drop in aromatics is especially sensitive at the near interface where 1 point fall of octane values is noted and a presence of light aromatics detected by GC in the brine.

3. Gasoline ageing after storage was rated as moderate as illustrated by limited increases of colour, contents of existent and potential gums, still matching quality specifications.

   Subsequently, the gasoline discharged from the cavern could be fully re-introduced in the gasoline pools of the 3 supplying refineries without requiring any re-processing. The product received was blended with octane improvers and adjusted with other available gasolines to match for the retail market either the specifications of 0,15 g/l leaded premium (0,25 g/l cancelled for environmental reasons) or the unleaded Europremium 95.

4. The potential gums in gasoline which normally turn into some existent gums for the products stored in above-ground tanks did not get through because of the privileged maintenance conditions in the cavern (no air, no UV, stable temperature, no volatility loss). This specific protection enhances the choice of salt caverns for the long storage of petroleum products.

5. The Manosque cavern findings confirmed previous experiments made in the German salt caverns of Blexen and Heide including the migration of aromatics at the interface from the gasoline layer into the brine layer.

6. A simulation program fed with gasoline ageing characteristics enabled to predict a further possible storage of at least 2 years in salt cavern without compromising its acceptable quality for sale on the domestic market.

9- FURTHER SAGESS EXPERIMENTS

The interesting results on the gasoline of cavern «V» encouraged SAGESS to extend this first experiment to cavern «P», another salt cavity filled with 313,000 M3 of an unleaded base gasoline (intended for 0,15 g/l leaded premium), supplied from the same refineries. Product which was stored in cavern «P» between March 1992 and March 1996 (3,5 years residence time) is currently being discharged for sale on the retail market.

Analysis of the so far discharged gasoline consolidated the basic conclusions for cavern «V» experiment :

- Trouble-free introduction into refineries gasoline pools (without reprocessing) after suitable quality control,
- Mix of original batches but gradual increase of densities and aromatics with balanced decrease of naphtenics/isoparaffins followed by a decrease,
- Little evolution of ageing characteristics.

GÉOSEL MANOSQUE - CAVERN V

EASTERN OVERHANGING VIEW

Cavern characteristics

Depth	590 - 660 m
Height	125 m
Maximum diameter	91 m
Capacity	195,000 m^3
Traps	5,000 m^3

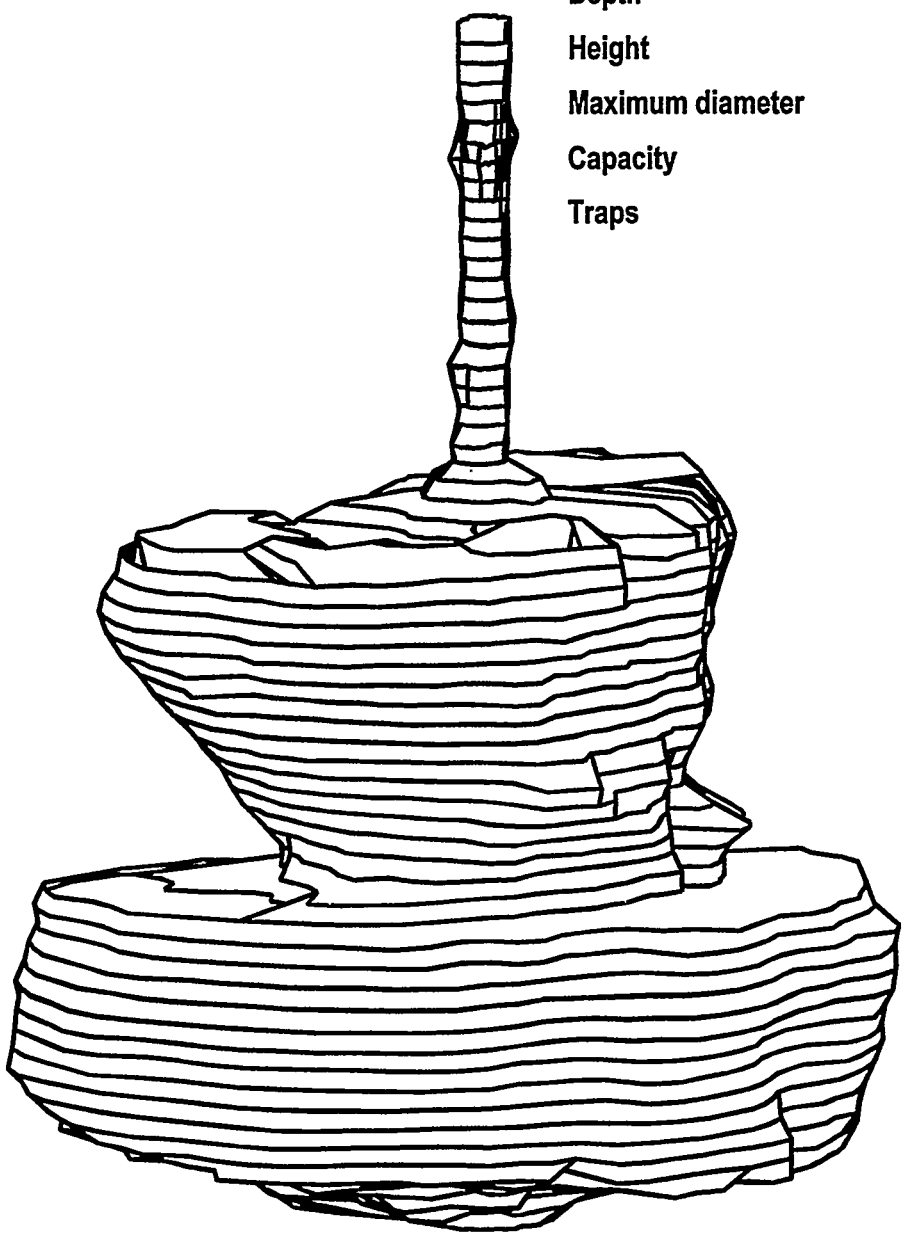

géostock

IASH '97
VANCOUVER - OCT - 1997

sagess

S.A.G.E.S.S.

Société Anonyme de GEstion des Stocks de Sécurité

☞ **A private company which fulfills a public service duty :**

Holding and controlling 1/4 of the French strategic petroleum reserves

SAGESS Strategic Stocks	Million m3
Gasolines	1.2
Diesel / Home Heating Fuels	3.8
Jet Fuels	0.2
Crude Oils	0.3

géostock

sagess

WHY STORING GASOLINE IN A SALT CAVERN ?

BALANCE OF TECHNICAL / ECONOMICAL FACTORS IS ATTRACTIVE

Technical

Salt cavern protects gasoline better than aboveground tanks

☛ No air, no UV responsible for ageing

No volatility loss

Storage temperature is stable (30 to 35° C range)

Economical

Storage times can be extended and costs are cheaper

géostock

CAVERN GASOLINE FEATURES

Fill history

PRODUCTS	STORAGE PERIODS
Diesel fuel	1971 ⇨ 1980
Naphta	1980 ⇨ 1981
Base gasoline for leaded	1981 ⇨ 1989
Base gasoline for leaded	1989 ⇨ 1996

Gasoline : 11 batches, 3 CAT - cracking refineries (base for leaded premium)

Storage time

Between 5 years 2 months and 7 years 8 months

Average # 7 years

HISTOGRAM OF CAVERN GASOLINE CONTENTS

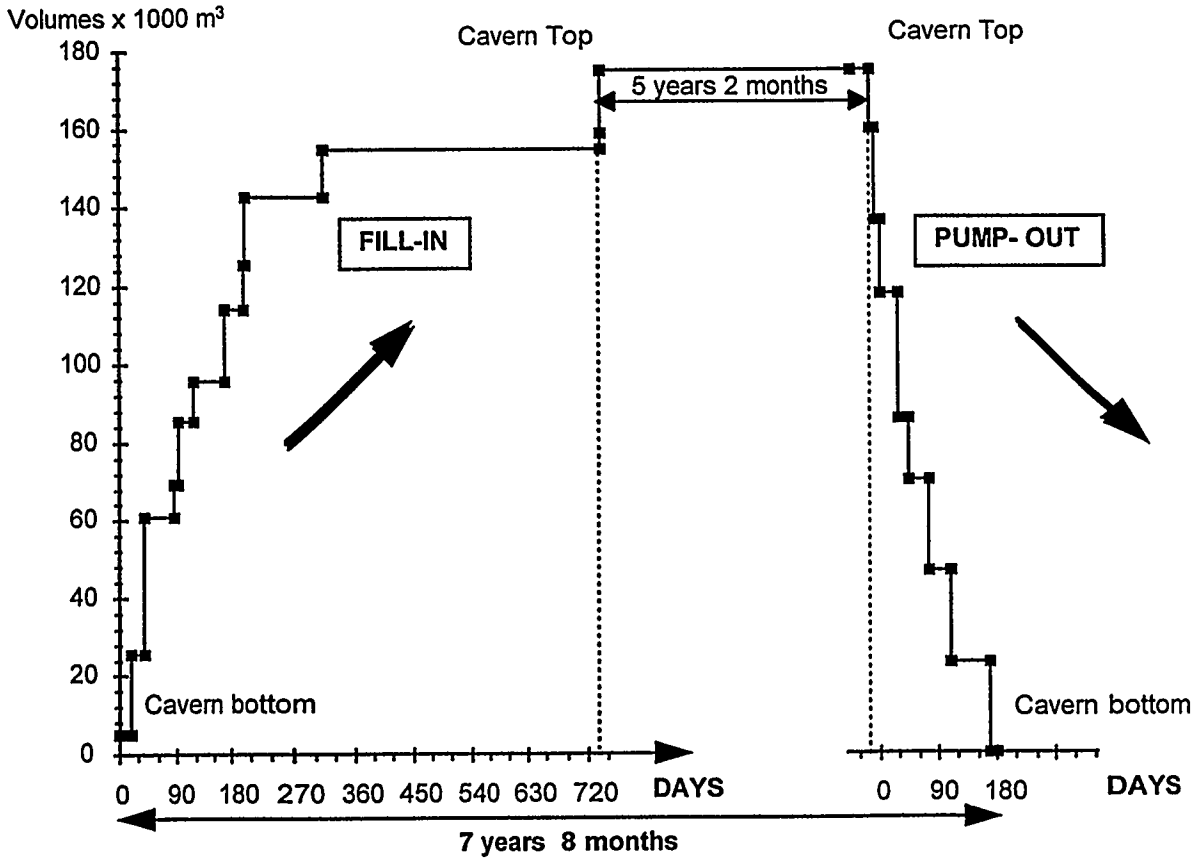

géostock

IASH '97
VANCOUVER - OCT - 1997

sagess

QUALITY CONTROL ANALYSIS

PRODUCT : LEAD-FREE GASOLINE STOCK FOR LEADED PREMIUM (0.25 G/L LEAD)

STORAGE TIME : 5-7 YEARS

		FILL-IN (11 BATCHES)			PUMP-OUT (8 LOTS)	
PROPERTY	**UNIT**	**RANGE OF VALUES**	**AVERAGE** *(weighted values)*	**SPECIFICATION**	**RANGE OF VALUES**	**AVERAGE** *(weighted values)*
Aspect	-	Clear and Bright		CaB	Clear and Bright	
Colour	-	Yellow pale	-		Light amber	
Density at 15°C	Kg/m3	746-778	757	720-770	754-758	756
DISTILLATION						
IBP	°C	27-38	34	-	33-41	37
50 %	°C	93-121	103	-	98-104	101
85 %	°C	138-167	152	180 max	143-154	148
90 %	°C	146-178	161	210 max	152-163	157
PF	°C	178-206	192	215 max	183-200	193

géostock

sagess

QUALITY CONTROL ANALYSIS

		FILL-IN (11 BATCHES)			PUMP-OUT (8 LOTS)	
PROPERTY	**UNIT**	**RANGE OF VALUES**	**AVERAGE** *(weighted values)*	**SPECIFICATION**	**RANGE OF VALUES**	**AVERAGE** *(weighted values)*
% Evaporated at 70 °C	% vol	15-30	24	10-47	24-30	26
% Evaporated at 100 °C	% vol	36-55	47	40-70	47-51	49
Residue	% vol	1-2	1,3	2 max	1-1,4	1,2
PVR at 37,8° C	HPa	500-720	590	450-790	484-731	604
Doctor test	-	Negative	-	Negative	Negative	-
Copper corrosion	Scale	1A-1B	1 A^+	1 B max	1A - 1B (1 out of 8)	$1A^+$
RON (clear)	Rating	92-96,2	94,9	-	94,5 - 95,6	95
MON (clear)	Rating	81,3-87,7	83,3	-	83 - 83,8	83,4
Existent Gum	mg/dl	0,5-6,0	2,0	10 max	1,1 - 5,5	3,5

NARROWER RANGES OF RESULTS ON GASOLINE AFTER STORAGE INDICATE MIXING

géostock

D15 AND DISTILLATION (E 100) VERSUS CAVERN DEPTH

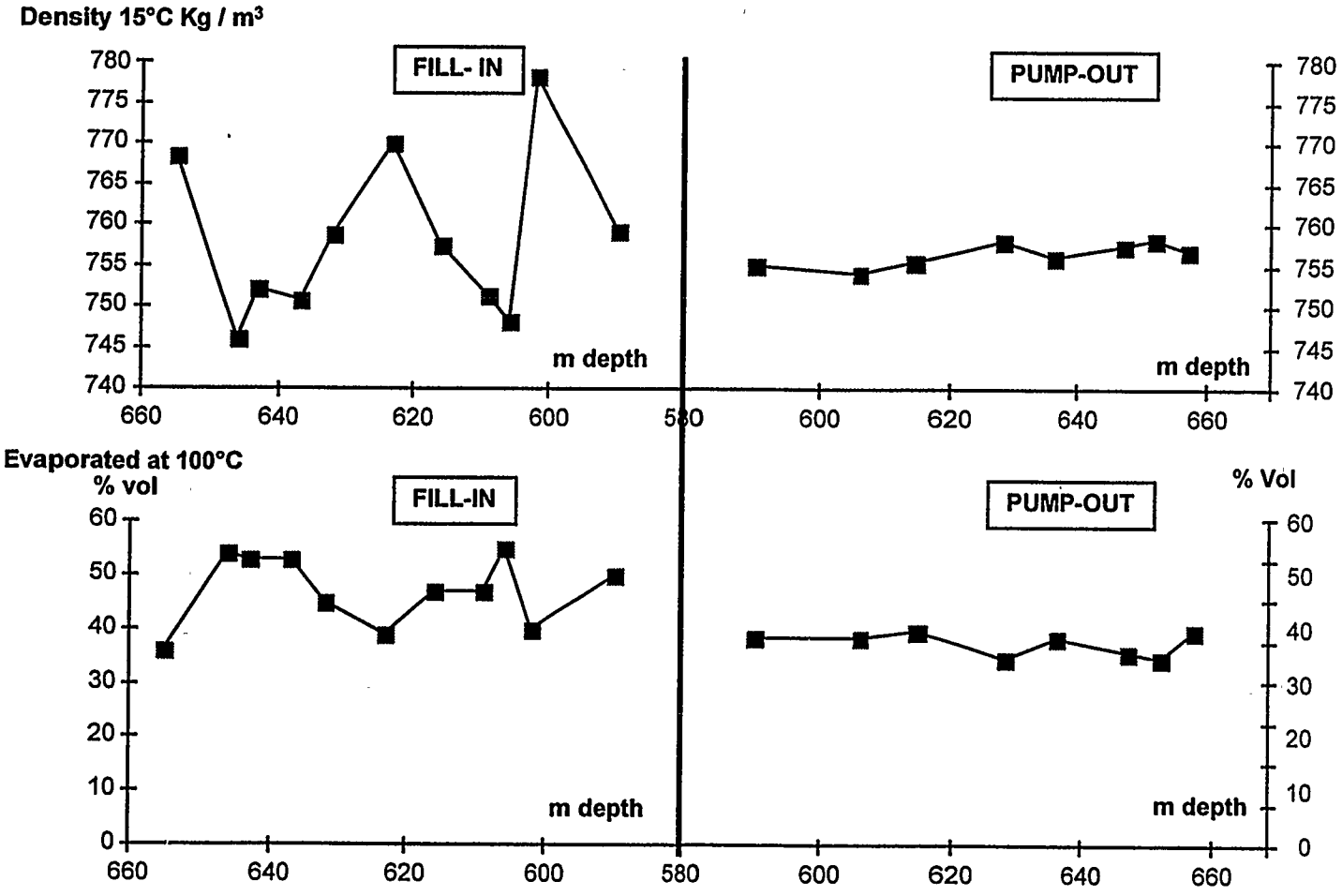

géostock

IASH '97
VANCOUVER - OCT - 1997

sagess

SEGMENT ANALYSIS

- AGEING CHARACTERISTICS -

	UNIT					
VOLUME AT DISCHARGE PUMP	**x 1,000 m3**	**10**	**55**	**110**	**166**	**INTERFACE**
EXISTENT GUM WASHED	mg / dl	4.3	5.8	4.4	4.3	4.0
INDUCTION PERIOD	minutes	> 1000	> 1000	> 1000	> 1000	84
POTENTIAL GUM WASHED (6 hours)	mg / dl	426	46	58	60	344
AROMATICS (FIA)	% Vol	43.0	47.7	51.9	44.5	36.2
RON (PIONA)	-	93.9	94.8	95.0	93.7	91.5
MON (PIONA)	-	82.2	83.0	83.0	82.0	80.3

géostock

sagess

BRINE ANALYSIS *

DENSITY 15°C	Kg/l	1.2005	ASTM D 4052
SALINITY	Kg/l	0.3	CALCULATION
TOTAL HYDROCARBONS	mg/l	6.2	GC ANALYSIS
BENZENE	mg/l	2.4	„
TOLUENE	mg/l	0.1	„
OTHER LIGHT AROMATICS	mg/l	< 0.1	„
OXYGEN	mg/l	0.4	„
BACTERIA CONTAMINATION	RLU**	NIL	LUMAC

* At gasoline/brine interface, at the end cavern discharge

** Relative Luminescence Unit

☛ **A limited migration of benzene and other light aromatics from gasoline into brine is confirmed by analysis**

géostock

6th International Conference
on Stability and Handling of Liquid Fuels
Vancouver, B. C., Canada
October 13-17, 1997

ASSESSING THE POTENTIAL FOR OXIDATIVE CRUDE OIL DEGRADATION DURING LONG-TERM STORAGE

J. B. Green*[1], J. Y. Shay[1], K. Q. Stirling[1], and H. N. Giles[2].

[1]BDM-PT, P.O. Box 2543, Bartlesville, OK 74005
[2]U.S. DOE, Strategic Petroleum Reserve Headquarters, Department of Energy, FE-43, 3G-070 Forrestal Building, 1000 Independence Ave., S.W., Washington, DC 20585-0340

Alteration of crude oil composition and properties is a major concern for those involved with its long-term storage or strategic stockpiling. Significant alteration of crude oil could potentially occur via any of several pathways: microbial degradation, contamination, precipitation of slightly soluble components, or oxidative degradation. Over the course of an ongoing program for support of the U.S. Strategic Petroleum Reserve (SPR), the authors have examined each of the pathways listed above. This paper will focus on assessing the potential for oxidative degradation of crude oil. In order to assess the maximum extent of degradation likely to occur, three crude oils were subjected to a modified version of the oxygen overpressure test used to test diesel fuel storage stability (ASTM D 5304). Hot (85°C) filtration and sediment washing were employed to avoid wax precipitation. The crude was aged for 16, 40, and 90 hours under pure oxygen using conditions prescribed in the test method. Additional tests were also carried out under air and inert (N_2) atmospheres. The resulting aged crude oil samples and sediments were subjected to a variety of analyses. Aging under pure oxygen at 90°C for 90 hours produced maximum sediment levels of 2.3–23 g/L for the range of crude oils tested. Sediment levels obtained under air or nitrogen were much lower, typically <0.3 g/L. Maximum sediment formation was directly proportional to either asphaltene or vanadium content of the crude oils examined. Both of these parameters correlate with the proportion of high molecular weight, slightly soluble crude oil components present. Sediments from oxidized crude oil exhibit atomic H/C ratios near 1.0, moderately elevated heteroatom contents compared to the respective >1,050°F resid, and relatively low (<1 wt%) levels of carbonyl and sulfoxide functional groups. Based on the results obtained, it was concluded that oxidative degradation of crude in SPR caverns is of minimal concern.

Introduction

Shortages of crude oil experienced in the 1970's led to establishment of crude oil reserves within the U.S. and other major oil importing nations. The U.S. Strategic Petroleum Reserve (SPR) was authorized by the Energy Policy and Conservation Act signed into law on December 22, 1975. This act provided for storage of more than 500 million barrels of oil that could be readily retrieved and refined in case of a crude oil supply interruption or other emergency.

Since that time, the SPR Headquarters of the U.S. Department of Energy has been actively engaged in preparation, filling, and monitoring of crude oil storage caverns. The caverns are formed in salt deposits located in Texas and Louisiana via solution mining; i.e., by injection of fresh or brackish water to form cavities within a given deposit. Movement of crude oil into or out

of caverns is accomplished by lowering or raising brine levels within each cavern. Periodic monitoring is carried out to ensure that no significant degradation of oil occurs during storage. An overview of the SPR caverns and monitoring program was published previously.[1]

Earlier, a significant effort was expended on determining factors contributing to buildup of minor amounts of an emulsion layer ("sludge") in selected SPR caverns over time. These results were presented in part at the *4th International Conference on Stability and Handling of Liquid Fuels*.[2-5] In short, sludge formation was found to largely result from natural settling phenomena and not from significant chemical or microbial degradation. Workers investigating sludge formed in crude oil stored above ground in Japan implicated asphaltene precipitation, wax precipitation, and oxidative condensation as potential mechanisms/causes for sludge buildup.[6,7]

Although oxidation or oxidative condensation was not found to be a significant factor causing sludge formation in SPR caverns, measurable oxygen infusion into caverns could occur via air dissolved in water used to displace oil in cavern operations as well as from air in purchased crude used to fill caverns. In order to assess the maximum potential for crude oil degradation via oxidation, samples of SPR crudes were aged under severe conditions using the oxygen overpressure storage stability test developed for diesel fuels (ASTM D 5304). Pure oxygen, air and inert atmospheres were employed during the testing. In addition to measurements of insolubles formation resulting from accelerated aging, analyses of aged oils and the insolubles themselves were carried out. The objectives of the work were to determine the extreme upper limit of crude oil degradation possible from storage under high concentrations of oxygen, as well as to obtain a realistic assessment of the potential for crude oil oxidation during long-term storage in SPR caverns under typical conditions (45°C, <10 ppm O_2).

Experimental

Three crude oil samples were selected. One was from a SPR cavern containing a mixture of sweet crude oils (BM113). A second was from another SPR cavern containing a mixture of sour crude oils (BM110). The third sample, from the Naval Petroleum Reserve (NPR1), was of intermediate quality. The storage stability of each sample was evaluated using a modified version of ASTM D 5304 (Standard Test Method for Assessing Distillate Fuel Storage Stability by Oxygen Overpressure). This is a short term test normally used to determine the stability of diesel fuels. The crude oil was filtered at ~85°C rather than the ambient temperature normally used. The isooctane used to rinse the filter was also heated. Heating was required because of the paraffinic nature of the crudes. The samples were stored at 90°C under 100 psig oxygen, air, or nitrogen for 16, 40, and 90 hours.

Filtered aliquots of crude recovered from each storage condition were tested for: specific gravity, carbon residue, acid number, viscosity, heptane insolubles, and loss of light ends via GC simulated distillation. Standard ASTM procedures were used for each test. Particulates obtained after storage were analyzed by infrared spectroscopy. For this analysis, nominal 10 mg/mL dichloromethane solutions were prepared, placed in 0.5 mm KBr cells, and scanned using a conventional dispersive infrared instrument. Determination of sulfoxides from infrared spectra is described elsewhere.[8] Calculation of carbonyl compound types was similar, except that a molar absorptivity of 620 $Lm^{-1}cm^{-1}$ was used. If sufficient quantities of particulate were available, elemental analyses for C, H, N, S, Ni, and V were also performed.

Results

Table 1 summarizes results from the accelerated storage stability tests. Test results are reported for three time periods for each of the three atmospheres (N_2, air, O_2) used. The reported insolubles include adherent (coatings formed on the test vessel) as well as filtered sediments.

Under a pure oxygen atmosphere, each of the crudes produced significant insolubles. However, the crude from the sweet cavern (BM113) required 90 hours to generate insolubles in excess of 1 g/L; it produced significantly less insolubles than the other two crudes at any given condition. The BM110 crude produced much higher levels of insolubles under air than either of the other two crudes. Formation of insolubles under nitrogen was uniformly low for all the crudes.

Table 2 summarizes properties of the vacuum resid (>1,050°F) obtained from each crude. Properties of the resids, instead of the whole crudes, have been selected in this case because most of the precursors for insolubles are present in the >1,050°F fraction. Inspection of the table reveals that the only properties which follow the trends in insoluble formation listed above in Table 1 are vanadium (V) and asphaltene contents. Figures 1 and 2 illustrate correlations between total insolubles formed under the most severe storage condition (90 hours under 100 psig O_2) with vandium and asphaltene contents, respectively. In each figure, V and asphaltene contents are expressed both on whole crude as well as >1,050°F resid bases. For vanadium (Figure 1), a better correlation was obtained whenever results were expressed on a resid basis. For asphaltene content (Figure 2), expression of data on a whole crude basis provided the better correlation.

Correlation of insoluble formation during aging with asphaltene content is not surprising since asphaltenes, by definition, comprise the least soluble components in a given crude. The correlation of insolubles with vanadium content may be fortuitous, since V content often tracks asphaltene content in many crudes. In any case, either parameter may prove useful toward predicting the

oxidation susceptibility and/or storage stability of crude in a given SPR cavern. Further work will be needed to establish the general applicability of either correlation, however.

Tables 3–5 list properties of unaged crudes as well as for liquids recovered from each storage condition. The higher specific gravity (lower API gravity) and higher viscosities (77° and 100°F) observed for the aged crudes can largely be attributed to losses of light ends incurred during storage and handling. Figures 3–5 show correlations of those properties with light end loss for NPR1, BM110, and BM113 crudes, respectively. Out of all the plots shown, only those corresponding to viscosity for BM110 crude (Figure 4) exhibit any significant nonlinearity attributable to compositional changes beyond simple evaporation of volatile constituents. As evident from the larger quantities of insolubles formed from BM110 crude compared to the others (Table 1), its composition may have been altered the most during storage, particularly from aging under pure oxygen.

Figure 6 illustrates insoluble formation under 100 psig oxygen as a function of time for each crude. As noted above, the BM110 crude formed the most insolubles at any given time, in accordance with its higher V and asphaltene contents. Under an oxygen atmosphere, insoluble formation is approximately linear with time for each crude. Figure 7 shows acid number data determined on filtered crudes in Tables 3–5. In contrast to insoluble formation, increases in acid number tended to level off with time, particularly for NPR1 and BM113 crudes. Also, acid number increased the most for the NPR1 crude, which exhibited only intermediate levels of insoluble formation during aging.

Figure 8 shows the relationship between acid number versus insoluble formation for each crude. The exponential increase in insolubles with acid number for NPR1 and BM113 crudes suggests that insoluble formation may be acid catalyzed, or otherwise accelerated. However, the linear relationship evident for BM110 indicates that for it, the two processes occur independently. In any case, it should be borne in mind that acid number may simply coincide with a host of other oxidation-induced compositional changes which have equal or greater effect on insoluble formation.

Tables 6–8 list results from infrared analysis of sediments obtained from determination of insolubles. Table 9 shows elemental analyses of selected sediments. Neither the oxygen nor sulfur contents determined from infrared analysis account for major proportions of the total elemental contents shown in Table 9. This finding in turn indicates that the bulk of sediment S and O exists in other types of functional groups.

In the case of sulfur, most of the total S probably exists in thiophenic structures which are carried more or less incidentally into the sediment through actions of other structural moieties present. The fact that the sediment with the highest sulfoxide content (NPR1, Table 6) contained only moderate levels of total sulfur (2 wt%) illustrates the prevalence of thiophenic or other inert

forms of sulfur in crudes and corresponding sediments. This in turn prevents total sulfur (Table 2) from being a useful predictor of insoluble formation. The very moderate and relatively uniform levels of sulfoxide groups observed in all sediments suggests that their formation via oxidation of sulfide groups is not a key element in the process of insoluble formation.

Similarly, although nitrogen is somewhat enriched in sediments compared to levels in whole >1,050°F resids (by a factor of 2 or less, compare Tables 2 versus 9), its degree of enrichment is similar to that of sulfur—thereby indicating incidental incorporation. However, although total nitrogen does not correlate with insoluble formation, a subset of nitrogen containing-species could conceivably be activated toward insolubles formation (e.g., vanadyl porphyrins).

Incorporation of significant levels of acids (presumably carboxylic acids) in sediment should result in much higher levels of carbonyl groups in sediments than those actually observed in the infrared analyses (Tables 6-8). Although the levels of total oxygen estimated by difference in Table 9 are admittedly approximate, they surpass those determined by infrared by a great enough degree that precipitation of acids or other carbonyl types can effectively be ruled out as the major mechanism for insoluble formation. However, the "catalysis" or promotion of insoluble formation by acids suggested by exponential plots for NPR1 and BM113 crudes in Figure 8 cannot be refuted (or confirmed) by the infrared data.

Discussion

Based on the available data, the most likely mechanism for insoluble formation during crude storage is one where molecular oxygen acts as a free radical initiator, hydrogen acceptor, or otherwise as a promoter of condensation/agglomeration reactions yielding species too large to be soluble in crude oil. Quite likely, reactive species such as phenols undergo oxidative coupling via schemes analogous to that proposed by Mochida, etal.,[6] for crude oil stored above ground, or White, etal.,[9] for coal liquids. The insolubles produced are highly aromatic (H/C~1, see Table 9) and somewhat enriched in heteroatoms compared to the whole >1,050°F resid.

The hypothesis that molecular oxygen "chews up" selected crude oil components to the point where they contain sufficient polar functional groups to become insoluble is totally inconsistent with the experimental data. In fact, direct oxidation of functional groups like sulfides (to sulfoxides) very likely retards insoluble formation by consuming available oxygen in a manner analogous to conventional antioxidant additives. This explains the disproportionately low degree of insolubles formation observed under air compared to pure oxygen (except for BM110 crude, see Table 1), as well as the induction time usually required (except for BM110 crude–see Figure 6).

The exceptional behavior for BM110 crude may result from a deficiency in oxidizable functionalities which could provide it comparable protection to that of the other crudes.

Vanadium or asphaltene contents are useful indicators of a given crude's potential toward insolubles formation. This is likely the case because both of these parameters indicate/correlate with levels of large molecules with inherently lower solubility in crude oil.

Finally, the "problem" of insolubles formation during crude oil storage should be placed into perspective. First, the highest level of insolubles observed was 23 g/L, or approximately 2.5 wt%. This result was obtained under a completely unrealistic condition of 100 psig (115 psia) pure O_2. The dissimilarity of insolubles produced from diesel fuel at such extreme conditions of temperature and oxygen partial pressure to those formed under actual long-term storage was noted earlier by Power and Davidson.[10] Secondly, the likelihood of achieving even a 1 psia oxygen partial pressure inside a SPR cavern is extremely remote. As noted above, most crudes are capable of consuming moderate levels of oxygen, through sulfoxide formation and analogous mechanisms, with no formation of insolubles. By far, the conditions employed here which best represent actual crude storage in SPR caverns are those employing inert (N_2) gas. Therefore, the impact of oxidation or oxidative coupling on crude oil composition or insolubles formation over time periods of even several decades should be negligible. This finding is in agreement with earlier studies of sludge formation and composition which indicated the absence of significant chemical or microbial degradation of SPR crude in storage.[2-5]

Acknowledgment. This work was supported by the U.S. Department of Energy, SPR Headquarters. The authors thank Susan Howard and Cheryl Dickson for manuscript and figure preparation, respectively.

References

(1) Giles, H. N.; Koenig, J. W. J.; Neihof, R. A.; Shay, J. Y.; Woodward, P. W. *Energy Fuels* **1991**, *5*, 602–608.

(2) Green, J. B.; Woodward, P. W.; Thomson, J. S.; Shay, J. Y.; Giles, H. N. In *Proceedings of the 4th International Conference on Stability and Handling of Liquid Fuels*; Giles, H. N., Ed.; vol. 1, DOE/CONF-911102; NTIS: Springfield, VA, 1992; pp 50–64.

(3) Thomson, J. S.; Grigsby, R. D.; Doughty, D. A.; Woodward, P. W.; Giles, H. N. *ibid*, pp 65–78.

(4) Green, J. B.; Yu, S. K.-T.; Woodward, P. W.; Giles, H. N. *ibid*, pp 79–93.

(5) Bryant, R. S.; Chase, K. L.; Stepp, A. K. *ibid*, pp 94–108.

(6) Mochida, I.; Sakanishi, K.; Fujitsu, H. *Oil Gas J.* **1986**, *Nov. 17*, 58–63.

(7) Hara, T. In *Proceedings of the 2nd International Conference on Long-term Storage Stabilities of Liquid Fuels*; Stavinoha, L. L., Ed.; vol. 1, Southwest Research Institute: San Antonio, TX, 1986; pp 1–12.

(8) Green, J. B.; Yu, S. K.-T.; Pearson, C.D.; Reynolds, J. W. *Energy Fuels* **1993**, *7*, 119–126.

(9) White, C. M.; Jones, L.; Li, N. C. *Fuel* **1983**, *62*, 1397–1403.

(10) Power, A. J., Davidson, R. G. *Fuel* **1986**, *65*, 1753–1755.

Table 1. Storage Stability of Crude Oil Aged at 90°C under 100 psig Gas Pressure

Crude	Aging Time (hours)	Total Insolubles (g/L)		
		Nitrogen	Air	Oxygen
NPR1 (94SPR021)	16	0.03	<0.01	0.26
	40	<0.01	0.06	5.7
	90	0.10	0.15	15
BM113 (95SPR094–095)	16	0.07	0.08	0.17
	40	0.07	0.12	0.41
	90	0.06	0.27	2.3
BM110 (95SPR027–028)	16	0.29	0.22	4.9
	40	0.33	3.1	9.1
	90	0.22	6.7	23

Table 2. Properties of Vacuum Resids (>1,050°F)

Crude	NPR1 (94SPR021)	BM113 (95SPR094–095)	BM110 (95SPR027–028)
>1,050°F resid[a]			
wt%	13.4	13.1	18.5
vol%	11.1	11.2	15.4
API Gravity	6.1	10.8	5.3
wt% S	1.58	1.19	3.61
wt% N	1.55	0.68	0.57
MCR, wt%	25.2	14.6	24.3
Viscosity, cSt			
180°F	235,682	2,844	45,470
210°F	33,861	885	8,458
Metals, ppm			
Ni	201	27.2	73.5
V	218 (29.2)[a]	32.0 (4.2)[a]	318 (58.8)[a]
Fe	138	10.4	5.1
C_7-asphaltenes, wt%	11.9 (1.6)[a]	3.85(0.50)[a]	14.1(2.6)[a]

[a] Yield or concentration on a whole crude basis.

Table 3. Properties of NPR1 Crude as a Function of Aging

Aging time	0 hours		16 Hours			40 Hours			90 Hours		
Atmosphere	U[a]	F[b]	N_2	Air	O_2	N_2	Air	O_2	N_2	Air	O_2
Specific gravity 60/60°F	0.852	0.877	0.886	0.885	0.888	0.883	0.888	0.887	0.882	0.884	0.885
API° gravity	34.5	29.9	28.2	28.4	27.8	28.8	27.9	28.0	28.9	28.6	28.4
Carbon residue, wt%	3.53		3.82	3.89	4.25	3.78	3.87	4.13	3.50	3.81	3.77
Acid number, mg KOH/g	0.22		0.25	0.29	0.90	0.25	0.40	1.80	0.25	0.53	2.50
Viscosity, cSt @ 77°F	5.93	13.37	19.22	20.27	21.34	17.04	22.75	24.02	21.10	20.57	20.17
Viscosity, cSt @ 100°F	4.37	8.33	11.55	11.11	12.55	10.39	12.53	12.09	9.91	10.88	11.42
C_7-asphaltenes, wt%			1.46	2.43	3.45	2.32	2.82	3.11	1.50	2.57	2.89
Distilled, % @ 200°F	8	2	1	1	1	1	<1	1	1	1	1
Distilled, % @ 300°F	21	13	9	10	9	11	9	9	10	9	10
Estimated light end loss, %	0	7	12	11	12	10	12	12	11	12	11

[a] Unfiltered
[b] Filtered

Table 4. Properties of BM113 (Sweet) Crude as a Function of Aging

Aging time	0 hours		16 Hours			40 Hours			90 Hours		
Atmosphere	U[a]	F[b]	N_2	Air	O_2	N_2	Air	O_2	N_2	Air	O_2
Specific gravity 60/60°F	0.846	0.869	0.873	0.878	0.877	0.875	0.876	0.879	0.876	0.877	0.878
API° gravity	35.7	31.3	30.5	29.7	29.8	30.3	30.0	29.4	30.1	29.8	29.7
Carbon residue, wt%	2.20	2.58	2.56	2.72	2.79	2.57	2.73	2.84	2.60	2.86	2.84
Acid number, mg KOH/g	0.09	0.09	0.10	0.14	0.33	0.10	0.28	0.65	0.10	0.53	0.95
Viscosity, cSt @ 77°F	7.20	14.21	16.05	19.49	24.09	20.51	18.55	21.03	19.05	19.63	19.02
Viscosity, cSt @ 100°F	4.88	8.98	10.31	12.11	12.06	11.07	11.33	12.78	11.76	11.77	12.10
C_7-asphaltenes, wt%	0.96	0.71	0.50	0.77	0.47	0.34	0.53	0.67	0.38	0.64	0.51
Distilled, % @ 200°F	8	2	1	<1	<1	<1	<1	<1	<1	<1	<1
Distilled, % @ 300°F	18	9	7	5	6	6	5	5	6	6	6
Estimated light end loss, %	-	9	11	13	12	12	13	13	12	12	12

[a] Unfiltered
[b] Filtered

Table 5. Properties of BM110 (Sour) Crude as a Function of Aging

Aging time	0 hours		16 Hours			40 Hours			90 Hours		
Atmosphere	U[a]	F[b]	N_2	Air	O_2	N_2	Air	O_2	N_2	Air	O_2
Specific gravity 60/60°F	0.864	0.886	0.895	0.898	0.897	0.894	0.901	0.902	0.896	0.904	0.897
API° gravity	32.3	28.2	26.6	26.0	26.2	26.7	25.5	25.3	26.4	25.0	26.2
Carbon residue, wt%	4.57	5.12	5.44	5.70	5.58	5.35	5.64	5.29	5.41	5.67	4.94
Acid number, mg KOH/g	0.11	0.13	0.16	0.13	0.34	0.16	0.29	0.63	0.16	0.40	1.17
Viscosity, cSt @ 77°F	11.53	20.11	28.69	32.17	31.97	27.56	37.51	39.17	29.79	45.40	32.84
Viscosity, cSt @ 100°F	7.33	12.86	17.41	19.74	19.42	16.77	22.69	23.67	17.98	26.81	19.94
C_7-asphaltenes, wt%	1.78	2.04	1.32	2.97	3.30	2.61	3.76	2.87	1.79	4.65	2.01
Distilled, % @ 200°F	7	1	<1	<1	<1	<1	<1	<1	<1	<1	<1
Distilled, % @ 300°F	16	8	4	4	3	5	2	2	3	1	3
Estimated light end loss, %	-	8	12	12	13	11	14	14	13	15	13

[a] Unfiltered
[b] Filtered

Table 6. Infrared Analysis of Sediments from Aged NPR1 Crude

Aging time (hours)	Atmosphere	Carbonyl oxygen (wt%)			Sulfoxide sulfur (wt%)
		Ketone type	Amide type	Total	
0	-	0.06	0.14	0.20	0.12
16	N_2	0.24	0.45	0.69	0.61
40	N_2	0.20	0.32	0.52	0.33
90	N_2	0.18	0.37	0.55	0.29
16	air	0.29	0.39	0.68	0.46
40	air	0.32	0.41	0.73	0.56
90	air	0.38	0.42	0.80	0.51
16	O_2	0.43	0.47	0.90	0.88
40	O_2	0.45	0.42	0.87	0.92
90	O_2	0.57	0.50	1.07	0.86

Table 7. Infrared Analysis of Sediments from Aged BM113 Crude

Aging time (hours)	Atmosphere	Carbonyl oxygen (wt% O)			Sulfoxide sulfur (wt% S)
		Ketone type	Amide type	Total	
0	-	ins[a]			
16	N_2	ins[a]			
40	N_2	ins[a]			
90	N_2	ins[a]			
16	air	ins[a]			
40	air	ins[a]			
90	air	0.45	0.28	0.73	0.42
16	O_2	0.40	0.32	0.72	0.31
40	O_2	0.43	0.32	0.75	0.34
90	O_2	0.51	0.36	0.87	0.54

[a] Insufficient sediment available for analysis.

Table 8. Infrared Analysis of Sediments from Aged BM 110 Crude

Aging time (hours)	Atmosphere	Carbonyl oxygen (wt% O)			Sulfoxide sulfur (wt% S)
		Ketone type	Amide type	Total	
0	-	0.10	0.19	0.29	0.19
16	N_2	0.07	0.18	0.25	0.23
40	N_2	0.08	0.17	0.25	0.21
90	N_2	0.08	0.19	0.27	0.23
16	air	0.17	0.21	0.38	0.19
40	air	0.22	0.21	0.43	0.25
90	air	0.25	0.25	0.50	0.41
16	O_2	0.23	0.23	0.46	0.26
40	O_2	0.28	0.25	0.53	0.53
90	O_2	0.45	0.33	0.78	0.60

Table 9. Elemental Analysis of Selected Sediments (wt%)

Crude	Aging Condition	C	H	N	S	O[a]
NPR1	40 hrs-O_2	82.3	7.96	1.66	2.00	6.1
NPR1	90 hrs-O_2	82.3	7.92	1.67	2.07	6.0
BM113	90 hrs- O_2	81.7	7.13	0.952	2.05	8.2
BM110	40 hrs-air	77.0	6.87	0.870	5.07	10.2
BM110	40 hrs-O_2	81.1	7.03	1.048	5.63	5.2
BM110	90 hrs- O_2	80.0	6.85	0.914	5.70	6.5

[a] O calculated by difference.

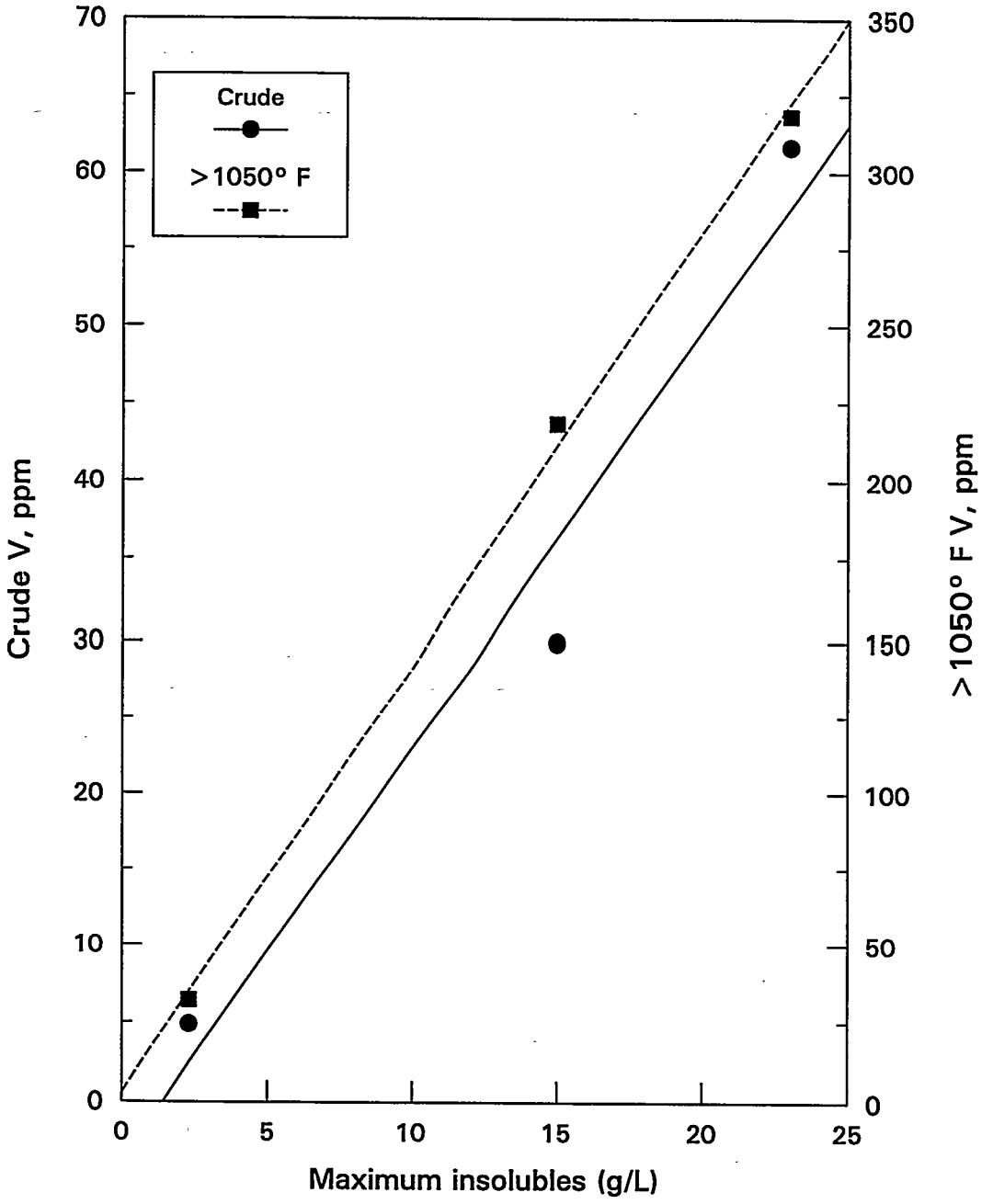

Figure 1. Correlation of maximum formation of insolubles (90 hrs, 100 psig oxygen) with vanadium content

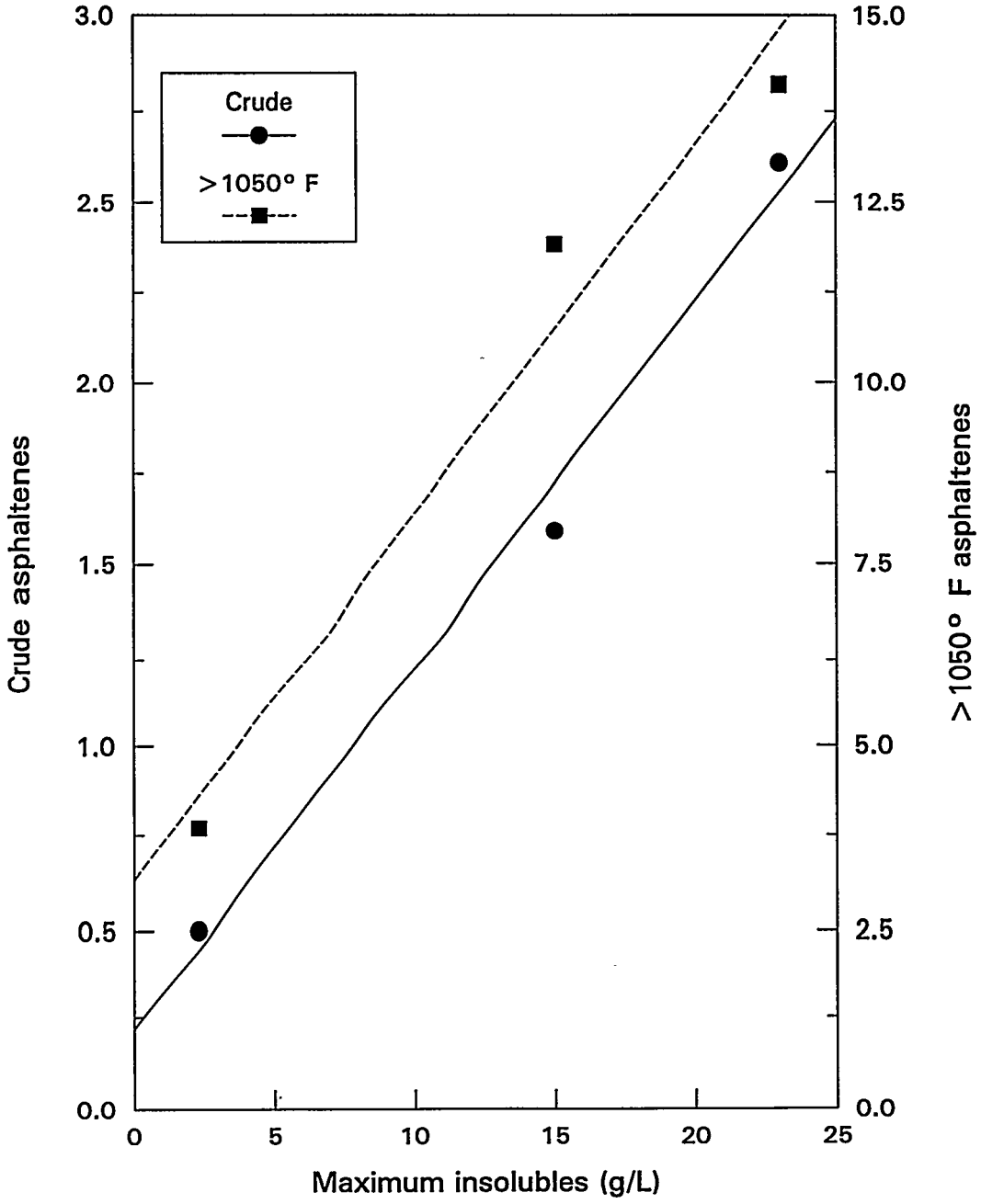

Figure 2. Correlation of maximum formation of insolubles (90 hrs, 100 psig oxygen) with asphaltene (heptane) content

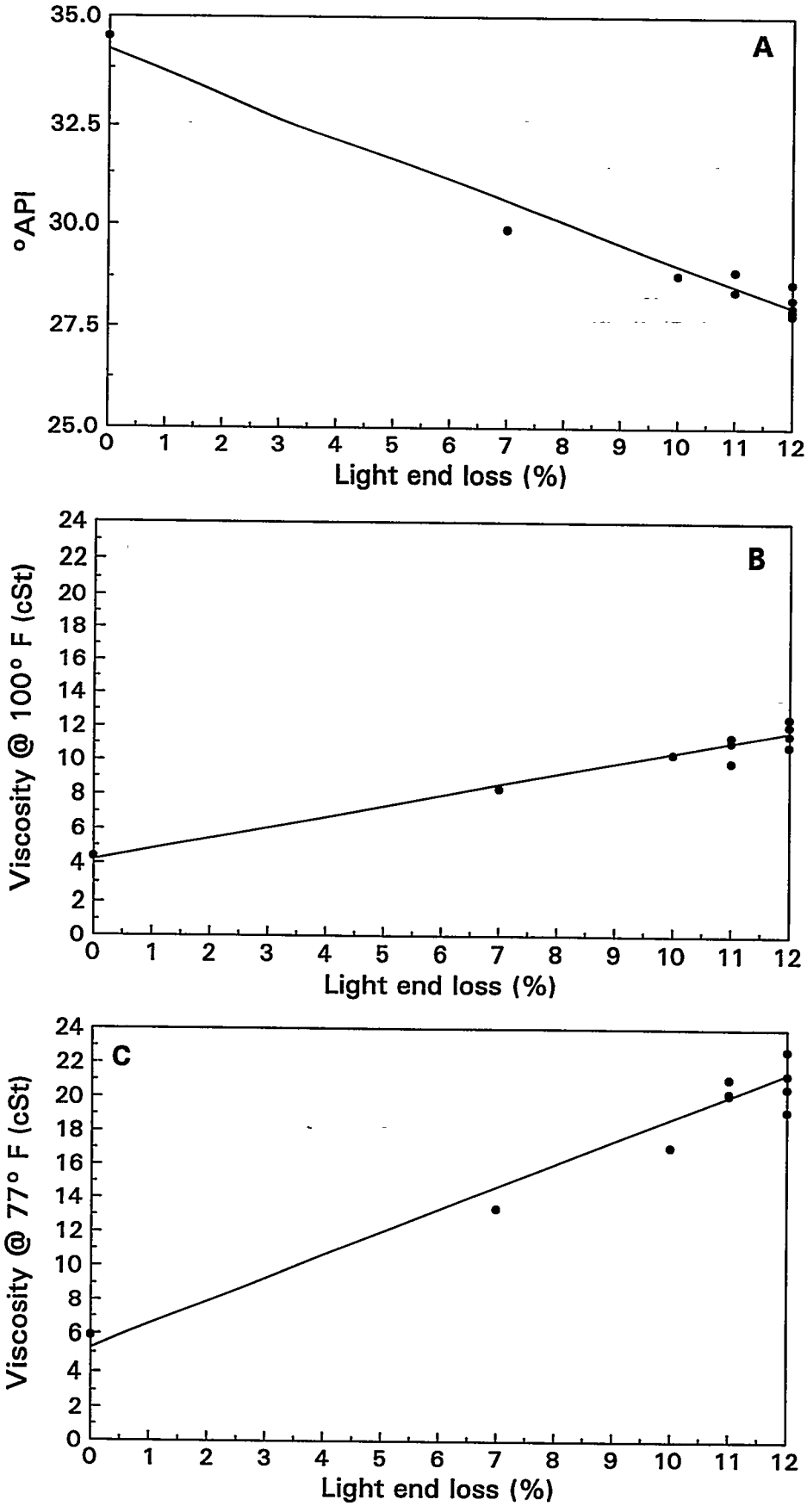

Figure 3. Correlations of light end loss with gravity and viscosity - NPR1

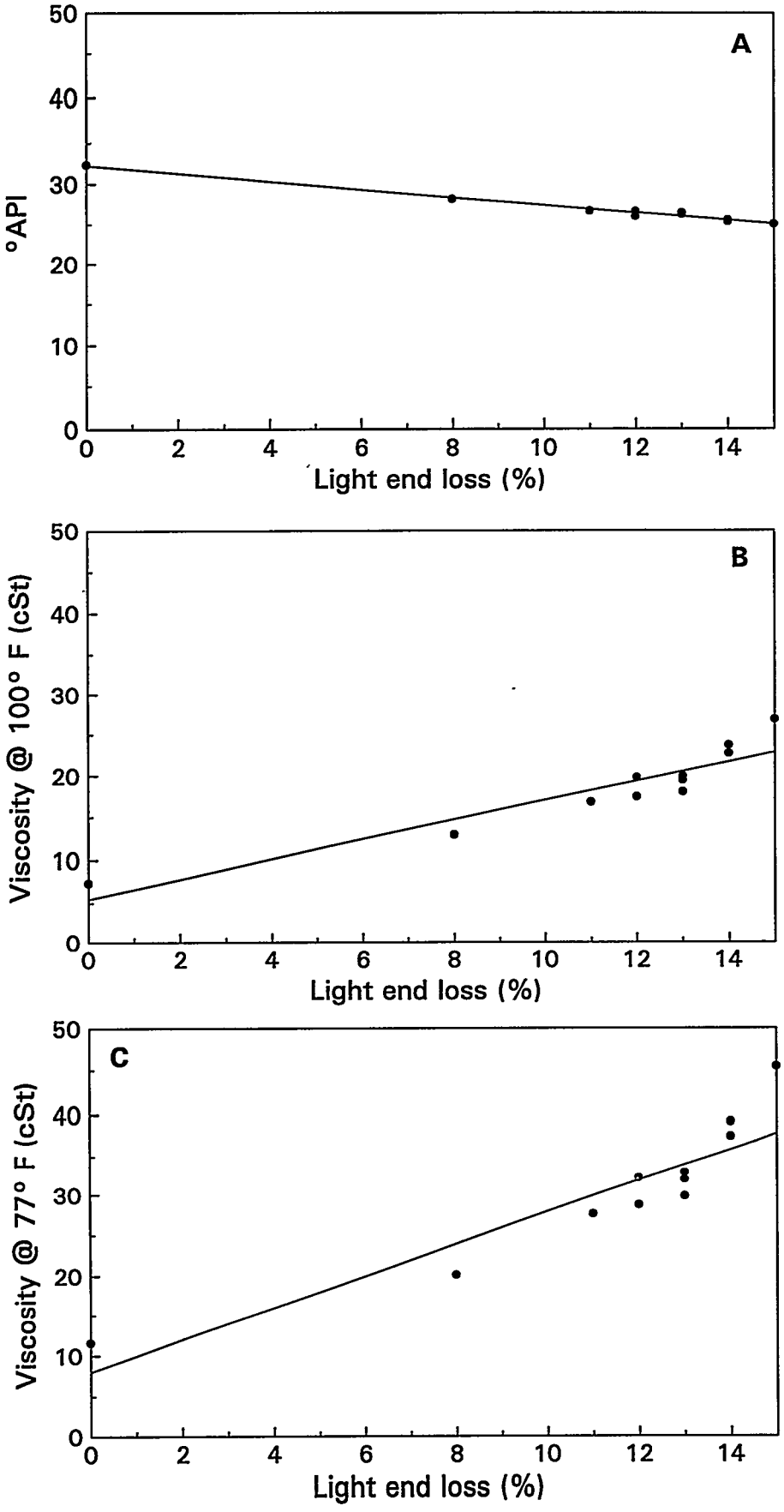

Figure 4. Correlations of light end loss with gravity and viscosity - BM110

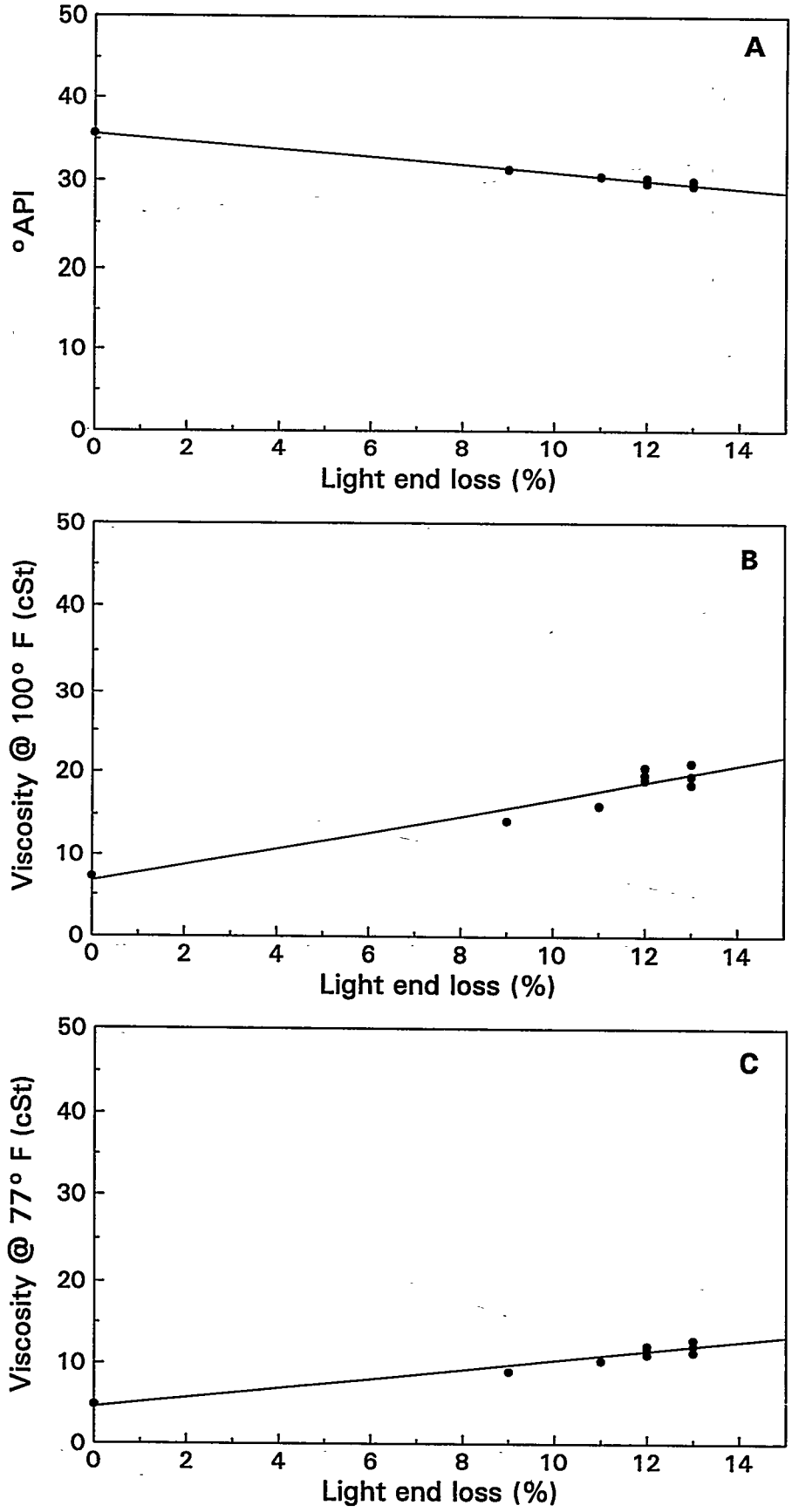

Figure 5. Correlations of light end loss with gravity and viscosity - BM113

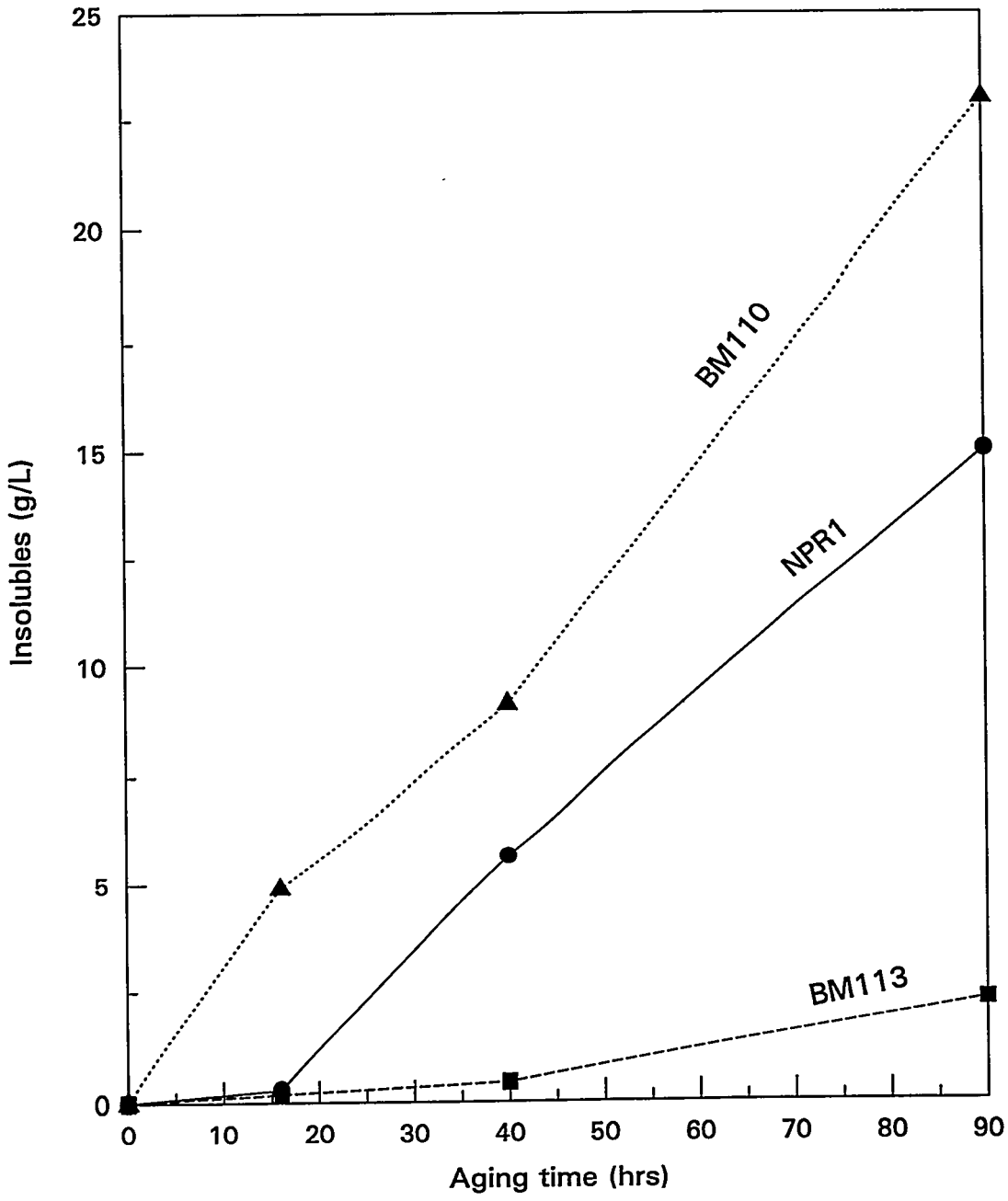

Figure 6. Formation of insolubles at 90° C, 100 psig oxygen as a function of time

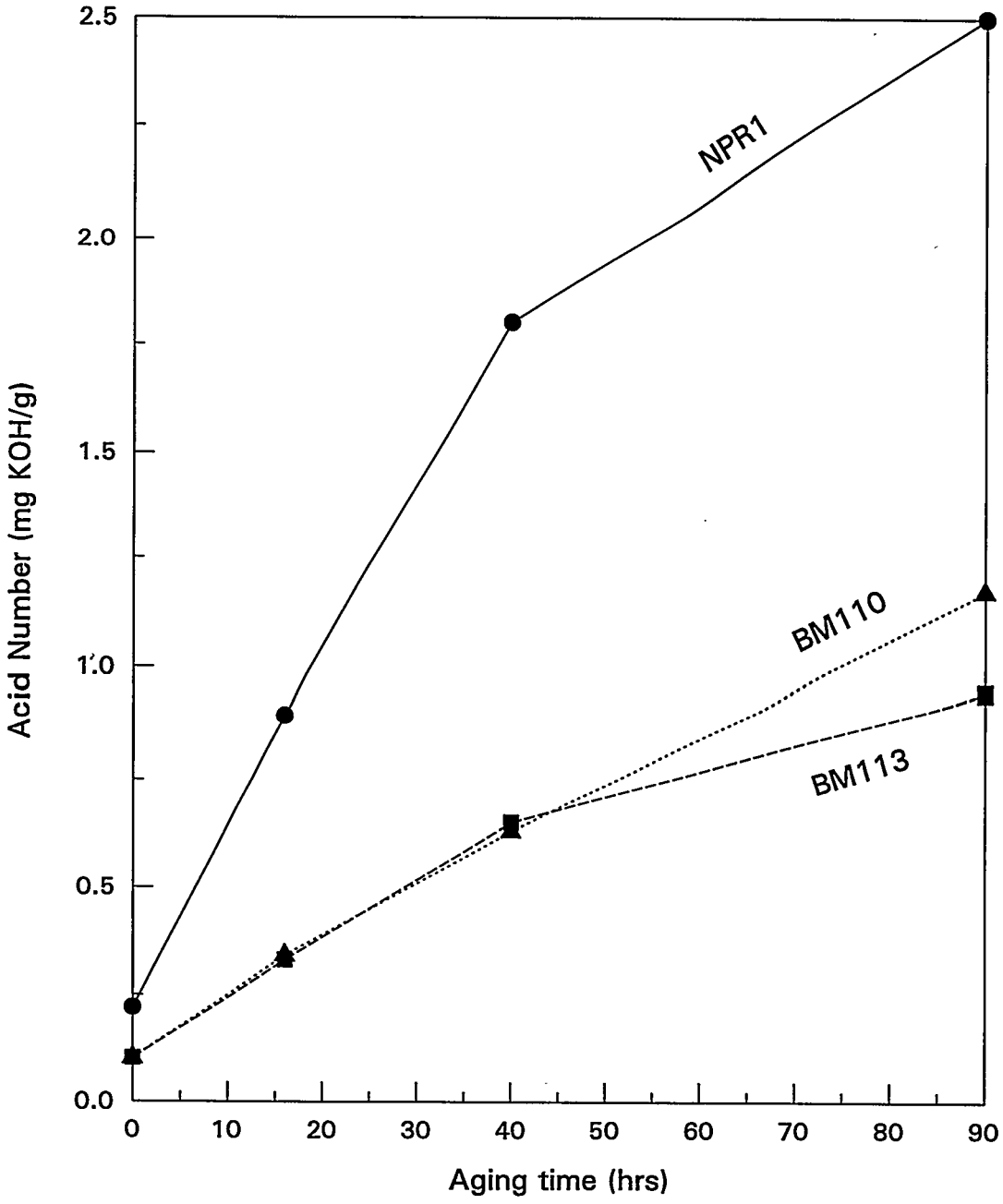

Figure 7. Increase in acid number with aging at 90° C, 100 psig oxygen

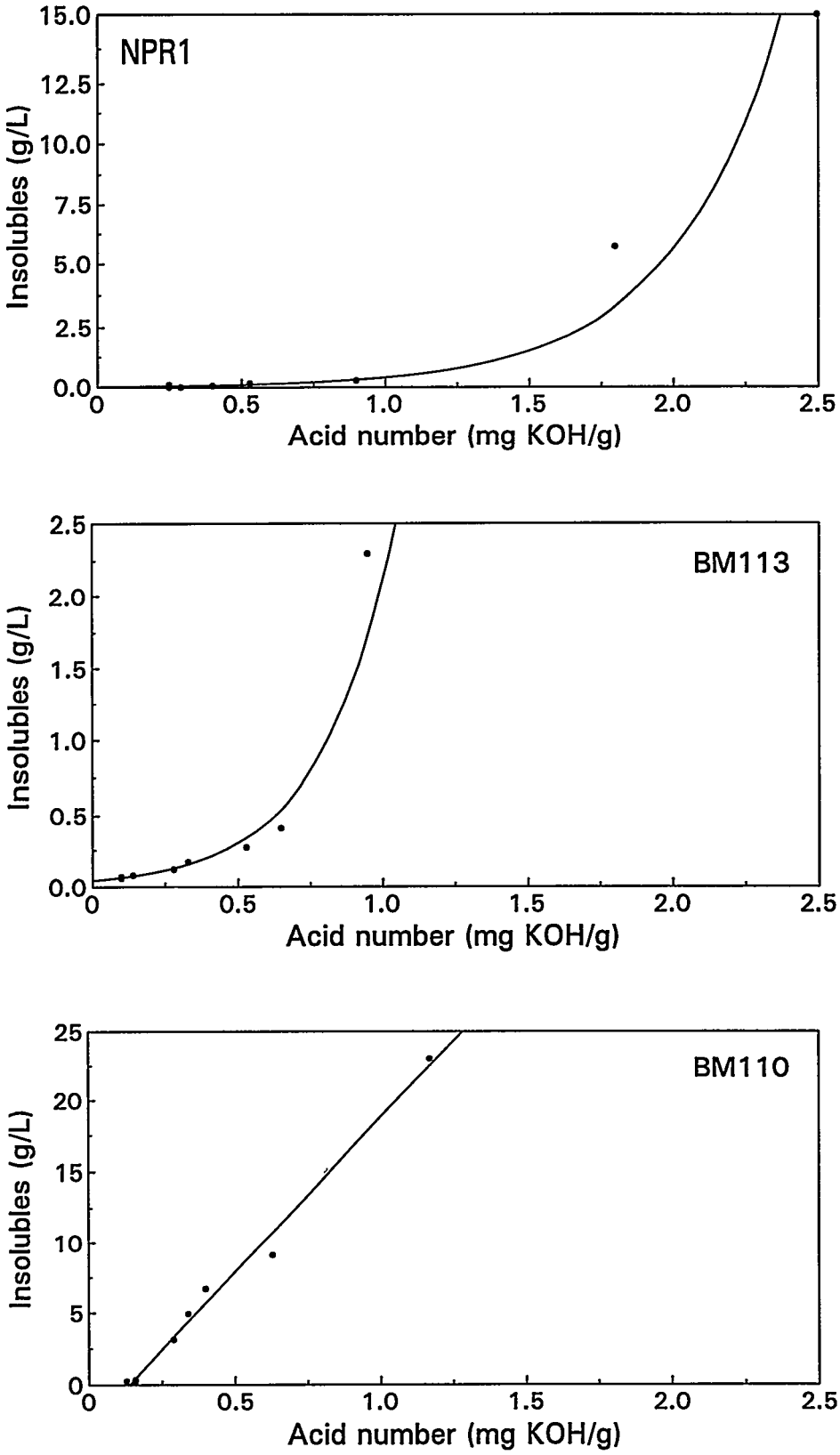

Figure 8. Correlation between acid number and formation of insolubles